Winter 1-25-2018

Integrating Management Zones and Canopy Sensing to Improve Nitrogen Recommendation Algorithms

Joel D. Crowther
University of Nebraska-Lincoln

INTEGRATING MANAGEMENT ZONES AND CANOPY SENSING TO IMPROVE NITROGEN RECOMMENDATION ALGORITHMS

by

Joel D. Crowther

A THESIS

Presented to the Faculty of

The Graduate College at the University of Nebraska

In Partial Fulfillment of Requirements

For the Degree of Master of Science

Major: Agronomy

Under the Supervision of

Professor Richard B. Ferguson and Professor Joe D. Luck

Lincoln, Nebraska

May, 2018

INTEGRATING MANAGEMENT ZONES AND CANOPY SENSING TO IMPROVE NITROGEN RECOMMENDATION ALGORITHMS

Joel Dewane Crowther, M.S.

University of Nebraska, 2018

Advisors: Richard B. Ferguson and Joe D. Luck

Fertilizer nitrogen use efficiency (NUE) in maize (*Zea mays* L.) production is historically inefficient, presenting significant environmental and economic challenges. Low NUE can be attributed to poor synchrony between soil N supply and crop demand, applying uniform rates of N fertilizer to spatially variable landscapes, and failure to account for temporal variability in crop response to N. Innovative N management strategies, including crop canopy sensing and management zones (MZ), are tools that have proven useful in increasing NUE. Several researchers have proposed that the integration of these two approaches may result in further improvements in NUE and in profitability by synthesizing both crop- and soil-based information for more robust N management. The objectives of this research were to identify soil and topographic variables that could be used to delineate MZ that appropriately characterize areas with differential crop response to N fertilizer and then to test a sensor-based N application algorithm and evaluate the potential of an integrated MZ- and sensor-based approach compared to uniform N management and to sensor-based N management alone. Management zones delineated with a field-specific approach were able to appropriately characterize the spatial variability in in-season crop response to N in all eight fields and in yield response to N in three of six fields. Sensor-based application resulted in significantly increased NUE compared to uniform N

management in six of eight fields, and marginal net return was significantly increased in four of eight fields. Delineated MZ appropriately classified areas of differing NUE in six of eight fields. Results from these studies indicate that integrating field-specific MZ and sensor-based N application has potential to increase NUE and profitability compared to sensor-based or MZ-based N management approaches alone. Additional research is needed to explore how to best incorporate static soil information into a sensor-based algorithm that can be generalized for a variety of soil, climatic, and managerial factors.

ACKNOWLEDGEMENTS

I would first like to thank my advisors, Joe Luck and Richard Ferguson, for their guidance, friendship, and unwavering trust in me. Despite their busy schedules, their doors were always open to me. Their confidence in me inspired confidence in myself as they granted me responsibilities few graduate students receive. I am also grateful to Tim Shaver for his support as a member of my supervisory committee.

I enjoyed immensely the opportunity to interact daily with my fellow graduate student and great friend, John Parrish. I have never worked with a more capable and hard-working person. We shared many stories and laughs while driving almost 50,000 road miles and several hundred field miles together these two years. From repairing the Veris on a frozen, windy morning to wrapping up a fertilizer application on a humid summer evening lit with fireflies, the experiences we have shared will not soon be forgotten.

I am grateful to the rest of the Project SENSE team—Brian Krienke, Dean Krull, Laura Thompson, Troy Ingram, Nathan Mueller, Keith Glewen, and Taro Mieno—for their support. Their wisdom and experience have made me a better scientist, and their humor during meetings and field days made for an enjoyable two years.

I am thankful to have been able to interact with other excellent graduate students and faculty, including Leonardo Bastos, Rachel Stevens, Bijesh Maharjan, Dennis McCallister, Dinesh Panday, Mohammed Naser, and Amanda Sanford in classes, lab meetings, and hallway conversations.

Thank you to the USDA National Institute of Food and Agriculture and UNL CASNR for providing the assistantship which allowed me to study at UNL. I am also grateful to the dozens of farmers and extension personnel with whom I interacted as a member of Project SENSE. Special thanks go to Cole Anderson, Brandon Hunnicutt, Paul Jarecke, Justin Krafka, Jenny Rees, Ken Seim, Glen Slater, and Lynn Yates, all of whom embody the phrase: “Nebraska Nice”. Your kindness to an outsider will be fondly remembered.

Most importantly, I thank my wife, Cindi, for her unwavering patience, love, and support throughout our time in Nebraska. She is always there when I need comfort or advice, and I could not have done this without her support. Hannah, our Nebraska baby, has brought so much joy to my life, and providing for her future has made this all worth it. I love you both!

Finally, I thank God for the blessings and opportunities He has provided me and for His guiding hand in my life. “I can do all things through Christ which strengtheneth me” (Philip. 4:13).

TABLE OF CONTENTS

List of Figures and Tables

List of Appendices

List of Equations

List of Abbreviations

AOI	Area-of-interest
CEC	Cation-exchange capacity
DEM	Digital Elevation Model
EC_a	Apparent electrical conductivity
EC_s	Shallow apparent electrical conductivity
EC_d	Deep apparent electrical conductivity
$Elev_{rel}$	Relative elevation
EONR	Economic optimum nitrogen rate
FPI	Fuzziness Performance Index
GPS	Global positioning system
GWP	Global warming potential
LSD	Least significant difference
MZ	Management zones
MZA	Management Zone Analyst
N	Nitrogen
N_2O	Nitrous oxide
NCE	Normalized Classification Entropy
NDRE	Normalized Difference Red Edge
NDVI	Normalized Difference Vegetation Index
NeDNR	Nebraska Department of Natural Resources
NH_3	Ammonia
NIR	Near-infrared
NO_3^-	Nitrate
N_{OPT}	Optimum nitrogen rate
NUE	Nitrogen use efficiency
P	Phosphorus
PFP_N	Partial factor productivity of applied nitrogen
R^2	Coefficient of determination
RCBD	Randomized complete block design
RE	Red edge
RMSE	Root mean square error
S	Sulfur
SI	Sufficiency Index
SOM	Soil organic matter
SR_{soil}	Simple ratio of soil optical reflectance
UAN	Urea ammonium nitrate
UTM	Universal Transverse Mercator
VI	Vegetation index

CHAPTER 1: A REVIEW OF CURRENT LITERATURE

Introduction

Nitrogen (N) is an essential for plant growth and is the nutrient that most often limits crop production (Lahda et al., 2005). Maize (*Zea mays* L.) requires high amounts of N, and consequently, applications of N fertilizer are generally required to achieve optimal yields. In 2015, worldwide demand for N fertilizer was over 110 million Mg (FAO, 2017).

Maize is the most widely grown crop in the US, with an estimated 36.8 million ha planted in 2017 (USDA NASS, 2017). It is also the largest user of N, accounting for around 40% of N fertilizer consumption in the US (Ribaudo et al., 2012). For this reason, maize is often the target of environmental impact policies where N is concerned (Snyder, 2012).

Crop fertilizer N use is historically inefficient. Estimates of maize N use efficiency (NUE) range from 35 to 75% (Morris et al., 2018). Applied N fertilizer that is not taken up by the crop or that is immobilized by soil microbes is subject to numerous loss mechanisms, including denitrification, volatilization, and leaching (Cassman et al., 2002). Nitrogen can also be lost from the plant as ammonia (NH_3) (Francis et al., 1993).

Low NUE over time has resulted in severe environmental consequences. Nitrogen loading from agricultural activity in the Mississippi-Atchafalaya River Basin has contributed to a continually expanding hypoxic zone in the Gulf of Mexico (Goolsby et al., 2001; Rabalais et al., 2001; Ribaudo et al., 2011). Increased loadings of N and phosphorus (P) have substantially altered the estuarine ecosystem of Chesapeake Bay

(Boesch et al., 2001). Surplus above-ground N also dramatically increases emissions of nitrous oxide (N_2O), a potent greenhouse gas (van Groenigen et al., 2010).

Closer to the source of maize production, over-application of N fertilizer has resulted in nitrate (NO_3^-) contamination of groundwater (Schepers et al., 1991; Ferguson, 2015). Many areas in the US have surpassed the maximum NO_3^- contaminant level of 10 $mg \cdot L^{-1}$ set by the US Environmental Protection Agency (Compton et al., 2011). Groundwater contaminated with NO_3^- poses a number of health risks, including Blue Baby syndrome in infants (Rubin et al., 2016). One source estimates that US $\$0.16 \cdot kg\ N^{-1}$ would be required to treat NO_3^--contaminated drinking water (Compton et al., 2011).

Causes of Low NUE

One of the major causes of low NUE in maize production is poor synchrony between soil N supply and crop demand (Shanahan et al., 2008). Cassman et al. (2002) estimated that around 75% of N fertilizer is applied prior to planting, including during the previous fall. This results in high levels of inorganic N in the soil profile, well before the stage of rapid crop uptake, and presents increased opportunity for N losses. In-season applications of N fertilizer coincide with the period of rapid uptake and therefore have great potential to increase NUE (Fageria and Baligar, 2005).

Another factor contributing to low NUE is failure to account for spatial variability by applying uniform rates of fertilizer N to spatially variable landscapes. Numerous field studies have shown that N supply within a field can be highly spatially variable (Reuss et al., 1977; Scharf et al., 2005; Shahandeh et al., 2005). Nitrogen mineralization of soil organic matter (SOM) can vary according to differences in soil temperature, water

availability, and local topography (Mahmoudjafari et al., 1997; Timlin et al., 1998). This results in spatial differences in the economic optimum N rate (EONR) within fields (Mamo et al., 2003). Scharf et al. (2005) found high within-field variability in EONR in a study of eight maize fields. Among the fields, median EONR varied between 63 and 208 $kg \cdot ha^{-1}$, with an average standard deviation of 58 $kg \cdot ha^{-1}$. In addition, EONR ranged from 0 to 280 $kg \cdot ha^{-1}$, the complete range of N rates, in five of eight fields. Soil texture also has a great influence on spatial variability in EONR (Shahandeh et al., 2011). Roberts et al. (2010) found that greater variability in EONR was measured in alluvial and loess soils than in claypan soils.

Producers typically apply enough N to meet the crop requirements of the most N-limiting areas of a field, resulting in frequent over-application of N fertilizer (Scharf et al., 2005). As such, there is a greater risk for N loss in areas of the field requiring less N (Shanahan et al., 2008). Variable-rate technology allows for site-specific management of N fertilizer, and has great potential to increase NUE. Mamo et al. (2003) found that variable-rate N applications would have resulted in 75 $kg \cdot ha^{-1}$ less N being applied than by applying a uniform rate, resulting in an economic benefit of $\$23 \cdot ha^{-1}$ compared to the uniform rate.

Further adding to the complexity, N requirement varies not only spatially, but also among years. Climate and management interactions result in high temporal variability in EONR and in crop yields (Cassman et al, 2002; Tremblay et al., 2012). Temporal variability in response to N has been documented in several studies (Mamo et al., 2003; Lambert et al., 2006; Dhital and Raun, 2016). Nitrogen is more susceptible than other

plant nutrients to hydrologic conditions, which are affected by annual precipitation and topography interactions. This subsequently affects mineralization of SOM, denitrification, and water availability. Sogbedji et al. (2001) found strong year-to-year variation in maize response to N. Annual field-averaged EONRs had a range of 65 $kg \cdot ha^{-1}$, with lower rates being highly associated with low early-season precipitation. Collectively, both spatial and temporal variability make accurate estimation of EONR difficult for many fields.

Management Zones

One method of accounting for within-field variability in crop N requirement is the practice of delineating management zones (MZ). Doerge (1999) defined MZ as "sub-regions of a field that express a homogeneous combination of yield-limiting factors for which a single crop input is appropriate to attain maximum efficiency of farm inputs". The concept of "farming by soil" (Larson and Robert, 1991) began during the mid-1980s by promoting the management of farm inputs by soil mapping unit (Mulla and Miao, 2016). However, researchers soon realized that considerable variability was present at scales finer than soil mapping units (Mulla et al., 1992; Franzen et al., 2002).

Myriad approaches to MZ delineation have been developed in the last 25 years. Khosla et al. (2010) reported that 162 delineation methods using 42 unique properties were used, either individually or in combination, in over 100 refereed publications published between 1992 and 2008. The most common approach to MZ delineation is the use of proximal soil sensing to measure soil apparent electrical conductivity (EC_a) (Khosla et al., 2010).

Several researchers have reported success in relating soil EC_a to variation in crop production (Kitchen et al., 1999; Corwin and Lesch, 2003; Bronson et al., 2005; Moral et al., 2010). Fleming et al. (2004) used soil EC_a alone for MZ delineation and found that it consistently identified areas of differing productivity across a field. When used in conjunction with other soil and crop properties, even greater prediction of variation in productivity is possible (Khosla et al., 2010). On-the-go sensors for mapping of soil EC_a use either electrical resistivity or electromagnetic induction methods, and several sensing systems are commercially available (Veris Technologies, Salina, KS; Geonics, Mississauga, ON, Canada; Dualem, Milton, ON, Canada). Mapping soil EC_a is an attractive method because it provides continuous, high-resolution data in real-time to map spatial patterns in field productivity (Mulla, 2013).

Measures of landscape attributes are also commonly used for MZ delineation. Topography is one of the five soil-forming factors (Jenny, 1941) and is often the only factor to vary significantly within many fields (Franzen et al., 2002). Topography affects crop yield by influencing the redistribution of soil particles, SOM, and soil nutrients through erosion and/or deposition (Kravchenko and Bullock, 2000). It also affects water availability both vertically and horizontally on the landscape. Hanna et al. (1982) found a significant effect of landscape position on water availability. Elevation and its derivatives, including slope and curvature, have commonly been used in conjunction with soil EC_a maps for MZ delineation (Fraisse et al., 2001; Schepers et al., 2004; Derby et al., 2007) or to enhance soil survey map units (Bobryk et al., 2016).

Soil organic matter has a large impact on soil N supply and is therefore another potential attribute for MZ classification. However, SOM can vary widely within fields, and often obtaining enough samples to accurately characterize field variability through traditional soil sampling and laboratory analysis is laborious cost prohibitive (Adamchuk et al., 2011). Historically, researchers have used bare soil imagery obtained from satellite or aerial remote sensing platforms to characterize soil variability by soil color, or reflectance in the visible region of the electromagnetic spectrum (Adamchuk et al., 2004). These have been used as predictors of SOM to delineate management zones with some success (Varvel et al., 1999; Chen et al., 2000; Stewart and McBratney, 2001; Schepers et al., 2004). However, bare soil imagery is becoming difficult to obtain given the increase in conversion to conservation tillage systems. Of the 112.8 million cropland hectares in the US, 62.1% use conservation tillage (USDA NASS, 2012).

Soil organic matter content, among other soil properties, is known to have a strong influence on soil reflectance, particularly in the visible (400-700 nm) and near-infrared (NIR) (750-1400 nm) regions of the electromagnetic spectrum (Baumgardner et al., 1985). An optical sensor developed by Veris Technologies (Salina, KS) provides an on-the-go measurement of SOM content using near infrared reflectance spectroscopy (NIRS). This technique measures diffusely scattered light from an illuminated sample (Christy, 2008). As SOM content increases, soil reflectance decreases throughout the visible and NIR spectrum (Baumgardner et al., 1985). The spectral response of the soil at a depth of ~5 cm is recorded in two wavelengths, one in the visible red region and one in

the NIR. This spectral data is then calibrated to estimate SOM using soil samples collected from representative areas in the field (Christy, 2008).

Numerous also are the statistical methods used to classify MZ. These include the ISODATA method (Fraisse et al., 2001; Guastaferro et al., 2010), non-parametric approaches (Aggelopooulou et al., 2013), a hierarchical approach (Fleming et al., 2000), and the fuzzy *c*-means (or *k*-means) method (Minasny and McBratney, 2002; Fridgen et al., 2004). Management Zone Analyst (MZA) (University of Missouri, USDA-ARS, Columbia, MO) is a free software program that uses a fuzzy *c*-means algorithm for clustering. In addition to ease of use, MZA has the advantage of providing results for a range of clusters so that the user can evaluate how many MZ should be used (Fridgen et al., 2004).

Managing N through the use of MZ often improves efficiency compared to uniform field management by helping to characterize the spatial variability in soil physical and chemical properties. However, MZ are often inconsistent in characterizing the spatial variability in crop N requirement because of the effect of temporal variability on crop N response (Shanahan et al., 2008). In a five-year study in Nebraska, Schepers et al. (2004) found temporal variability to greatly affect MZ, and the use of MZ to direct variable N application would have been appropriate in only three of five years. They concluded that a static, soil-based MZ approach alone is likely inadequate for directing variable applications of N due to the inability to account for temporal variability.

Crop Canopy Sensing

One tool with the potential to manage all three factors influencing low NUE is crop canopy sensing. This strategy is known as a reactive approach to N fertilizer management because the sensors can identify and correct N stress that has already occurred during the growing season (Ping et al., 2008; Shanahan et al., 2008). Rather than using indirect measures of growing condition from the soil or from atmospheric conditions, canopy sensors use the crop itself as a bio-indicator to assess crop N status and direct real-time, variable-rate, in-season applications of N fertilizer (Adamchuk et al., 2011). Sensor-based N management is better able to account for spatial and temporal variability and also helps to achieve greater synchrony between N supply and crop N demand, as the majority of N fertilizer is applied in-season during the period of rapid N uptake. Canopy sensors have been used successfully to direct in-season variable-rate N fertilizer applications in several crops, including maize (Scharf and Lory, 2009; Holland and Schepers, 2010), wheat (*Triticum aestivum* L.) (Raun et al., 2005; Solie et al., 2012), cotton (*Gossypium hirsutum* L.) (Oliveira et al., 2013; Raper and Varco, 2015), rice (*Oryza sativa* L.) (Tubaña et al., 2012; Xue et al., 2014), and sugarcane (*Saccharum* spp.) (Amaral et al., 2015).

Crop canopy sensors make use of the relationship between leaf and canopy reflectance to crop response to make quantitative estimates of in-season N requirement (Hatfield et al., 2008). As electromagnetic radiation is incident upon a plant, much of that radiation is absorbed for photosynthesis, especially in the visible region. Radiation not absorbed by the plant is reflected, and this reflectance can be measured by optical

sensors. In the visible region, reflectance is strongly correlated to plant pigments, primarily chlorophyll. As leaf chlorophyll content increases, reflectance in the visible wavelengths decreases, especially in the visible blue (400-500 nm) and visible red (600-700 nm) regions (Hatfield et al., 2008). Very little incident radiation in the NIR region is absorbed by crop leaves due to scattering by the leaf mesophyll cells (Walter-Shea et al., 1991). As such, NIR reflectance tends to increase with increased biomass and crop vigor. Given that N affects these properties, N sufficiency is strongly related to canopy reflectance, especially in the visible red (600-700 nm) and NIR regions (Walburg et al., 1982).

Many commercially-available canopy sensing systems use active sensor technology. Active sensors work by emitting modulated light in two or more wavelengths in the visible and NIR regions. This polychromatic light source simultaneously emits light from each wavelength, and photodetectors within the sensor then measure the reflectance from the crop canopy. Using a single light source reduces errors associated with drift in irradiance (Holland et al., 2004), and using the modulated light source as opposed to a passive sensor system allows the sensor to differentiate between natural background light and the sensor-emitted light (Barker and Sawyer, 2013).

To make use of canopy reflectance information, a number of vegetation indices (VIs) have been developed that combine reflectance in two or more regions of the electromagnetic spectrum. One of the first and most widely used VIs is the Normalized Difference Vegetation Index (NDVI), which has the following equation (Rouse et al., 1973):

$$NDVI = \frac{R_{NIR} - R_{RED}}{R_{NIR} + R_{RED}} \quad [1.1]$$

where

R_{NIR} = near-infrared reflectance

R_{RED} = red reflectance

NDVI has been used to direct in-season variable-rate N fertilizer applications with some success (Raun et al., 2005; Samborski et al., 2009; Kitchen et al., 2010). However, under high-biomass conditions, reflectance in the red region becomes saturated, and further increases in chlorophyll content do not affect reflectance (Gitelson and Merzlyak, 1996). The red-edge (700-740 nm) region does not suffer this saturation effect, and thus has been found to be a better predictor of chlorophyll content and canopy N status (Li et al., 2014; Holland and Schepers, 2010). The Normalized Difference Red Edge (NDRE) VI replaces red reflectance from NDVI with reflectance in the red-edge region (Gitelson and Merzlyak, 1994):

$$NDRE = \frac{R_{NIR} - R_{RE}}{R_{NIR} + R_{RE}} \quad [1.2]$$

where

R_{NIR} = NIR reflectance

R_{RE} = red-edge reflectance

In order to assess crop N status, canopy reflectance of plants yet to be fertilized is compared to reflectance from plants receiving an adequate amount of N fertilizer such that N is not a limiting factor (Schepers et al., 1992; Shanahan et al., 2008). This N-sufficient reference is used to calculate a Sufficiency Index (SI) with the following equation (Peterson et al., 1993; Varvel et al., 1997):

$$SI = \frac{VI_{Target}}{VI_{Reference}} \quad [1.3]$$

where

$0 \leq SI \leq 1$

VI_{Target} = vegetation index of target crop

$VI_{Reference}$ = vegetation index of high-N reference

Essentially, lower SI values signify that unfertilized plants are more deficient, and so will require more N fertilizer to achieve their yield potential (Shanahan et al., 2008).

Establishing a high-N reference area in the field can be problematic. The reference area must be moved to a new area of the field each year in order to accurately represent the nutrient status of the rest of the field each year (Holland and Schepers, 2013). In addition, applying high amounts of N fertilizer is restricted in some countries or situations (Holland and Schepers, 2013). Furthermore, this approach can cause a nutrient imbalance between N and sulfur (S) and increase the severity of S deficiency in maize, resulting in artificially low VI values and correspondingly low fertilizer N recommendations (Franzen et al., 2016b). One alternative to the high-N reference method

is the use of a statistical approach, known as a virtual reference, to identify adequately fertilized plants without the need for applying high amounts of N fertilizer in an area the field (Holland and Schepers, 2013). This procedure involves sensing a portion of the field, observing a wide range of plant vigor and N status. The 95th percentile value is selected from a histogram of VI values, and this value is used as $VI_{Reference}$ to generate SI in equation 1.3.

Numerous algorithms have been developed to convert sensor reflectance data into an in-season N fertilizer application rate (Solari et al., 2010; Scharf et al., 2011; Solie et al., 2012; Franzen et al., 2014). Holland and Schepers (2010) developed a generalized N application algorithm for use with crop canopy sensors. They describe the plant growth function as a typical N rate by yield response function (quadratic or quadratic plateau) (Franzen et al., 2016a). The algorithm uses an estimated optimum N rate (N_{OPT}) along with the calculated SI to control the model. It also allows for incorporating economics into the N_{OPT} term and accounts for fertilizer N already applied as well as any N credits. The final form of the algorithm is as follows (Holland and Schepers, 2010):

$$N_{APP} = (MZ_i \cdot N_{OPT} - N_{PreFert} - N_{CRD} + N_{COMP}) \cdot \sqrt{\frac{(1-SI)}{\Delta SI}} \qquad [1.4]$$

where

N_{APP} = nitrogen application rate

MZ_i = MZ scalar; $i \in \{1,2,3,..,n\}$ zones and $0 \leq MZ_i \leq 2$

N_{OPT} = EONR or the maximum N rate prescribed by producers

$N_{PreFert}$ = Total fertilizer N applied before sensor-based N application

N_{CRD} = N credit for previous crop, NO_3^- in irrigation water, manure, etc.

N_{COMP} = N in excess of N_{OPT} required by the crop under soil-limiting conditions at a given growth stage

SI = Sufficiency Index of target crop

$\Delta SI = 1 - SI(0)$; the difference between $SI = 1$ and the *y*-intercept of the N response curve

There are several commercially-available active crop canopy sensing systems, including GreenSeeker (NTech Industries, Ukiah, CA), OptRx (Ag Leader Technology, Ames, IA), CropSpec (Topcon Positioning Systems, Olathe, KS), and N-Sensor ALS (Yara, Oslo, Norway).

The use of these systems to direct variable-rate, in-season N fertilizer applications in cereal cropping systems has resulted in positive environmental and economic returns (Kitchen et al., 2010; Roberts et al., 2010). Raun et al. (2002) experimented with sensor-based N application in wheat and found that, averaged over locations, NUE was improved by >15% when compared with traditional uniform practices. The savings in fertilizer N with similar grain yield had a value of >\$25·ha^{-1}. Scharf et al. (2011) conducted fifty-five replicated on-farm experiments in maize comparing sensor-based variable-rate N application to uniform producer-selected rates. Relative to the uniform rate, sensor-based management increased partial profit by \$42·ha^{-1}, and applied N was reduced by 16 kg·ha^{-1}. Li et al. (2016) modeled the long-term environmental benefits of sensor-based N fertilization and found that, when compared with uniform application, sensor-based management can significantly decrease both gaseous and aqueous N losses.

Total N fertilizer use was reduced by 11% with no significant reduction in grain yield. Variable-rate fertilization mitigated soil N_2O emissions, volatilized NH_3 loss, and NO_3^- leaching by 10, 23, and 16%, respectively. When considering emissions associated with farm input production, variable-rate N management resulted in 10% less global warming potential (GWP), 22% less acidification potential, and 16% less eutrophication potential than the producer-chosen uniform rate.

Integrated Soil-Based MZ and Canopy Sensing Approach

Crop canopy sensors and their corresponding algorithms are not without their limitations. With no direct knowledge of the soil and topographic characteristics underneath the growing crop, the sensor cannot accurately predict how spatial variability may affect future N mineralization or losses that are not expressed in the crop at the time of sensing. Areas of the field appearing to be highly N-deficient at the time of sensing receive correspondingly high in-season N rates, but often this excess N is not utilized, as these areas may simply have lower yield potential due to soil and topographic factors. This lack of soil-based information has resulted in poor algorithm performance in certain subfield regions due to local spatial variability (Ferguson, unpublished data, 2015). Researchers agree that refinements are needed in order to account for additional soil, climatic, and managerial factors (Shanahan et al., 2008; Stevens, 2014; Bean, 2016), combining both anticipatory and reactive decision-making (Ping et al., 2008). Schepers et al. (2004) and others (Holland and Schepers, 2010; Solari et al., 2008) have suggested combining MZ and in-season crop canopy sensing to better predict EONR throughout the field and achieve greater NUE.

Roberts et al. (2012) experimented with an integrated MZ and canopy sensor approach on six irrigated fields in Nebraska, USA. They found potential for this integrated approach to increase NUE and economic return over current management practices, particularly in silt loam fields with eroded slopes. However, they believed additional research was needed to further refine current algorithms and explore how to best integrate the two N management strategies. Furthermore, they advocated for additional similar field studies to establish a consistent set of variables for use in MZ delineation.

Research Objectives

The objectives of this master's research were to:

1. Identify soil and topographic variables that are related to in-season canopy reflectance and yield for soil-based MZ delineation.
2. Determine if delineated MZ can identify areas with differential crop response to N fertilizer.
3. Test a sensor-based N application algorithm compared to uniform N management in a variety of soil conditions.
4. Evaluate the potential of an integrated MZ- and sensor-based N management approach to sensor-based N management alone.

References

Adamchuk, V.I., J.W. Hummel, M.T. Morgan, and S.K. Upadhaya. 2004. On-the-go soil sensors for precision agriculture. Comput. Electron. Agric. 44:71-91.

Adamchuk, V.I., R.A. Viscarra Rossel, K.A. Sudduth, and P.S. Lammers. 2011. Sensor fusion for precision agriculture. In: Thomas, C. (Ed.), *Sensor Fusion—Foundation and Applications.* (pp. 27-40). Rijeka, Croatia: InTech.

Aggelopooulou, K., A. Castrignanò, T. Gemtos, and D. De Benedetto. 2013. Delineation of management zones in an apple orchard in Greece using a multivariate approach. Comput. Electron. Agric. 90:119-130.

Amaral, L.R., J.P. Molin, and J.S. Schepers. 2015. Algorithm for variable-rate nitrogen application in sugarcane based on active crop canopy sensor. Agron. J. 107:1513-1523.

Barker, D.W., and J.E. Sawyer. 2013. Factors affecting active canopy sensor performance and reflectance measurements. Soil Sci. Soc. Am. J. 77:1673-1683.

Baumgardner, M.F., L.F. Silva, L.L. Biehl, and E.R. Stoner. 1985. Reflectance properties of soils. Adv. Agron. 38:1-44.

Bean, G.M. 2016. Canopy sensing algorithm performance and modification using soil and weather information. MS thesis, Univ. Missouri, Columbia.

Bobryk, C.W., D.B. Myers, N.R. Kitchen, J.F. Shanahan, K.A. Sudduth, S.T. Drummond, B. Gunzenhauser, and N.N. Gomez Raboteaux. 2016. Validating a digital soil map with corn yield data for precision agriculture decision support. Agron. J. 108:957-965.

Boesch, D.F., R.B. Brinsfield, and R.E. Magnien. 2001. Chesapeake Bay eutrophication: Scientific understanding, ecosystem restoration, and challenges for agriculture. J. Environ. Qual. 30:303-320.

Bronson, K.F., J.D. Booker, S.J. Officer, R.J. Lascano, S.J. Maas, S.W. Searcy, and J. Booker. 2005. Apparent electrical conductivity, soil properties and spatial covariance in the U.S. Southern High Plains. Precis. Agric. 6:297-311.

Cassman, K.G., A.R. Dobermann, and D.T. Walters. 2002. Agroecosystems, nitrogen-use efficiency, and nitrogen management. Ambio. 31:132-140.

Chen, F., D.E. Kissel, L.T. West, and W. Adkins. 2000. Field-scale mapping of surface soil organic carbon using remotely sensed imagery. Soil Sci. Soc. Am. J. 64:746-753.

Christy, C.D. 2008. Real-time measurement of soil attributes using on-the-go near infrared reflectance spectroscopy. Comput. Electron. Agric. 61:10-19.

Compton, J.E., J.A. Harrison, R.L. Dennis, T.L. Greaver, B.H. Hill, S.J. Jordan, H. Walker, and H.V. Campbell. 2011. Ecosystem services altered by human changes in the nitrogen cycle: A new perspective for US decision making. Ecol. Lett. 14:804-815.

Corwin, D.L., and S.M. Lesch. 2003. Application of soil electrical conductivity to precision agriculture: Theory, principles, and guidelines. Agron. J. 95:455-471.

Derby, N.E., F.X.M. Casey, and D.W. Franzen. 2007. Comparison of nitrogen management zone delineation methods for corn grain yield.

Dhital, S., and W.R. Raun. 2016. Variability in optimum nitrogen rates for maize. Agron. J. 108:2165-2173.

Doerge, T. 1999. Defining management zones for precision farming. Crop Insight. 8:21. Pioneer Hi-Bred International, Inc.

Fageria, N.K., and V.C. Baligar. 2005. Enhancing nitrogen use efficiency in crop plants. Adv. Agron. 88:97-185.

Ferguson, R.B. 2015. Groundwater quality and nitrogen use efficiency in Nebraska's Central Platte River Valley. J. Environ. Qual. 44:449-459.

Fleming, K.L., D.F. Heermann, and D.G. Westfall. 2004. Evaluating soil color with farmer input and apparent soil electrical conductivity for management zone delineation. Agron J. 96:1581-1587.

Food and Agriculture Organization of the United Nations (FAO). 2017. World fertilizer trends and outlook to 2020. [Online]. Available at http://www.fao.org/publications/card/en/c/cfa19fbc-0008-466b-8cc6-0db6c6686f78 (verified 30 August 2017).

Fraisse, C.W., K.A. Sudduth, and N.R. Kitchen. 2001. Delineation of site-specific management zones by unsupervised classification of topographic attributes and soil electrical conductivity. Transactions of the ASAE. 44:155-166.

Francis, D.D., J.S. Schepers, and M.F. Vigil. 1993. Post-anthesis nitrogen loss from corn. Agron. J. 85:659-663.

Franzen, D.W., D.H. Hopkins, M.D. Sweeney, M.K. Ulmer, and A.D. Halvorson. 2002. Evaluation of soil survey scale for zone development of site-specific nitrogen management. Agron J. 94:381-389.

Franzen, D., N. Kitchen, K. Holland, J. Schepers, and W. Raun. 2016a. Algorithms for in-season nutrient management in cereals. Agron. J. 108:1775-1781.

Franzen, D., L.K. Sharma, and H. Bu. 2014. Active optical sensor algorithms for corn yield prediction and a corn side-dress nitrogen rate aid. NDSU Circ. SF1176-5, North Dakota State Univ. Ext. Serv., Fargo, ND.

Franzen, D.W., L.K. Sharma, H. Bu, and A. Denton. 2016b. Evidence for the ability of active-optical sensors to detect sulfur deficiency in corn. Agron. J. 108:2158-2162.

Fridgen, J.J., N.R. Kitchen, K.A. Sudduth, S.T. Drummond, W.J. Wiebold, and C.W. Fraisse. 2004. Management Zone Analyst (MZA): Software for subfield management zone delineation. Agron. J. 96:100-108.

Gitelson, A.A., and M.N. Merzlyak. 1994. Quantitative estimation of chlorophyll-a using reflectance spectra: Experiments with autumn chestnut and maple leaves. J. Photochem. Photobiol. 22:247-252.

Gitelson, A.A., and M.N. Merzlyak. 1996. Signature analysis of leaf reflectance spectra: Algorithm development for remote sensing of chlorophyll. J. Plant. Physiol. 148:494-500.

Goolsby, D.A., W.A. Battaglin, B.T. Aulenbach, and R.P. Hooper. 2001. Nitrogen input to the Gulf of Mexico. J. Environ. Qual. 30:329-336.

Guastaferro, F., A. Castrignanò, D. De Benedetto, D. Sollitto, A. Troccoli, and B. Cafarelli. 2010. A comparison of different algorithms for the delineation of management zones. Precis. Agric. 11:600-620.

Hanna, A.Y., P.W. Harlan, and D.T. Lewis. 1982. Soil available water as influenced by landscape position and aspect. Agron. J. 74:999-1004.

Hatfield, J.L., A.A. Gitelson, J.S. Schepers, and C.L. Walthall. 2008. Application of spectral remote sensing for agronomic decisions. Agron. J. 100:117-131.

Holland, K.H., and J.S. Schepers. 2010. Derivation of a variable rate nitrogen application model for in-season fertilization of corn. Agron. J. 102:1415-1424.

Holland, K.H., and J.S. Schepers. 2013. Use of a virtual-reference concept to interpret active crop canopy sensor data. Precis. Agric. 14:71-85.

Holland, K.H., J.S. Schepers, J.F. Shanahan and G.L. Horst. 2004. Plant canopy sensor with modulated polychromatic light source. pp. 148-160. *In* D.J. Mulla, (ed.) Proc. 7th International Conference on Precision Agriculture and Other Precision Resources Management, Minneapolis, MN, 25-28 July.

Jenny, H. 1941. Factors of soil formation. New York, NY: McGraw-Hill Book Co.

Johnson, C.K., D.A. Mortensen, B.J. Wienhold, J.F. Shanahan, and J.W. Doran. 2003. Site-specific management zones based on soil electrical conductivity in a semiarid cropping system. Agron. J. 95:303-315.

Khosla, R., D.G. Westfall, R.M. Reich, J.S. Mahal, and W.J. Gangloff. 2010. Spatial variation and site-specific management zones. *In* M.A. Oliver (Ed.),

Geostatistical applications in precision agriculture (pp. 195-219). New York, NY: Springer.

Kitchen, N.R., K.A. Sudduth, and S.T. Drummond. 1999. Soil electrical conductivity as a crop productivity measure for claypan soils. J. Prod. Agric. 12:607-617.

Kitchen, N.R., K.A. Sudduth, S.T. Drummond, P.C. Scharf, H.L. Palm, D.F. Roberts, and E.D. Vories. 2010. Ground-based canopy reflectance sensing for variable-rate nitrogen corn fertilization. Agron. J. 102:71-84.

Kravchenko, A.N., and D.G. Bullock. 2000. Correlation of corn and soybean grain yield with topography and soil properties. Agron J. 92:75-83.

Ladha, J.K., H. Pathak, T.J. Krupnik, J. Six, and C. van Kessel. 2005. Efficiency of fertilizer nitrogen in cereal production: Retrospects and prospects. Adv. Agron. 87:85-156.

Lambert, D.M., J. Lowenberg-DeBoer, and G.L. Malzer. 2006. Economic analysis of spatial-temporal patterns in corn and soybean response to nitrogen and phosphorus. Agron. J. 98:43-54.

Larson, W.E., and P.C. Robert. 1991. Farming by soil. *In* R. Lal and F.J. Pierce (Eds.), *Soil management for sustainability* (pp. 103-112). Ankeny, IA: Soil and Water Conserv. Soc.

Li, A., B.D. Duval, R. Anex, P. Scharf, J.M. Ashtekar, P.R. Owens, and C. Ellis. 2016. A case study of environmental benefits of sensor-based nitrogen application in corn. J. Environ. Qual. 45:675-683.

Li, F., Y. Miao, G. Feng, F. Yuan, S. Yue, X. Gao, Y. Liu, B. Liu, S. Ustin, X. Chen. 2014. Improving estimation of summer maize nitrogen status with red edge-based spectral vegetation indices. Field Crops Res. 157:111-123.

Mahmoudjafari, M., G.J. Kluitenberg, J.L. Havlin, J.B. Sisson, and A.P. Schwab. 1997. Spatial variability of nitrogen mineralization at the field scale. Soil Sci. Soc. Am. J. 61:1214-1221.

Mamo, M., G.L. Malzer, D.J. Mulla, D.R. Huggins, and J. Strock. 2003. Spatial and temporal variation in economically optimum nitrogen rate for corn. Agron. J. 95:958-964.

Minasny, B., and A.B. McBratney. 2002. FuzME version 3.0. Australian Centre for Precision Agriculture. The University of Sidney, Australia.

Moral, F.J., J.M. Terrón, and J.R. Marques da Silva. 2010. Delineation of management zones using mobile measurements of soil apparent electrical conductivity and multivariate geostatistical techniques. Soil Tillage Res. 106:335-343.

Morris, T.F., T.S. Murrell, D.B. Beegle, J.J. Camberato, R.B. Ferguson, J. Grove, Q. Ketterings, P.M. Kyveryga, C.A.M. Laboski, J.M. McGrath, J.J. Meisinger, J. Melkonian, B.N. Moebius-Clune, E.D. Nafziger, D. Osmond, J.E. Sawyer, P.C. Scharf, W. Smith, J.T. Spargo, H.M. van Es, and H. Yang. 2018. Strengths and limitations of nitrogen rate recommendations for corn and opportunities for improvement. Agron. J. 110: 1-37.

Mulla, D. 2013. Twenty five years of remote sensing in precision agriculture: Key advances and remaining knowledge gaps. Biosyst. Eng. 114:358-371.

Mulla, D.J., A.U. Bhatti, M.W. Hammond, and J.A. Benson. 1992. A comparison of winter wheat yield and quality under uniform versus spatially variable fertilizer management. Agric. Ecosyst. Environ. 38:301-311.

Mulla, D., and Y. Miao. 2016. Precision farming. In P.S. Thenkabail (Ed.), *Land resources monitoring, modeling, and mapping with remote sensing*. pp. 161-178. Boca Raton, FL: CRC Press.

Oliveira, L.F., P.C. Scharf, E.D. Vories, S.T. Drummond, D. Dunn, W.G. Stevens, K.F. Bronson, N.R. Benson, V.C. Hubbard, and A.S. Jones. 2013. Calibrating canopy reflectance sensors to predict optimal mid-season nitrogen rate for cotton. Soil Sci. Soc. Am. J. 77:173-183.

Peterson, T.A., T.M. Blackmer, D.D. Francis, and J.S. Schepers. 1993. Using a chlorophyll meter to improve N management. NebGuide G93-1171-A. Coop. Ext. Serv., Univ. of Nebraska, Lincoln.

Ping, J.L., R. B. Ferguson, and A. Dobermann. 2008. Site-specific nitrogen and plant density management in irrigated maize. Agron. J. 100:1193-1204.

Rabalais, N.N., R.E. Turner, and W.J. Wiseman, Jr. 2001. Hypoxia in the Gulf of Mexico. J. Environ. Qual. 30:320-329.

Raper, T.B., and J.J. Varco. 2015. Canopy-scale wavelength and vegetative index sensitivities to cotton growth parameters and nitrogen status. Precis. Agric. 16:62-76.

Raun, W.R., J.B. Solie, G.V. Johnson, M.L. Stone, R.W. Mullen, K.W. Freeman, W.E. Thomason, and E.V. Lukina. 2002. Improving nitrogen use efficiency in cereal

grain production with optical sensing and variable rate application. Agron. J. 94:815-820.

Raun, W.R., J.B. Solie, M.L. Stone, K.L. Martin, K.W. Freeman, R.W. Mullen, H. Zhang, J.S. Schepers and G.V. Johnson. 2005. Optical sensor-based algorithm for crop nitrogen fertilization. Comm. Soil Sci. Plant Anal. 36:2759-2781.

Reuss, J.O., P.N. Soltanpour, and A.E. Ludwick. 1977. Sampling distribution of nitrates in irrigated fields. Agron. J. 69:588-592.

Ribaudo, M., J. Delgado, L. Hansen, M. Livingston, R. Mosheim, and J. Williamson. 2011. Nitrogen in agricultural systems: Implications for conservation policy. Economic Res. Rep. ERR-187. USDA, Washington, DC.

Ribaudo, M., Livingston, M., and J. Williamson. 2012. Nitrogen management on U.S. corn acres, 2001-10. U.S. Dept. of Agriculture, Economic Research Service. EB-20.

Roberts, D.F. 2009. An integrated crop- and soil-based strategy for variable-rate nitrogen management in corn. PhD dissertation, Univ. Nebraska, Lincoln.

Roberts, D.F., R.B. Ferguson, N.R. Kitchen, V.I. Adamchuk, and J.F. Shanahan. 2012. Relationships between soil-based management zones and canopy sensing for corn nitrogen management. Agron. J. 104:119-129. doi:10.2134/agronj2011.0044

Roberts, D.F., N.R. Kitchen, P.C. Scharf, and K.A. Sudduth. 2010. Will variable-rate nitrogen fertilization using corn canopy reflectance sensing deliver environmental benefits? Agron. J. 102:85-95.

Rouse, J.W., R.H. Haas, J.A. Schell, and D.W. Deering. 1973. Monitoring vegetation systems in the Great Plains with ERTS. Proc. Third Earth Resources Technology Satellite-1 Symposium, Goddard Space Flight Center, NASA SP-351, Science and Technical Information Office, NASA, Washington, DC, pp. 309-317.

Rubin, J.C., A.M. Struffert, F.G. Fernández, and J.A. Lamb. Maize yield and nitrogen use efficiency in upper Midwest irrigated sandy soils. Agron. J. 108:1681-1691.

Samborski, S.M., N. Tremblay and E. Fallon. 2009. Strategies to make use of plant sensors-based diagnostic information for nitrogen recommendations. Agron. J. 101:800-816.

Scharf, P.C., N.R. Kitchen, K.A. Sudduth, J.G. Davis, V.C. Hubbard, and J.A. Lory. 2005. Field-scale variability in optimal nitrogen fertilizer rate for corn. Agron. J. 97:452-461.

Scharf, P.C., and J.A. Lory. 2009. Calibrating reflectance measurements to predict optimal sidedress nitrogen rate for corn. Agron. J. 101:615-625.

Scharf, P.C., D.K. Shannon, H.L. Palm, K.A. Sudduth, S.T. Drummond, N.R. Kitchen, L.J. Mueller, V.C. Hubbard, and L.F. Oliveira. 2011. Sensor-based nitrogen applications out-performed producer-chosen rates for corn in on-farm demonstrations. Agron J. 103:1683-1691.

Schepers, A.R., J.F. Shanahan, M.A. Liebig, J.S. Schepers, S.H. Johnson, and A. Luchiari, Jr. 2004. Appropriateness of management zones for characterizing spatial variability of soil properties and irrigated corn yields across years. Agron. J. 96:195-203.

Schepers, J.S., D.D. Francis, M. Vigil, and F.E. Below. 1992. Comparison of corn leaf nitrogen and chlorophyll meter readings. Comm. Soil Sci. Plant Anal. 23:2173-2187.

Schepers, J.S., M.G. Moravek, E.E. Alberts, and K.D. Frank. 1991. Maize production impacts on groundwater quality. J. Environ. Qual. 20:12-16.

Shahandeh, H., A.L. Wright, and F.M. Hons. 2011. Use of soil nitrogen parameters and texture for spatially-variable nitrogen fertilization. Precis. Agric. 12:146-163.

Shahandeh, H., A.L. Wright, F.M. Hons, and R.J. Lascano. 2005. Spatial and temporal variation of soil nitrogen parameters related to soil texture and corn yield. Agron. J. 97:772-782.

Shanahan, J.F., N.R. Kitchen, W.R. Raun, and J.S. Schepers. 2008. Responsive in-season nitrogen management for cereals. Comput. Electron. Agric. 61:51-62.

Snyder, C.S. 2012. Are Midwest corn farmers over-applying fertilizer N? Better Crops Plant Food 96:3-4.

Sogbedji, J.M., H.M. van Es, S.D. Klausner, D.R. Bouldin, and W.J. Cox. 2001. Spatial and temporal processes affecting nitrogen availability at the landscape scale. Soil Tillage Res. 58:233-244.

Solari, F., J.F. Shanahan, R.B. Ferguson, and V.I. Adamchuk. 2010. An active sensor algorithm for corn nitrogen recommendations based on a chlorophyll meter algorithm. Agron. J. 102:1090-1098.

Solari, F., J. Shanahan, R. Ferguson, J. Schepers, and A. Gitelson. 2008. Active sensor reflectance measurements of corn nitrogen status and yield potential. Agron. J. 100:571-579.

Solie, J.B., A.D. Monroe, W.R. Raun, and M.L. Stone. 2012. Generalized algorithm for variable-rate nitrogen application in cereal grains. Agron. J. 104:378-387.

Stevens, L.J. 2014. A regional investigation of in-season nitrogen requirement for maize using model and sensor-based recommendation approaches. MS thesis, Univ. Nebraska, Lincoln.

Stewart, C.M., and A.B. McBratney. 2001. Using bare soil imagery to determine management zones for the variable-rate application of inputs for cotton. pp. 319-324. *In* G. Grenier and S. Blackmore (eds.) ECPA 2001: Proc. 3rd European Conf. on Precision Agriculture, Montpelier, France, 18-20 June. agro-Montpelier ENSAM, Montpelier, France.

Timlin, D.J., Y. Pachepsky, V.A. Snyder, and R.B. Bryant. 1998. Spatial and temporal variability of corn grain yield on a hillslope. Soil Sci. Soc. Am. J. 62:764-773.

Tremblay, N., Y.M. Bouroubi, C. Bélec, R.W. Mullen, N.R. Kitchen, W.E Thomason, S. Ebelhar, D. B. Mengel, W.R. Raun, D.D. Francis, E.D. Vories, and I. Ortiz-Monasterio. 2012. Corn response to nitrogen is influenced by soil texture and weather. Agron. J. 104:1658-1671.

Tubaña, B.S., D.L. Harrell, T. Walker, J. Teboh, J. Lofton and Y. Kanke. 2012. In-season canopy reflectance-based estimation of rice yield response to nitrogen. Agron. J. 104:1604-1611.

U.S. Department of Agriculture, National Agricultural Statistics Service (USDA NASS). 2017. Acreage. [Online]. Available at http://usda.mannlib.cornell.edu/MannUsda/viewDocumentInfo.do?documentID=1000 (verified 30 August 2017).

U.S. Department of Agriculture, National Agricultural Statistics Service (USDA NASS). 2012. Land use practices by size of farm: 2012. [Online]. Available at https://www.agcensus.usda.gov/Publications/2012/ (verified 13 September 2017).

van Groenigen, J.W., G.L. Velthof, O. Oenema, K.J. van Groenigen, and C. van Kessel. 2010. Towards an agronomic assessment of N_2O emissions: A case study for arable crops. Eur. J. Soil Sci. 61:903-913.

Varvel, G.E., J.S. Schepers, and D.D. Francis. 1997. Ability for in-season correction of nitrogen deficiency in corn using chlorophyll meters. Soil Sci. Soc. Am. J. 61:1233-1239.

Varvel, G.E., M.R. Schlemmer, and J.S. Schepers. 1999. Relationship between spectral data from aerial image and soil organic matter and phosphorus levels. Precis. Agric. 1:291-300.

Walburg, G., M.E. Bauer, C.S.T. Daughtry, and T.L. Housley. 1982. Effects of nitrogen nutrition on the growth, yield, and reflectance characteristics of corn canopies. Agron. J. 74:677-683.

Walter-Shea, E.A., J.M. Norman, B.L. Blad, and B.F. Robinson. 1991. Leaf reflectance and transmittance in soybean and corn. Agron. J. 83:631-636.

Xue, L., G. Li, X. Qin, L. Yang, and H. Zhang. 2014. Topdressing nitrogen recommendation for early rice with an active sensor in South China. Precis. Agric. 15:95-110.

CHAPTER 2: EVALUATING RELATIONSHIPS BETWEEN MANAGEMENT ZONES AND ACTIVE CROP CANOPY SENSING FOR IMPROVED NITROGEN MANAGEMENT IN MAIZE

ABSTRACT

Active crop canopy sensors and management zones (MZ) are two methods of directing variable-rate, in-season nitrogen (N) fertilizer applications in maize (*Zea mays* L.). Researchers have suggested that integrating these two approaches may result in improved performance of sensor-based N application algorithms through increased N use efficiency (NUE) and profitability. The objectives of this research study were to (1) identify soil and topographic variables that are related to in-season canopy reflectance and yield for soil-based MZ delineation and (2) determine if delineated MZ can identify areas with differential crop response to N fertilizer. Nitrogen ramp blocks containing six randomized N rates (0 to 280 kg·ha^{-1}, in 56 kg·ha^{-1} increments) were placed end-to-end in field-length strips at eight irrigated maize fields in east central Nebraska in 2016 and 2017. Soil and topographic variables that were evaluated for MZ delineation in each field included soil apparent electrical conductivity (EC_a), soil optical reflectance, soil organic matter (SOM), relative elevation, and slope. Maize response to N was evaluated with in-season canopy reflectance measurements (normalized difference red edge; NDRE) and grain yield. Relationships between maize response variables and measured soil and topographic attributes were evaluated and used to delineate MZ. Yield response to N rate was highly variable both among and within fields. Soil EC_a had the highest correlations to crop

response overall and was used as a clustering variable in five of eight fields. Crop response was correlated to SOM in fields with high variability in SOM and was used as a clustering variable in three of eight fields. Economic analysis showed a potential advantage by using soil-based MZ compared to producer-chosen uniform N rates in five of eight fields. Delineated MZ were able to identify areas with differential soil chemical properties and crop response to N fertilizer. Zone 1 properly identified areas with significantly higher NDRE values in all eight fields and with significantly different yield response in three of six fields. Integrating soil-based MZ and sensor-based N management has potential to achieve further economic benefits.

Abbreviations: EC_a, apparent electrical conductivity; EONR, economic optimum nitrogen rate; MZ, management zones; NDRE, normalized difference red edge; NIR, near-infrared; NUE, nitrogen use efficiency; RE, red edge; RMSE, root mean square error; SI, sufficiency index; SOM, soil organic matter.

INTRODUCTION

Maize is the most widely grown crop in the US, and it is also the largest user of nitrogen (N) fertilizer (Morris et al, 2018). For this reason, maize is often the target of environmental impact policies where N is concerned (Snyder, 2012). Fertilizer N use in cereal production is historically inefficient, with estimates of maize N use efficiency (NUE) ranging from 35 to 75% (Morris et al., 2018). Applied N fertilizer that is not taken up by the crop is subject to numerous loss mechanisms, including denitrification, volatilization, and leaching (Cassman et al., 2002). Low NUE over time has resulted in severe environmental consequences in several regions of the US.

Three major factors contributing to low NUE in maize production include: (1) poor synchrony between soil N supply and crop demand (Shanahan et al., 2008), (2) applying uniform rates of fertilizer N to spatially variable landscapes, and (3) failure to account for temporal variability in crop response to N. High levels of inorganic N in the soil profile resulting from large pre-plant applications of fertilizer N increases the potential for N losses. In-season applications of N fertilizer coincide with the period of rapid crop uptake and therefore have great potential to increase NUE (Fageria and Baligar, 2005). Numerous field studies have shown that N supply within a field can be highly spatially variable (Scharf et al., 2005; Shahandeh et al., 2005). This variability is caused by differences in soil temperature, soil organic matter (SOM) mineralization, soil texture, water availability, and local topography. As producers typically apply enough N fertilizer to meet the crop requirements of the most N-limiting areas of a field, N fertilizer is frequently over-applied, increasing the risk for N loss in areas of the field requiring less

N. Climate and management interactions also result in high temporal variability in the economic optimum nitrogen rate (EONR) and in crop yields (Tremblay et al., 2012). Collectively, these three factors make accurate estimation of EONR difficult for many fields. Innovative N management strategies that can account for these factors are needed to increase NUE and mitigate detrimental environmental impacts.

Delineating fields into management zones (MZ) is one method for managing within-field variability to increase NUE. Management zones are regions of a field with homogenous soil and landscape attributes, resulting in similar yield-limiting factors and corresponding uniform levels of crop inputs (Doerge, 1999). Myriad approaches to MZ delineation have been developed in the last 25 years (Khosla et al., 2010). Some common attributes that have been used—either individually or in combination—for MZ delineation include soil apparent electrical conductivity (EC_a) (Kitchen et al., 1999; Fleming et al., 2004), yield maps (Flowers et al., 2005), imagery (Schepers et al., 2004), topography (Fraisse et al., 2001), and soil survey maps (Franzen et al., 2002).

The statistical methods used to classify MZ are diverse. These include the ISODATA method, non-parametric approaches, a hierarchical approach, and the fuzzy *c*-means (or *k*-means) method. Management Zone Analyst (MZA) (University of Missouri, USDA-ARS, Columbia, MO) is a free software program that uses a fuzzy *c*-means algorithm for clustering. In addition to ease of use, MZA has the advantage of providing results for a range of clusters so that the user can evaluate how many MZ should be used (Fridgen et al., 2004).

While managing N through the use of MZ often improves efficiency compared to uniform field management by helping to characterize the spatial variability in soil physical and chemical properties, MZ are often inconsistent in characterizing the spatial variability in crop N requirement because of the effect of temporal variability on crop N response (Shanahan et al., 2008). In a five-year study in Nebraska, Schepers et al. (2004) found temporal variability to greatly affect MZ, and the use of MZ to direct variable-rate N fertilizer application would have been appropriate in only three of five years. They concluded that a static, soil-based MZ approach alone is likely inadequate for directing spatially variable applications of N fertilizer due to the inability to account for temporal variability.

One tool with the potential to manage all three factors causing low NUE is crop canopy sensing. This strategy is known as a reactive approach to N fertilizer management because the sensors can identify and correct N stress that has already occurred during the growing season (Ping et al., 2008). Rather than using indirect measures of growing condition from the soil or from atmospheric conditions, canopy sensors use the crop itself as a bio-indicator to assess crop N status and direct real-time, variable-rate, in-season applications of N fertilizer (Adamchuk et al., 2011). Sensor-based N management is better able to account for spatial and temporal variability and also helps to achieve greater synchrony between N supply and crop N demand, as the majority of N fertilizer is applied in-season during the period of rapid N uptake. Canopy sensors have been used successfully to direct in-season variable-rate N fertilizer applications in several crops,

including maize (Holland and Schepers, 2010), wheat (Solie et al., 2012), cotton (Oliveira et al., 2013), rice (Tubaña et al., 2012), and sugarcane (Amaral et al., 2015).

Crop canopy sensors make use of the relationship between leaf and canopy reflectance to crop response to make quantitative estimates of in-season N status (Hatfield et al., 2008). Active crop canopy sensors emit modulated light in two or more wavelengths in the visible (400-700 nm) and near-infrared (NIR) (750-1400 nm) regions of the electromagnetic spectrum, and measure the reflectance from the crop canopy with photodetectors. Reflectance in these wavelengths is combined into vegetation indices, which are correlated with chlorophyll content and N sufficiency (Walburg et al., 1982). In order to assess crop N status, canopy reflectance of plants yet to be fertilized is compared to reflectance from plants receiving an adequate amount of N fertilizer such that N is not a limiting factor (Shanahan et al., 2008). This N-sufficient reference is used to calculate a Sufficiency Index (SI) with the following equation (Peterson et al., 1993):

$$SI = \frac{VI_{Target}}{VI_{Reference}} \quad [2.1]$$

where

$0 \leq SI \leq 1$

VI_{Target} = vegetation index of target crop

$VI_{Reference}$ = vegetation index of high-N reference

Essentially, lower SI values signify that unfertilized plants are more deficient, and so will require more N fertilizer to achieve their yield potential (Shanahan et al., 2008).

Numerous algorithms have been developed to convert sensor reflectance data into an in-season N fertilizer application rate (Scharf et al., 2011; Solie et al., 2012; Franzen et

al., 2014). Holland and Schepers (2010) developed a generalized N application algorithm for use with crop canopy sensors. They describe the plant growth function as a typical N rate by yield response function (quadratic or quadratic plateau) (Franzen et al., 2016). The algorithm uses an estimated optimum N rate (N_{OPT}) along with the calculated SI to control the model. It also allows for incorporating economics into the N_{OPT} term and accounts for fertilizer N already applied as well as any N credits.

The use of these systems to direct variable-rate, in-season N fertilizer applications in cereal cropping systems has resulted in positive environmental and economic returns (Kitchen et al., 2010; Roberts et al., 2010). Raun et al. (2002) experimented with sensor-based N application in wheat and found that, averaged over locations, NUE was improved by >15% when compared with traditional uniform practices. The savings in fertilizer N with similar grain yield had a value of >\$25·ha^{-1}. Scharf et al. (2011) conducted 55 replicated on-farm experiments in maize comparing sensor-based variable-rate N application to uniform producer-selected rates. Relative to the uniform rate, sensor-based management increased partial profit by \$42·ha^{-1}, and applied N was reduced by 16 kg·ha^{-1}.

Crop canopy sensors and their corresponding algorithms are not without their limitations. With no direct knowledge of the soil and topographic characteristics underneath the growing crop, the sensor cannot accurately predict how spatial variability may affect future N mineralization or losses that are not expressed in the crop at the time of sensing. This lack of soil-based information has resulted in poor algorithm performance in certain subfield regions due to local spatial variability (Ferguson,

unpublished data, 2015). Researchers agree that refinements are needed in order to account for additional management, soil, and climatic factors (Shanahan et al., 2008), combining both anticipatory and reactive decision-making (Ping et al., 2008). Schepers et al. (2004) and others (Holland and Schepers, 2010; Solari et al., 2008) have suggested combining MZ and in-season crop canopy sensing to better predict EONR throughout the field and achieve greater NUE.

Roberts et al. (2012) experimented with an integrated MZ and canopy sensor approach on six irrigated fields in Nebraska, USA and found potential for this integrated approach to increase NUE and economic return over current management practices, particularly in silt loam fields with eroded slopes. However, they believed further research was needed to refine current algorithms and explore how to best integrate the two N management strategies. Furthermore, they advocated for additional similar field studies to establish a consistent set of variables for use in MZ delineation. Therefore, the objectives of this research study were to (1) identify soil and topographic variables that are related to in-season canopy reflectance and yield for soil-based MZ delineation and (2) determine if delineated MZ can identify areas with differential crop response to N fertilizer.

MATERIALS AND METHODS

Research Fields

Experiments were conducted on eight maize fields, all center-pivot irrigated, during the 2016 (Fields AR16, CA16, HU16, and KR16) and 2017 (Fields AR17, HU17, JA17, and KR17) growing seasons. Fields were located in east central Nebraska, USA (Fig. 2.1). Fields AR16, KR16, AR17, HU17, and KR17 were relatively flat (< 5 m of relief), while there were substantial differences in elevation (~7-20 m) and topography for Fields CA16, HU16, and JA17. The sites were grouped into four classifications based on soil texture and topography: sandy loam, relatively level (KR16 and KR17), silt loam, relatively level (AR16, AR17, HU17), silt loam, eroded slopes (CA16 and HU16), and sandy loam, eroded slopes (JA17). One to four soil series were represented at each site (Table 2.1).

Experimental Treatments

Tillage practices, crop rotation, hybrid selection, planting date, seeding rate, irrigation, and other field management decisions and operations were managed by individual producers (Table 2.2). Plots were arranged in a 2 x 3 randomized complete block design (RCBD) (Fig. 2.2). Plots were 6, 8, or 12 rows (0.76-m row spacing) in width, depending on producer equipment (Table 2.3). Plot length was 15.2 m with 0.6 m buffers in 2016, and 12.2 m with 3.6 m buffers in 2017 (Fig. 2.2). Blocks were placed end-to-end in a field length strip, with the number of blocks per field varying from 10 to 16 (Table 2.3). Treatment layout maps for all fields can be found in Appendix 1.

Nitrogen treatments consisted of six rates ranging from 0 to 280 $kg \cdot ha^{-1}$ in 56 $kg \cdot ha^{-1}$ increments. Field AR16 had 84 $kg \cdot ha^{-1}$ applied before planting, so rates on that site ranged from 84 to 308 $kg \cdot ha^{-1}$, in 45 $kg \cdot ha^{-1}$ increments. Field JA17 received a pre-emergence N fertilizer application of 39 $kg \cdot ha^{-1}$. Field KR17 received an N application of 23 $kg \cdot ha^{-1}$ as ammonium sulfate (21-0-0-24) at the V4 growth stage to correct a sulfur deficiency. A base N fertilizer rate of 56 $kg \cdot ha^{-1}$ was applied to all but the check plots between the V2 and V5 growth stages (Table 2.3). Field JA17 had a decreased base rate of 17 $kg \cdot ha^{-1}$ to account for the pre-emergence N application. The remaining N fertilizer was applied between the V9 and VT growth stages (Table 2.3). The N fertilizer source for all treatments was either 28 or 32% urea ammonium nitrate (UAN) solution (Table 2.3). Nitrogen fertilizer was applied with a high-clearance applicator (Hagie DTS 10, Hagie Manufacturing Co., Clarion, IA), and the fertilizer was applied through a straight stream nozzle between each row. Flow rate was controlled with a pulse-width modulation spray rate controller (PinPoint, Capstan Ag Systems, Topeka, KS). Fertilizer application data were collected with a flowmeter at a rate of 1 Hz and were filtered to exclude erroneous data points.

Field Data Collection

Soil Data

Spatial soil data collected for each field included soil apparent electrical conductivity (EC_a) and soil optical reflectance (red and NIR bands). These attributes were collected for each field prior to planting (except for Field HU17, for which data were collected following harvest) using a Veris MSP3 on-the-go soil sensing platform (Veris

Technologies, Inc., Salina, KS). The MSP3 instrument uses two arrays of coulter-electrode pairs to measure soil EC_a at depths of 0 to 0.3 m (shallow EC_a—EC_s) and 0 to 0.9 m (deep EC_a—EC_d) simultaneously. The MSP3 also measures soil optical reflectance with an active optical sensor located ~5 cm deep in the soil measuring in red and near-infrared (NIR) wavelengths. The simple ratio (SR_{soil}) $\left(\frac{NIR}{Red}\right)$ was calculated from the reflectance readings. 25 soil samples were collected to a depth of 20 cm across the range of EC_s and reflectance values for the field, and results were used by Veris Technologies to calibrate the optical reflectance readings to estimate soil organic matter (SOM). A global positioning system (GPS) receiver was mounted on the MSP3 sensor to log geographic coordinates as the instrument made parallel passes ~18 m apart throughout the field.

Elevation for each field as 2-m Digital Elevation Model (DEM) grids was retrieved from the Nebraska Department of Natural Resources (NeDNR) LiDAR Repository (NeDNR, 2010). Elevation data for the experimental sites was collected in 2009 (Fields CA16, HU16, and HU17) and 2010 (Fields AR16, KR16, AR17, JA17, and KR17). Relative elevation ($Elev_{rel}$) was calculated for each field by subtracting all grids by the minimum elevation within the field. Slope was calculated with the same grid size as the DEMs using the Spatial Analyst package in ArcMap 10.4 (ESRI, Redlands, CA). Summary statistics for the spatial data can be found in Appendix 1.

All spatial data were projected into the Universal Transverse Mercator (UTM) Zone 14N (NAD83 Datum) projection. To obtain values of each data layer for each plot, ordinary kriging was used to interpolate each layer (EC_s, EC_d, SR_{soil}, SOM, $Elev_{rel}$, and

Slope). Interpolation was conducted using the Geostatistical Analyst package in ArcMap 10.4. Plots were buffered by one row (0.76 m) on each side and by 2 m at each edge to reduce the possibility of any potential buffer effect between plot N applications. As an additional precaution, pivot tracks were buffered by 1 m. Buffered plots measured 11.2 m in length in 2016 and 9.0 m in 2017, with width varying according to plot row width. Data were extracted from this rectangular area-of-interest (AOI) using zonal statistics or join in ArcMap 10.4.

Crop Response Data

Canopy reflectance was measured at the time of the in-season N application (V9 to VT growth stage) for each plot using an OptRx active canopy sensor (Ag Leader Technology, Ames, IA) (Table 2.3). Canopy reflectance in the red-edge (RE) (730 nm) and NIR (780 nm) wavelengths was used to calculate the normalized difference red edge (NDRE) vegetation index using the following equation (Gitelson and Merzlyak, 1994):

$$NDRE = \frac{R_{NIR} - R_{RE}}{R_{NIR} + R_{RE}} \quad [2.2]$$

where

R_{NIR} = NIR reflectance

R_{RE} = red-edge reflectance

The sensor was mounted to the front of the high-clearance applicator approximately 0.3-0.6 m above the crop canopy. The sensor was positioned over either of the center two rows of each plot in the nadir view. Differential GPS location and reflectance data were logged with a GeoSCOUT X data logger (Holland Scientific, Lincoln, NE). Canopy reflectance measurements were collected at a rate of 1 Hz while the vehicle traveled at a

speed of ~1.5 m·sec^{-1}, resulting in raw data points ~1.5 m apart. Sensor readings were extracted for each plot AOI using zonal statistics in ArcMap 10.4. Sensor readings within the plots were buffered in the same manner as the soils and elevation data.

Yield Data

The entirety of the center two rows of each plot was harvested at physiological maturity with a two-row combine. Due to an improper calibration, Field JA17 was harvested a second time, using rows adjacent to the center two. A Gleaner K combine (AGCO Corp., Duluth, GA) was used for 2016 sites, and the 2017 sites were harvested with a Kincaid 8-XP plot combine (Kincaid Equipment Manufacturing, Haven, KS). Both combines were equipped with a HarvestMaster HM800 GrainGage (Juniper Systems, Logan, UT) for measurement of plot weight, moisture, and test weight. Harvested weight was adjusted to a moisture of 155 g kg^{-1}. Yield was further cleaned by adjusting plot area due to pivot tracks, lodging, and poor stand.

Yield response to N rate models were fit to each treatment block using a quadratic-plateau function. This function has been found to best describe maize yield response to N in previous research by Cerrato and Blackmer (1990) and Scharf et al. (2005). PROC NLIN in SAS 9.4 (SAS Institute Inc., Cary, NC) was used to compute the quadratic-plateau function for each block (Table 2.4). Two parameters, the coefficient of determination (R^2) and root mean square error (RMSE), were calculated for each model and used to evaluate goodness of fit using the following equations:

$$R^2 = 1 - \frac{ESS}{TSS} \qquad [2.3]$$

$$RMSE = \sqrt{\frac{ESS}{(n-2)}} \quad [2.4]$$

where

$ESS =$ model error sum of squares
$TSS =$ total sum of squares
$n =$ number of observations

Each of the 109 response functions was plotted along with the observations it described and visually inspected for fit. In a few cases, it appeared that the initial NLIN procedure may not have found the best function, so the NLIN procedure was run again with different starting parameters. This resulted in improved fit of the quadratic-plateau function in a few instances. Additionally, one outlier observation was removed from a small number of blocks when negative yield response to N occurred in order to improve model fit.

Parameters (*a*, *b*, and *c*) from the quadratic model:

$$Yield = a + b(Applied\ N) + c(Applied\ N)^2 \quad [2.5]$$

were evaluated using a process described by Scharf et al. (2005). When the linear (*b*) coefficient of the quadratic-plateau model was negative (i.e. yield decreased with the first increment of N fertilizer), yield was modeled as unresponsive to N. When the quadratic (*c*) coefficient of the quadratic model was positive, or when PROC NLIN in SAS failed to converge, a linear function was fit to the data, using PROC REG in SAS 9.4. Yield was modeled as a linear function when $p < 0.10$ and the slope of the line was significantly greater than zero. Otherwise, yield was modeled as unresponsive to N. Unresponsive treatment blocks were excluded from further analysis.

Parameters *b* and *c* from the quadratic-plateau models were used to calculate EONR for each treatment block (Table 2.4). EONR was determined with a maize grain price of \$120.07·Mg^{-1} (\$3.05·bu^{-1}) and a N fertilizer cost of \$0.99·kg^{-1} (\$0.45·lb^{-1}). EONR was calculated based on the equation:

$$EONR = \frac{(\$0.99/\$120.07 - b)}{2c} \quad [2.6]$$

where b and c were the linear and quadratic coefficients of the quadratic-plateau function, and $b > 0$ and $c < 0$ (Scharf et al., 2005). EONR was constrained to never exceed the highest N rate for each field.

Management Zone Delineation

In order to explore relationships between the measured soil and crop variables, a Pearson correlation analysis was conducted using PROC CORR in SAS 9.4. The first analysis explored relationships between check plot yield and NDRE for all check plots. A second analysis utilized all but the check plots, which at the time of sensing had received the same rate of N fertilizer. NDRE was the only crop variable used in the second analysis. Yield for all plots was not explored due to the confounding treatment effect of N on the measured variables.

Using Global (all fields combined) and Field-Specific approaches, the two variables with the highest significant correlation ($p < 0.05$ and $R > 0.50$) to either NDRE or check yield for each field were selected as input variables for clustering in Management Zone Analyst (MZA) 1.0.1 (USDA-ARS and University of Missouri, Columbia, MO) (Fridgen et al., 2004). To increase the number of observations for

clustering and to increase the overall spatial area of the MZ, all soil and landscape data collected from the plots as well as adjacent to them were used as inputs into MZA, resulting in a total area of 12-30 ha. In the software, Mahalanobis distance was selected as the measure of similarity except when variables with identical units were used. In these instances Euclidean distance was chosen.

Two indices are calculated by MZA to help determine the optimum number of classes. The Normalized Classification Entropy (NCE) quantifies the disorganization created by dividing data into classes (Lark and Stafford, 1997). The Fuzziness Performance Index (FPI) determines the amount of membership sharing (fuzziness) among classes (Odeh et al., 1992). Class number is optimized when both NCE and FPI are minimized, meaning a low degree of membership sharing and low disorganization from the clustering process (Fridgen et al., 2004).

Management Zone Validation

Following MZ delineation for each field, zones were evaluated to determine if there were differences between MZ in terms of response to N. For an initial exploration of MZ, differences in four soil chemical properties—pH, Mehlich-III phosphorus (P), SOM, and cation-exchange capacity (CEC)—were tested. To do this, sample points were grouped by MZ and an *F*-test was performed to determine if these properties differed between MZ.

Canopy reflectance (expressed as NDRE) is one input in the Holland-Schepers sensor-based N recommendation algorithm (Holland and Schepers, 2010) and consequently was used as one variable to test zonal differences within each field. To

accomplish this, treatment blocks were disregarded and plots were placed into two groups—those that had received no N fertilizer and those that had received a base rate of 56 kg·ha^{-1}. Because the remaining N fertilizer was applied simultaneously with canopy reflectance sensing, all non-check plots had received the same amount of N at the time of sensing. NDRE values were averaged within each plot and an *F*-test was used to evaluate zonal differences.

In order to evaluate MZ delineation using yield response to N rate, treatment blocks within each field were disregarded, and plots were grouped according to target N rate within each zone. Only plots located in a block that successfully fit a quadratic-plateau function were used. Plot yields and as-applied N fertilizer rates were averaged for each target N rate within each zone. A quadratic-plateau model with six observations was fitted using procedures identical to those outlined previously. Statistical differences between the two models for each field were tested by combining the data for the two zones and re-fitting a quadratic-plateau model to the combined data set (Roberts et al., 2012). With the resulting models for Zone 1, Zone 2, and the combined model, a Chow *F*-test was performed to determine whether the models for each zone were statistically different (Chow, 1960):

$$F_{k,n_1+n_2-2k} = \frac{\left(SSE_C-(SSE_1+SSE_2)\right)/k}{(SSE_1+SSE_2)/(n_1+n_2-2k)} \qquad [2.7]$$

where SSE_C, SSE_1, and SSE_2 are equal to the residual sum of squares from the combined, Zone 1, and Zone 2 models, respectively; n_1 and n_2 are the number of observations in Zone 1 and Zone 2, respectively; and k is equal to the total number of model parameters.

RESULTS AND DISCUSSION

Yield Response to Nitrogen

The average yield at EONR for all eight sites was 14.2 $Mg \cdot ha^{-1}$, indicating favorable growing conditions and production practices for these experiments (Table 2.3). Out of 109 total blocks, yield response to N was described using a quadratic-plateau function in 62 blocks, a linear function in 23 blocks, and a nonresponsive function in 24 blocks (Table 2.4). Plots for each individual block can be found in Appendix 1. The average R^2 for the 85 responsive plots was 0.88, and median R^2 was 0.91. A cumulative distribution function for R^2 values is shown in Fig. 2.3. Sixty percent of all responsive functions had $R^2 \geq 0.90$.

Only 57% of blocks were able to be described by a quadratic-plateau function for yield response to N. This is much lower than the results of the study by Scharf et al. (2005), in which 93% of their blocks were described using a quadratic-plateau function. Just two fields (AR16 and JA17) were responsible for nearly half of the 47 blocks for which a quadratic-plateau function could not be fit. Field AR16 did not have a proper check plot, and the lowest N rate was 84 $kg \cdot ha^{-1}$. Combined with soybean as a previous crop and >3% SOM levels throughout the field, most of the blocks showed no yield response to N. Field JA17 was highly variable in topography. In one area, elevation ranged 3.3 m in the 43-m length of one block. This highly localized variability did not provide equal growing conditions for the entire block area and likely affected water and nutrient availability as well as crop stand. This resulted in little or sometimes even negative yield response to N in many of the blocks of this field.

EONR varied greatly both among and within the eight fields in this study. Median EONR ranged from to 110 to 198 kg·ha^{-1} between fields (Fig. 2.4). Yield at EONR was not significantly related to EONR (p = 0.42). Yield level explained on average only 1% of the variability in EONR (R^2 = 0.01). This is similar to the results found by Scharf et al. (2006), who found yield to be a very weak predictor of EONR. They concluded that spatial variability in EONR was due mainly to variations in soil N supply and N uptake efficiency, rather than to variations in crop demand for N. These findings may have negative implications for traditional yield-based N fertilizer recommendations derived from a mass balance approach (Lory and Scharf, 2003).

Within-field variability in EONR was also high, with a range of 80 kg·ha^{-1} or more for six of eight fields (Fig. 2.4). The level of between-field and within-field spatial variability in EONR confirms the value of variable-rate N fertilizer application provided that EONR can be accurately predicted across the field.

Selection of Soil Variables for Management Zone Delineation

The first objective of this research was to determine which soil and landscape variables could identify areas with differential crop response to N and could therefore be used to delineate MZ. To accomplish this, measured soil and landscape variables, including EC_a at two depths (EC_s and EC_d), soil optical reflectance (SR_{soil}), SOM, elevation ($Elev_{rel}$), and slope were evaluated to determine their relationship to check plot yield and in-season canopy reflectance (NDRE) (Table 2.5).

Results from this analysis of all sites combined (Global Approach) indicated that no variable was significantly correlated to check yield (p < 0.10). Relative elevation and

slope were significantly correlated to NDRE ($p < 0.05$), but the correlation was weak (R = -0.21, -0.25). Check yield and NDRE were significantly correlated to each other ($p < 0.001$; $R = 0.67$). Most of the soil and topographic variables were significantly correlated to one another, with the highest correlation occurring between EC_s and EC_d ($R = 0.94$). Shallow EC_a was significantly correlated ($p < 0.001$) to every other soil and topography variable. Soil organic matter was moderately correlated to both EC_s and EC_d (R = 0.65, 0.71), which has also been reported by Serrano et al. (2014).

To remove confounding N treatment effects on the correlation between crop and soil variables, a second analysis looked at correlations to in-season NDRE for all but the check plots, which at the time of sensing had an equal rate of N fertilizer applied (Table 2.6). Four variables—SOM, SR_{soil}, Slope, and $Elev_{rel}$—were significantly correlated to NDRE at $p < 0.05$, though weakly (R = 0.17, -0.14, -0.14, -0.11). With no significant correlation to check yield and only weak correlations to NDRE, no variable was chosen to cluster MZ in an approach with all fields combined (Global Approach). The eight fields chosen varied widely in soil texture, SOM levels, and topography, making it difficult to explain crop response accurately for all of them using the same one or two soil properties. Correlations were subsequently evaluated on a field-by-field basis (Field-Specific Approach).

Next, correlation analyses between soil and topographic variables, NDRE, and check yield were evaluated for each individual site (Table 2.7, see also Appendix 1). The two variables with the highest significant correlation ($p < 0.05$ and $R > 0.5$) to either NDRE or check yield for each field were selected as clustering variables in MZA, except

for Fields CA16 and JA17, where only one variable was used. Shallow EC_a was chosen as a clustering variable in five of eight fields, and EC_d was chosen as a clustering variable in four of eight fields. Soil organic matter was chosen in three of eight fields, and $Elev_{rel}$ was selected in two of eight fields.

There did not appear to be a pattern between the four field classification groups and the variables chosen for MZ delineation. However, for the four sites where EC_s had a significant ($p < 0.05$) correlation to both check yield and NDRE, the correlations were positive for sites with coarse-textured soils (KR16 and KR17) and negative for sites with fine-textured soils (HU16 and HU17). For the sandy fields, areas with higher soil EC_s had higher clay content, water-holding capacity, and SOM, resulting in improved crop growth. For the silt loam fields, increased EC_s corresponded to areas with higher slopes or with increased clay content and poorer drainage where conditions are less suitable for optimal crop growth in most growing seasons.

Interestingly, SR_{soil} and SOM were not significantly correlated at $p < 0.10$ for either approach that used all sites (Global Approach). A proprietary calibration procedure by Veris Technologies related soil optical reflectance to SOM using directed soil samples and laboratory analysis. However, SOM calibrations for the eight sites were rated by Veris Technologies as high quality (two sites), average (three sites), and questionable (two sites), with one site being unable to be calibrated (data not shown).

When evaluated with a Field-Specific approach, there were significant ($p < 0.10$) correlations between SR_{soil} and SOM when both check and non-check plots were used for five of eight fields. However, correlations were negative for four of the five fields and

positive for the remaining field. This may explain the lack of significant correlation when using all fields combined.

Soil organic matter content for all sites ranged from 0.6 to 5.0% (Table 2.1). Baumgardner et al. (1969) found that SOM content plays a dominant role in bestowing spectral properties to soils when SOM exceeds 2%. As SOM content drops below 2%, it becomes less effective in masking the effects on reflectance of other soil constituents. This may explain why Field KR16 was unable to be calibrated, as it had a range in SOM of 0.6 to 1.7%. Other factors causing varying degrees of correlation between soil optical reflectance and SOM levels include the level of wear on the sapphire window through which the sensor views the soil, the level of crop residue present during sensing, and varying soil moisture caused by local topographic variability in each field.

Management Zone Delineation

Results from MZA were evaluated using two indices calculated by MZA—NCE and FPI. Class number is optimized when both NCE and FPI are minimized (Fridgen et al., 2004). The FPI indicated that optimal clustering occurred with five MZ in two fields, with three MZ in two fields, and with two MZ in four fields (Fig. 2.5). For NCE, optimal clustering occurred with two MZ for all eight fields (Fig. 2.5). To simplify analysis, each field was clustered into two MZ.

A map of delineated MZ for Field HU17 is presented in Fig. 2.6. Classification maps for all fields are included in Appendix 1. For all sites, Zone 1 consisted of more productive soils with higher SOM content while Zone 2 classified the less productive areas of the field. For the sandy level fields (KR16 and KR17), Zone 1 contained soils

with higher soil EC_a and corresponding higher SOM content. The fields with eroded slopes (CA16, HU16, JA17) had more productive areas in the level, upland positions of the landscape, while Zone 2 areas were associated with steep slopes and drainage areas, and lower SOM, with conditions less suitable for growth. Silt loam level fields (AR16, AR17, HU17) had more productive Zone 1 areas associated with lower soil EC_a in slight depressions.

Management Zone Validation

Soil Chemical Properties

Management zones were first evaluated to see if there were any differences between MZ in soil chemical properties, including pH, Mehlich-III P, SOM, and CEC (Table 2.8). The property that showed significant ($p < 0.05$) between-zone differences most often was CEC, occurring in five of eight fields. It is interesting to note that CEC was significantly greater in Zone 1 for the fields with coarse-textured soils (KR16 and JA17) and significantly greater in Zone 2 for the fields with fine-textured soils (AR16, HU16, HU17). This increased CEC for the Zone 1 soils in sandy fields is likely related to increased clay content in these areas given the fact that these fields had positive correlations between crop growth and soil EC_a, while the opposite was true for the silt loam fields (Table 2.7). Measured SOM recorded significant differences between MZ in three of eight fields. Phosphorus and pH did not prove to be valuable indicators of zonal differences, each returning a significant difference in only one of eight fields.

Normalized Difference Red Edge Index

The second objective of this study was to determine if delineated MZ can identify areas with differential crop response to N fertilizer. In order for MZ to be used together with canopy sensor-based N management, MZ should be able to properly identify areas within a field with differing levels of N sufficiency. Researchers have found NDRE to be a good measure of in-season crop N status (Li et al., 2014), and it was consequently used for MZ validation.

For six of seven fields, Zone 1 properly identified areas with significantly higher NDRE values and potentially greater N sufficiency than Zone 2 when using the check plots ($p < 0.05$; Fig. 2.7). When all other plots were analyzed, Zone 1 identified areas with higher NDRE values in six of eight fields. When considering both groups (check plots and all other plots), there was a significant difference in NDRE between zones for at least one of the groups for all eight fields. These results indicate that using appropriate soil and topographic variables to delineate field-specific MZ can characterize in-season variability in NDRE and subsequently, N status. This is in contrast to results concluded by Inman et al. (2008). However, their study used a different vegetation index, the Normalized Difference Vegetation Index (NDVI), which, under high-biomass conditions, can become saturated and fail to accurately reflect chlorophyll content (Gitelson and Merzlyak, 1996). They also collected reflectance data using a passive sensor in an aircraft rather than with a ground-based active sensor.

Yield

Yield response to N rate was another crop response variable used to test whether MZ statistically differed within each field. Yield response to N rate models in Zones 1 and 2 were significantly different ($p < 0.05$) for Fields KR16, HU17, and KR17 (Table 2.9; Fig. 2.8). They were not significantly different for Fields AR16, CA16, and AR17, and comparisons could not be made in Fields HU16 and JA17. For these two fields (HU16 and JA17), all blocks showing a quadratic-plateau response were located in one zone. Fields AR16 and AR17 had very little variability, and each field contained highly productive soils across both zones. This resulted in very small differences between zones in optimal yield (0.61 and 0.01 $Mg \cdot ha^{-1}$, respectively) and EONR (23 and 11 $kg \cdot ha^{-1}$, respectively) (Table 2.9). The models for Zones 1 and 2 in Field CA16 were very close to being significantly different ($p = 0.058$), and zonal EONR varied by 96 $kg \cdot ha^{-1}$, the greatest range of any of the fields studied.

Maximum yield difference between zones was greatest in Field KR16 (3.46 $Mg \cdot ha^{-1}$) and Field KR17 (2.39 $Mg \cdot ha^{-1}$). Though these fields had a very great difference in optimum yield, there were minimal differences in EONR between zones (11 and 28 $kg \cdot ha^{-1}$ for Fields KR16 and KR17, respectively). Zone 1 for both of these fields contained areas with more productive soil, resulting in significantly increased yields compared to Zone 2. However, because the soil was likely supplying more N in these favorable conditions, less N was required from N fertilizer additions (Morris et al., 2018). This can also be confirmed in the fact that, for 4 of 6 fields in this study, Zone 2 EONR was greater than EONR for Zone 1. The results from this study indicate that soil-based

MZ delineated using field-specific variables are able to appropriately classify areas with differing yield response to N rate in fields with medium to high spatial variability. Accounting for this within-field variability through the use of soil-based MZ has potential to increase the performance of sensor-based N recommendation algorithms.

Economic Considerations

An economic analysis compared current producer N fertilizer application rates for each field (Table 2.2) to applying a zone-based uniform N rate based on the calculated EONR for each zone (Table 2.9). This analysis was performed for the six fields for which quadratic-plateau functions for yield response to N were fitted by zone. The study areas in Fields AR16, CA16, KR16, AR17, HU17, and KR17 were 29.6, 12.8, 14.8, 18.7, 24.2, and 16.4 ha, respectively. Assuming an N fertilizer cost of $\$0.99 \cdot kg^{-1}$ ($\$0.45 \cdot lb^{-1}$), the potential savings or loss resulting from zone-based application was determined. There was a total savings/loss of $\$16 \cdot ha^{-1}$, $\$117 \cdot ha^{-1}$, $-\$11 \cdot ha^{-1}$, $\$95 \cdot ha^{-1}$, $\$137 \cdot ha^{-1}$, and $\$92 \cdot ha^{-1}$ for Fields AR16, CA16, KR16, AR17, HU17, and KR17, respectively. Extrapolating this savings to a typical center pivot in Nebraska with an area of ~60 ha, the savings/loss is $982, $6991, -$681, $5674, $8244, and $5505 for these fields. The loss on Field KR16 is due to the EONR for both zones being greater than the producer's uniform N rate. The substantial economic benefit measured in five of six fields suggests a potential benefit to applying N fertilizer according to delineated MZ.

CONCLUSIONS

Economic optimum N rate varied greatly both among and within fields in this study. Within-field EONR ranged 80 kg $N \cdot ha^{-1}$ or more for six of eight fields. The high level of spatial variability in EONR confirms the value of variable-rate N fertilizer application if EONR can be accurately predicted across the field.

No soil or topographic variable was significantly correlated to crop response in an approach using all sites combined. When evaluated on a field-specific basis, soil EC_a had the highest correlations to crop response overall and was used as a clustering variable in five of eight fields. Crop response was correlated to SOM in fields with high variability in SOM and was used as a clustering variable in three of eight fields.

Field-specific MZ were delineated using a combination of EC_a, SOM, and elevation layers. These MZ identified significantly different areas of in-season crop response (NDRE) in all eight fields and different areas of yield response to N rate in three of six fields. Results from this study indicate that soil and topographic properties can be used to delineate field-specific MZ that properly identify spatial variability in crop response to N measured both in-season (NDRE) and by grain yield.

An economic analysis showed a potential benefit to variable-rate N fertilizer applications using soil-based MZ compared to a uniform rate in five of six fields analyzed. Further economic benefits may be achieved by integrating MZ and sensor-based N management.

REFERENCES

Adamchuk, V.I., R.A. Viscarra Rossel, K.A. Sudduth, and P.S. Lammers. 2011. Sensor fusion for precision agriculture. In: Thomas, C. (Ed.), *Sensor Fusion—Foundation and Applications.* (pp. 27-40). Rijeka, Croatia: InTech.

Amaral, L.R., J.P. Molin, and J.S. Schepers. 2015. Algorithm for variable-rate nitrogen application in sugarcane based on active crop canopy sensor. Agron. J. 107:1513-1523.

Baumgardner, M.F., S. Kristof, C.J. Johannsen, and A. Zachary. 1969. Effects of organic matter on the multispectral properties of soils. Indiana Acad. Sci. Proc. 79:413-422.

Cassman, K.G., A.R. Dobermann, and D.T. Walters. 2002. Agroecosystems, nitrogen-use efficiency, and nitrogen management. Ambio. 31:132-140.

Cerrato, M.E., and A.M. Blackmer. 1990. Comparison of models for describing corn yield response to nitrogen fertilizer. Agron. J. 82:138-143.

Chow, G.C. 1960. Tests of equality between sets of coefficients in two linear regressions. Econometrica 28:591-605.

Doerge, T. 1999. Defining management zones for precision farming. Crop Insight. 8:21. Pioneer Hi-Bred International, Inc.

Fageria, N.K., and V.C. Baligar. 2005. Enhancing nitrogen use efficiency in crop plants. Adv. Agron. 88:97-185.

Fleming, K.L., D.F. Heermann, and D.G. Westfall. 2004. Evaluating soil color with farmer input and apparent soil electrical conductivity for management zone delineation. Agron J. 96:1581-1587.

Flowers, M., R. Weisz, and J.G. White. 2005. Yield-based management zones and grid sampling strategies: Describing soil test and nutrient variability. Agron. J. 97:968-982.

Fraisse, C.W., K.A. Sudduth, and N.R. Kitchen. 2001. Delineation of site-specific management zones by unsupervised classification of topographic attributes and soil electrical conductivity. Transactions of the ASAE. 44:155-166.

Franzen, D.W., D.H. Hopkins, M.D. Sweeney, M.K. Ulmer, and A.D. Halvorson. 2002. Evaluation of soil survey scale for zone development of site-specific nitrogen management. Agron J. 94:381-389.

Franzen, D., N. Kitchen, K. Holland, J. Schepers, and W. Raun. 2016. Algorithms for in-season nutrient management in cereals. Agron. J. 108:1775-1781.

Franzen, D., L.K. Sharma, and H. Bu. 2014. Active optical sensor algorithms for corn yield prediction and a corn side-dress nitrogen rate aid. NDSU Circ. SF1176-5, North Dakota State Univ. Ext. Serv., Fargo, ND.

Fridgen, J.J., N.R. Kitchen, K.A. Sudduth, S.T. Drummond, W.J. Wiebold, and C.W. Fraisse. 2004. Management Zone Analyst (MZA): Software for subfield management zone delineation. Agron. J. 96:100-108.

Gitelson, A.A., and M.N. Merzlyak. 1994. Quantitative estimation of chlorophyll-a using reflectance spectra: Experiments with autumn chestnut and maple leaves. J. Photochem. Photobiol. 22:247-252.

Gitelson, A.A., and M.N. Merzlyak. 1996. Signature analysis of leaf reflectance spectra: Algorithm development for remote sensing of chlorophyll. J. Plant. Physiol. 148:494-500.

Hatfield, J.L., A.A. Gitelson, J.S. Schepers, and C.L. Walthall. 2008. Application of spectral remote sensing for agronomic decisions. Agron. J. 100:117-131.

Holland, K.H., and J.S. Schepers. 2010. Derivation of a variable rate nitrogen application model for in-season fertilization of corn. Agron. J. 102:1415-1424.

Inman, D., R. Khosla, R. Reich, and D.G. Westfall. 2008. Normalized difference vegetation index and soil color-based management zones in irrigated maize. Agron. J. 100:60-66.

Khosla, R., D.G. Westfall, R.M. Reich, J.S. Mahal, and W.J. Gangloff. 2010. Spatial variation and site-specific management zones. *In* M.A. Oliver (Ed.), *Geostatistical applications in precision agriculture* (pp. 195-219). New York, NY: Springer.

Kitchen, N.R., K.A. Sudduth, and S.T. Drummond. 1999. Soil electrical conductivity as a crop productivity measure for claypan soils. J. Prod. Agric. 12:607-617.

Kitchen, N.R., K.A. Sudduth, S.T. Drummond, P.C. Scharf, H.L. Palm, D.F. Roberts, and E.D. Vories. 2010. Ground-based canopy reflectance sensing for variable-rate nitrogen corn fertilization. Agron. J. 102:71-84.

Lark, R.M., and J.V. Stafford. 1997. Classification as a first step in the interpretation of temporal and spatial variation of crop yield. Annals Appl. Biol. 130:111-121.

Li, F., Y. Miao, G. Feng, F. Yuan, S. Yue, X. Gao, Y. Liu, B. Liu, S. Ustin, X. Chen. 2014. Improving estimation of summer maize nitrogen status with red edge-based spectral vegetation indices. Field Crops Res. 157:111-123.

Lory, J.A., and P.C. Scharf. 2003. Yield goal versus delta yield for predicting fertilizer nitrogen need in corn. Agron. J. 95:994-999.

Morris, T.F., T.S. Murrell, D.B. Beegle, J.J. Camberato, R.B. Ferguson, J. Grove, Q. Ketterings, P.M. Kyveryga, C.A.M. Laboski, J.M. McGrath, J.J. Meisinger, J. Melkonian, B.N. Moebius-Clune, E.D. Nafziger, D. Osmond, J.E. Sawyer, P.C. Scharf, W. Smith, J.T. Spargo, H.M. van Es, and H. Yang. 2018. Strengths and limitations of nitrogen rate recommendations for corn and opportunities for improvement. Agron. J. 110: 1-37.

Nebraska Department of Natural Resources. 2010. Elevation data. URL: https://dnr.nebraska.gov/data/elevation-data.

Odeh, I.O.A., A.B. McBratney, and D.J. Chittleborough. 1992. Soil pattern recognition with fuzzy c-means: application to classification and soil-landform interrelationships. Soil Sci. Soc. Am. J. 56:505-516.

Oliveira, L.F., P.C. Scharf, E.D. Vories, S.T. Drummond, D. Dunn, W.G. Stevens, K.F. Bronson, N.R. Benson, V.C. Hubbard, and A.S. Jones. 2013. Calibrating canopy reflectance sensors to predict optimal mid-season nitrogen rate for cotton. Soil Sci. Soc. Am. J. 77:173-183.

Peterson, T.A., T.M. Blackmer, D.D. Francis, and J.S. Schepers. 1993. Using a chlorophyll meter to improve N management. NebGuide G93-1171-A. Coop. Ext. Serv., Univ. of Nebraska, Lincoln.

Ping, J.L., R. B. Ferguson, and A. Dobermann. 2008. Site-specific nitrogen and plant density management in irrigated maize. Agron. J. 100:1193-1204.

Raun, W.R., J.B. Solie, G.V. Johnson, M.L. Stone, R.W. Mullen, K.W. Freeman, W.E. Thomason, and E.V. Lukina. 2002. Improving nitrogen use efficiency in cereal grain production with optical sensing and variable rate application. Agron. J. 94:815-820.

Roberts, D.F. 2009. An integrated crop- and soil-based strategy for variable-rate nitrogen management in corn. PhD dissertation, Univ. Nebraska, Lincoln.

Roberts, D.F., R.B. Ferguson, N.R. Kitchen, V.I. Adamchuk, and J.F. Shanahan. 2012. Relationships between soil-based management zones and canopy sensing for corn nitrogen management. Agron. J. 104:119-129. doi:10.2134/agronj2011.0044

Roberts, D.F., N.R. Kitchen, P.C. Scharf, and K.A. Sudduth. 2010. Will variable-rate nitrogen fertilization using corn canopy reflectance sensing deliver environmental benefits? Agron. J. 102:85-95.

Scharf, P.C., N.R. Kitchen, K.A. Sudduth, and J.G. Davis. 2006. Spatially variable corn yield is a weak predictor of optimal nitrogen rate. Soil Sci. Soc. Am. J. 70:2154-2160.

Scharf, P.C., N.R. Kitchen, K.A. Sudduth, J.G. Davis, V.C. Hubbard, and J.A. Lory. 2005. Field-scale variability in optimal nitrogen fertilizer rate for corn. Agron. J. 97:452-461.

Scharf, P.C., D.K. Shannon, H.L. Palm, K.A. Sudduth, S.T. Drummond, N.R. Kitchen, L.J. Mueller, V.C. Hubbard, and L.F. Oliveira. 2011. Sensor-based nitrogen applications out-performed producer-chosen rates for corn in on-farm demonstrations. Agron J. 103:1683-1691.

Schepers, A.R., J.F. Shanahan, M.A. Liebig, J.S. Schepers, S.H. Johnson, and A. Luchiari, Jr. 2004. Appropriateness of management zones for characterizing spatial variability of soil properties and irrigated corn yields across years. Agron. J. 96:195-203.

Serrano, J., S. Shahidian, and J. Marques da Silva. 2014. Spatial and temporal patterns of apparent electrical conductivity: DUALEM vs. Veris sensors for monitoring soil properties. Sens. J. 14:10024-10041.

Shahandeh, H., A.L. Wright, F.M. Hons, and R.J. Lascano. 2005. Spatial and temporal variation of soil nitrogen parameters related to soil texture and corn yield. Agron. J. 97:772-782.

Shanahan, J.F., N.R. Kitchen, W.R. Raun, and J.S. Schepers. 2008. Responsive in-season nitrogen management for cereals. Comput. Electron. Agric. 61:51-62.

Snyder, C.S. 2012. Are Midwest corn farmers over-applying fertilizer N? Better Crops Plant Food 96:3-4.

Solari, F., J. Shanahan, R. Ferguson, J. Schepers, and A. Gitelson. 2008. Active sensor reflectance measurements of corn nitrogen status and yield potential. Agron. J. 100:571-579.

Solie, J.B., A.D. Monroe, W.R. Raun, and M.L. Stone. 2012. Generalized algorithm for variable-rate nitrogen application in cereal grains. Agron. J. 104:378-387.

Tremblay, N., Y.M. Bouroubi, C. Bélec, R.W. Mullen, N.R. Kitchen, W.E Thomason, S. Ebelhar, D. B. Mengel, W.R. Raun, D.D. Francis, E.D. Vories, and I. Ortiz-Monasterio. 2012. Corn response to nitrogen is influenced by soil texture and weather. Agron. J. 104:1658-1671.

Tubaña, B.S., D.L. Harrell, T. Walker, J. Teboh, J. Lofton and Y. Kanke. 2012. In-season canopy reflectance-based estimation of rice yield response to nitrogen. Agron. J. 104:1604-1611.

Walburg, G., M.E. Bauer, C.S.T. Daughtry, and T.L. Housley. 1982. Effects of nitrogen nutrition on the growth, yield, and reflectance characteristics of corn canopies. Agron. J. 74:677-683.

FIGURES AND TABLES

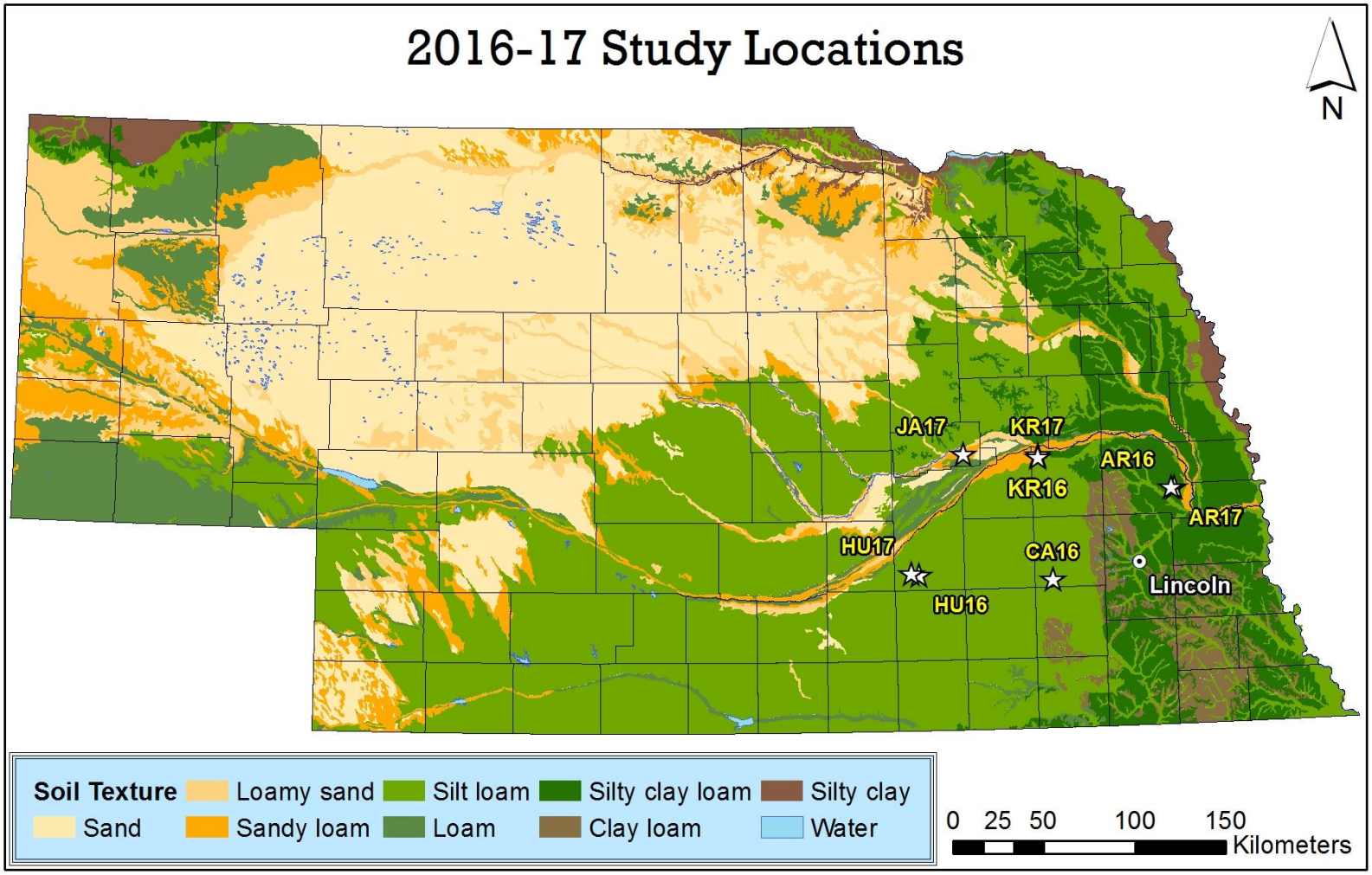

Fig 2.1. Study site locations within the state of Nebraska. SSURGO surface soil texture also shown.

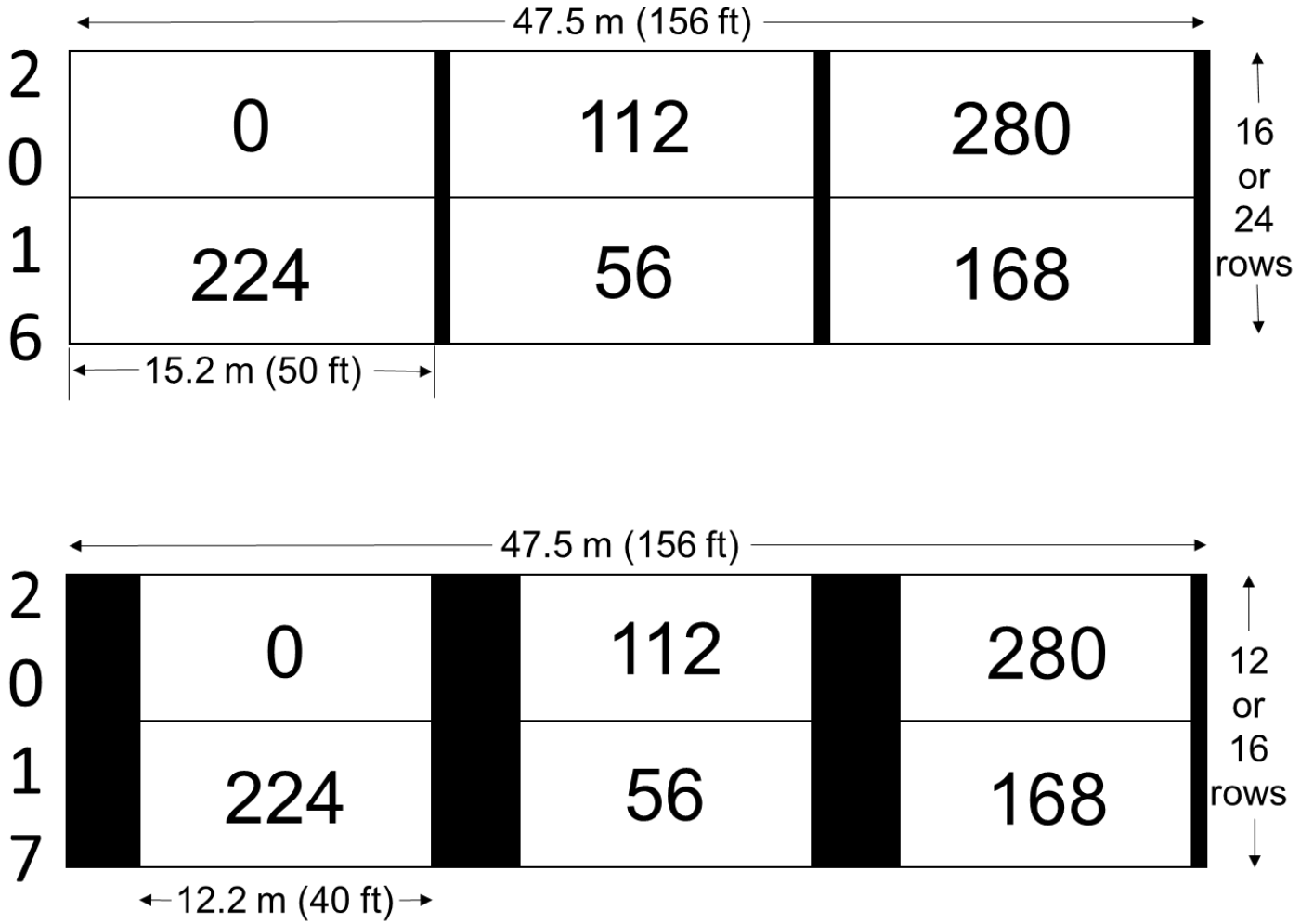

Fig 2.2. Small plot RCBD treatment layouts for 2016 and 2017. Example N rates in kg·ha^{-1}.

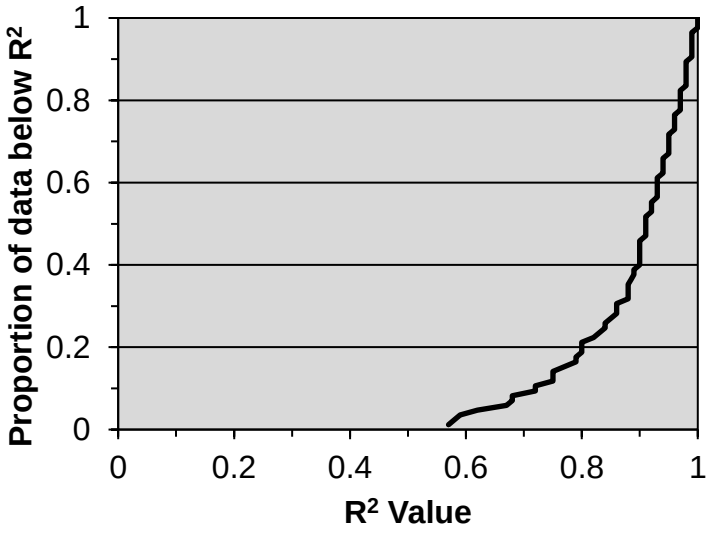

Fig 2.3. Cumulative distribution function for the coefficient of determination (R^2) for all 85 plots modeled as responsive to N (24 plots were modeled as unresponsive). 60% of the models fit the yield data with $R^2 \geq 0.90$.

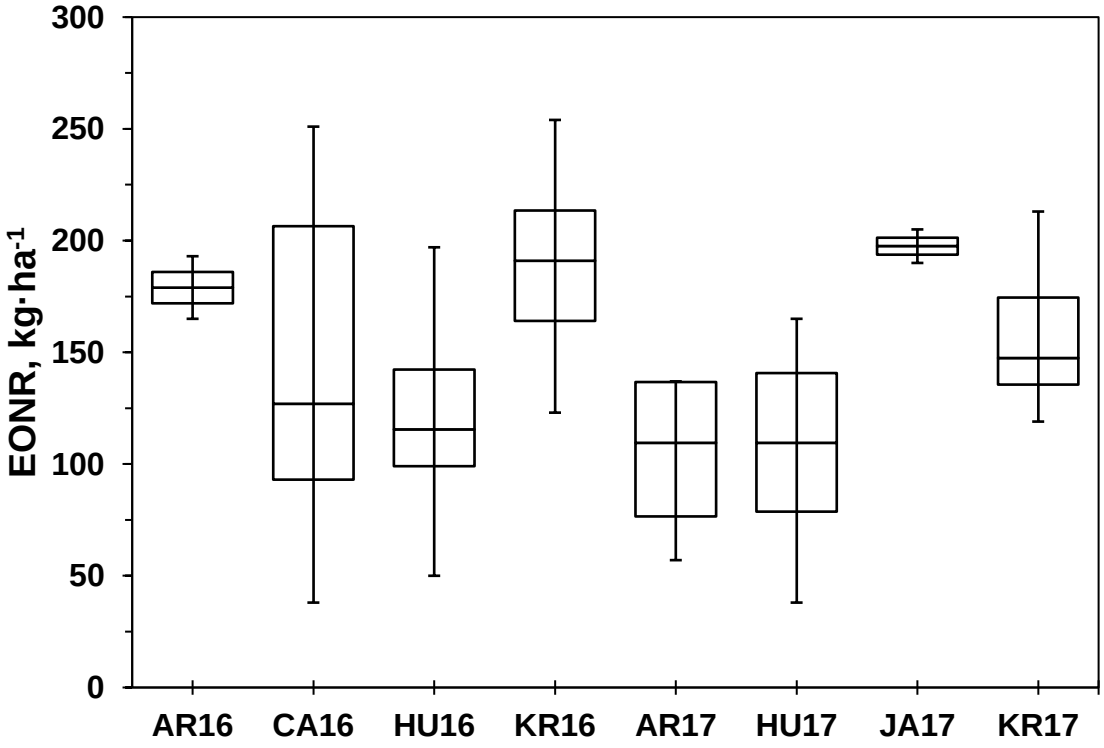

Fig. 2.4. Box-and-whiskers plot of economic optimum N rate (EONR) distributions for all eight sites. The upper and lower limits of each box signify the 75th and 25th percentiles for EONR, the horizontal line in the center of the box indicates the median, and the whiskers represent the full range of EONR observed.

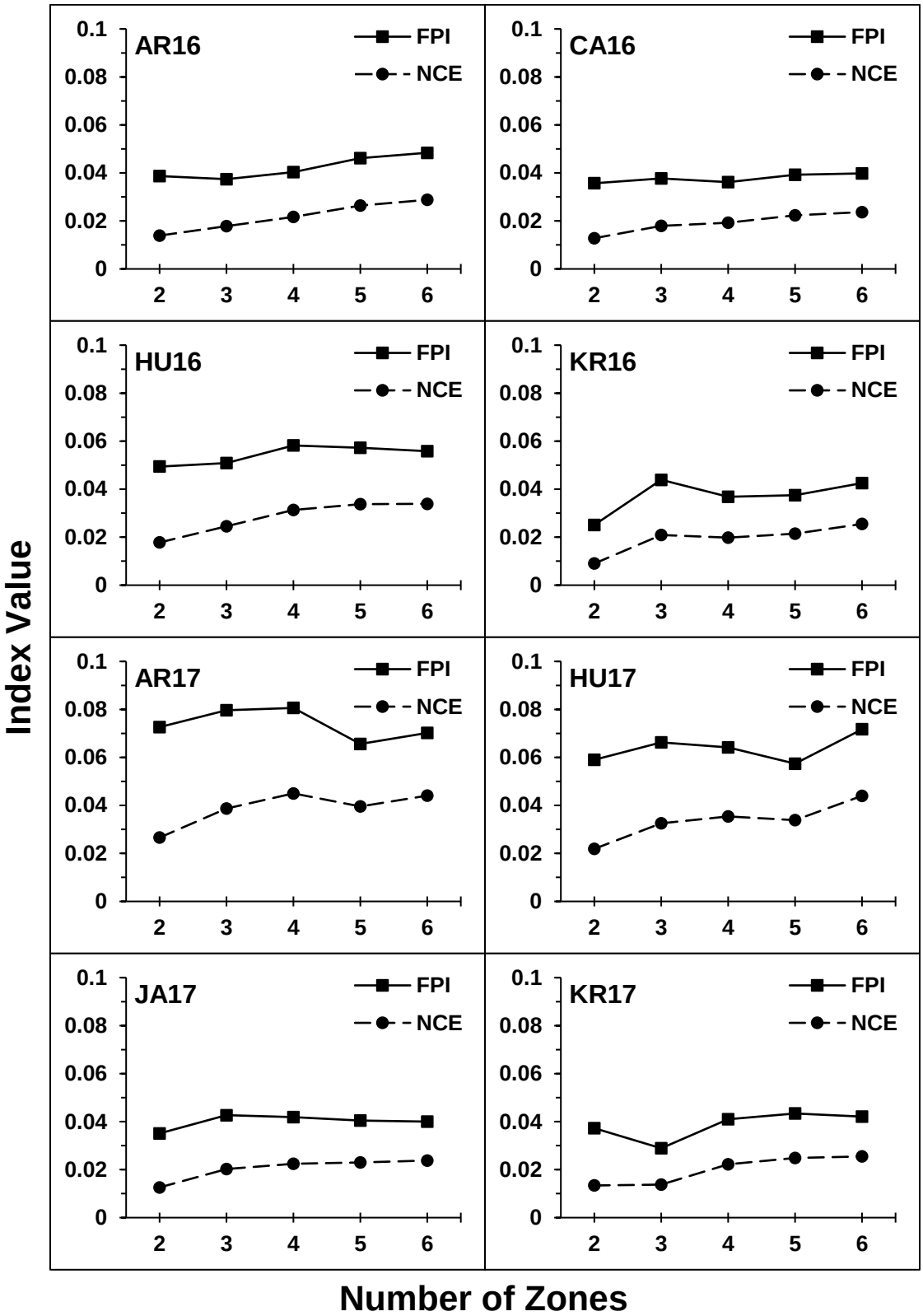

Fig 2.5. FPI and NCE values calculated in MZA for all fields.

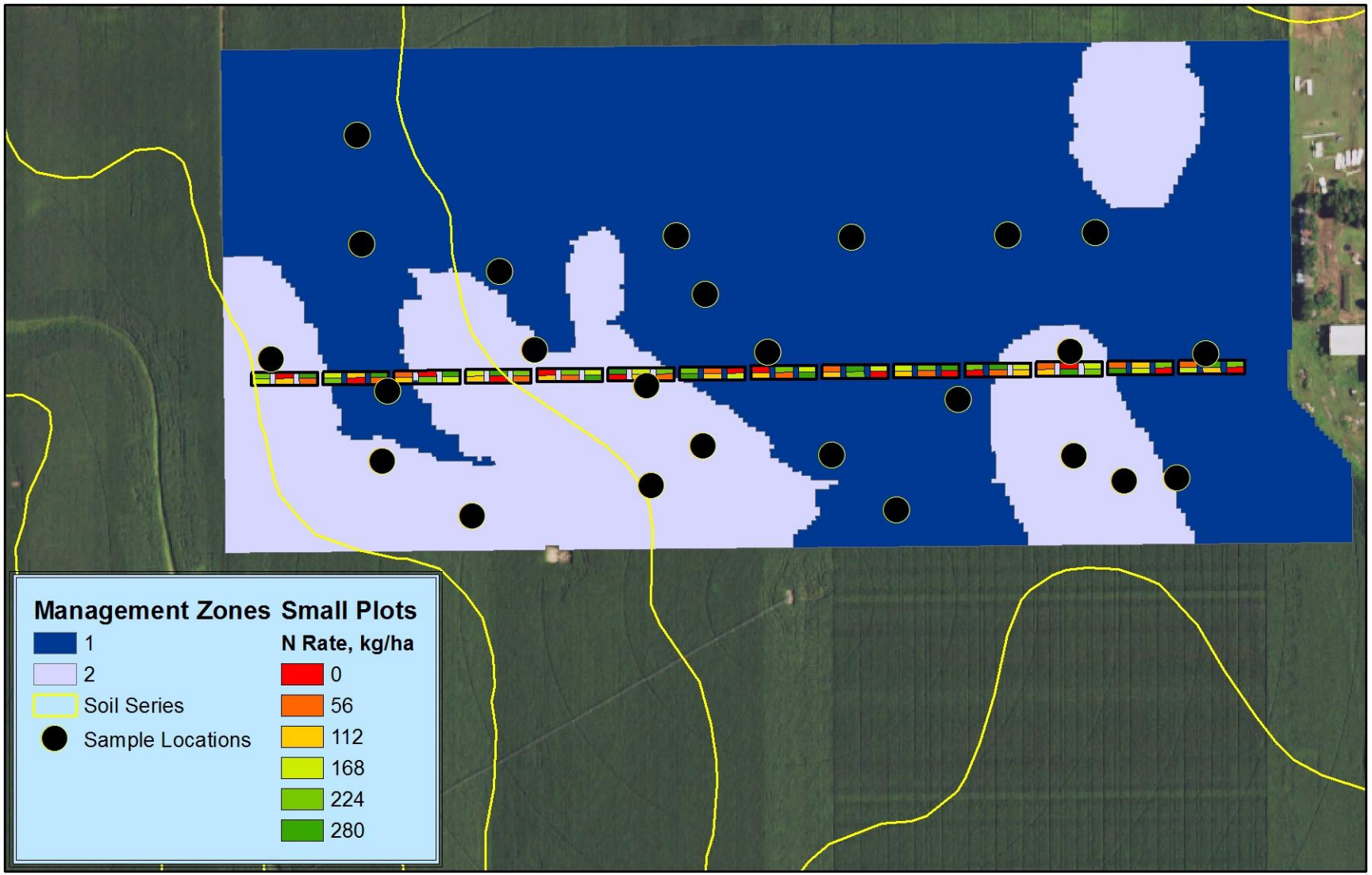

Fig. 2.6. Management zone delineation for Field HU17 using EC_s and SOM.

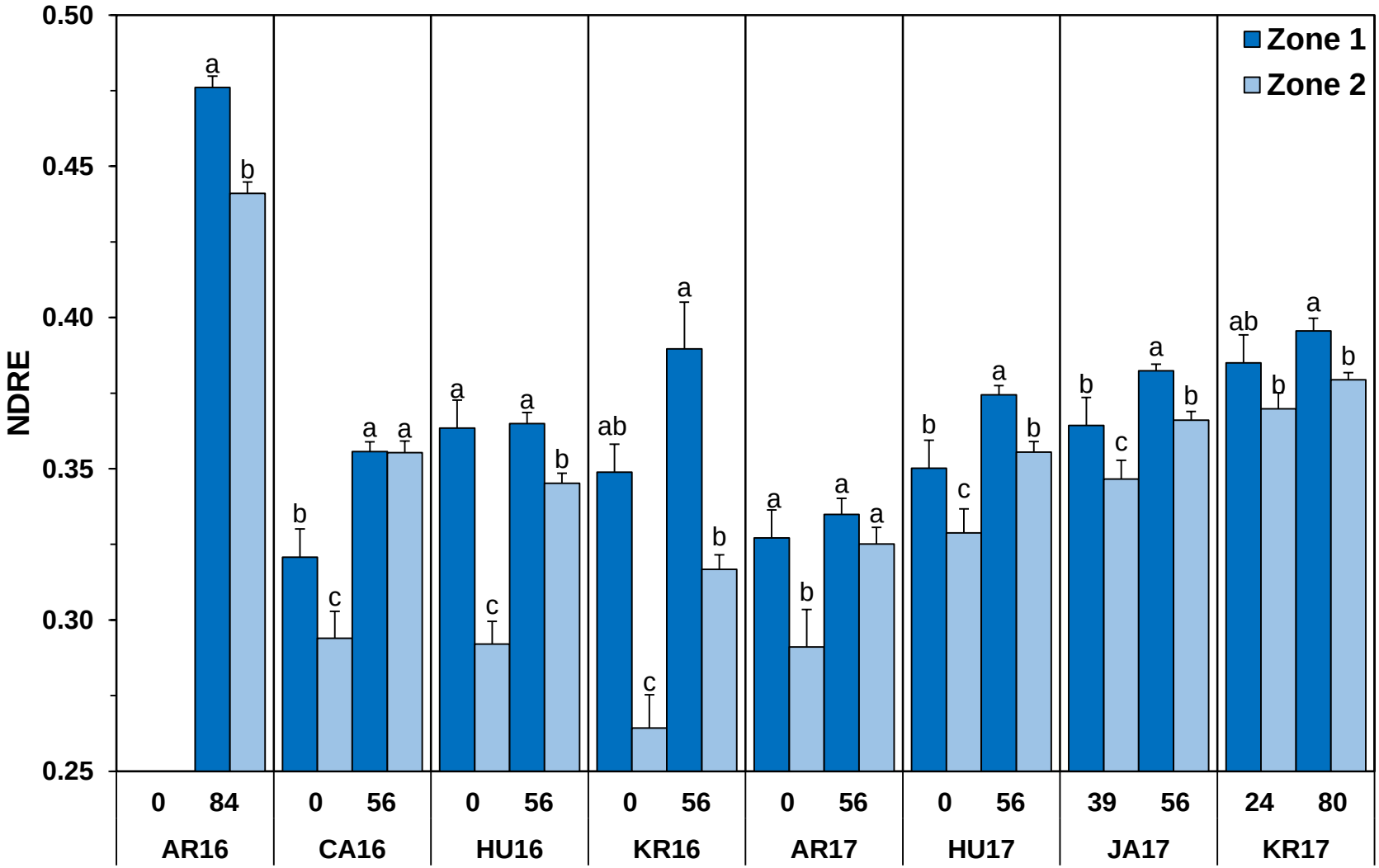

Fig. 2.7. In-season canopy reflectance (NDRE) by N rate by zone for each field. Bars with the same letter are not significantly different. Error bars represent standard error for each treatment.

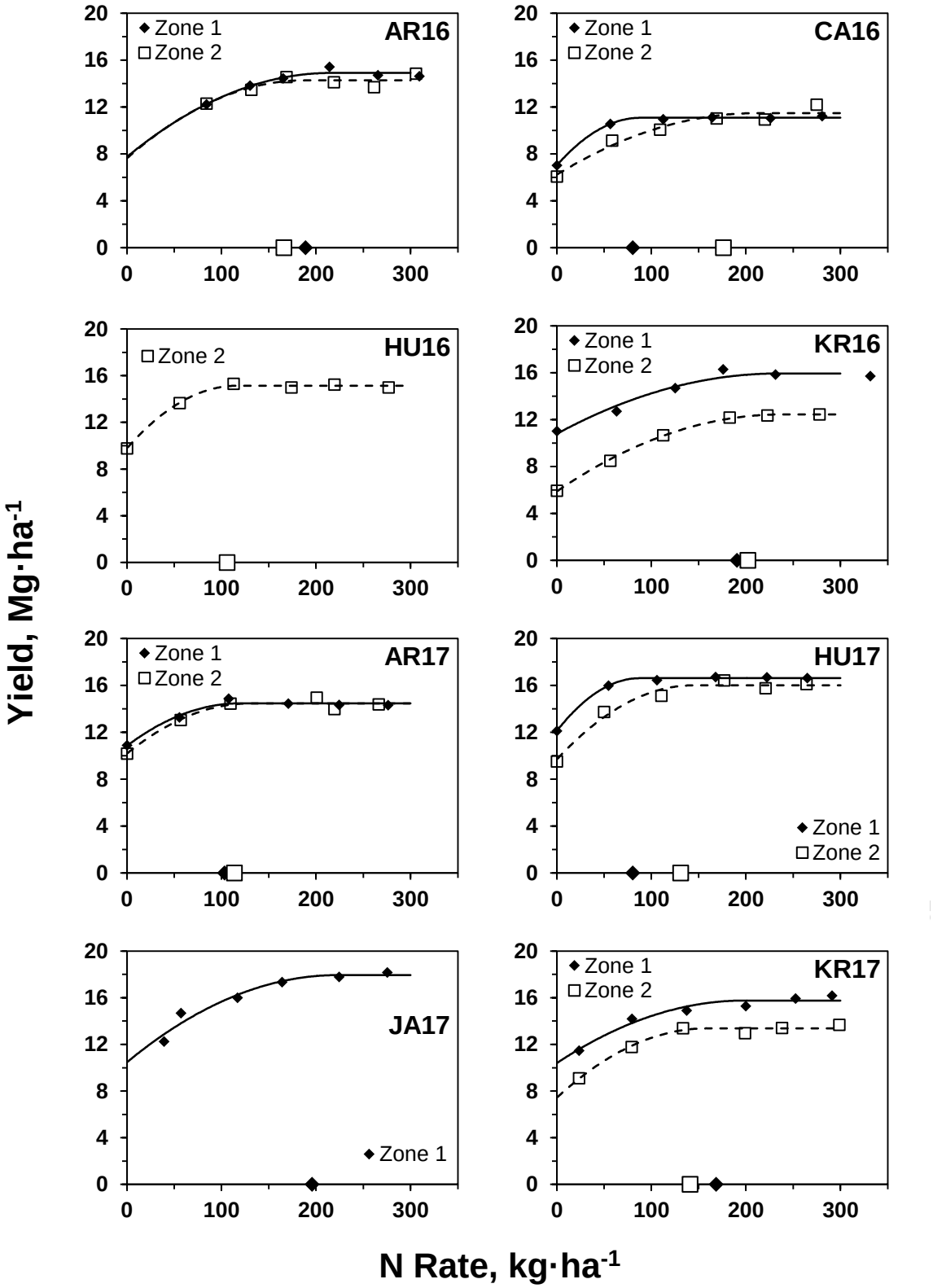

Fig. 2.8. Yield response to N rate by zone within each field. Zone 1 and 2 EONR is designated on the *x*-axis with the corresponding zone symbol.

Table 2.1. Field location, soil series, and soil classification for all fields.

Field ID	Year	Legal Description	Soil Series	Soil Great Group	Slope	SOM Range†
AR16	2016	T.14N-R.9E., Sec 19, NW ¼, N ½	Filbert silt loam	Vertic Argialbolls	0-1%	2.9-5.0%
			Tomek silt loam	Pachic Argiudolls	0-2%	
			Yutan silty clay loam	Mollic Hapludalfs	2-6%, eroded	
CA16	2016	T.9N-R.2E., Sec 19, NW ¼, W ½, S ½	Deroin silty clay loam	Mollic Hapludalfs	6-11%, severely eroded	1.9-3.6%
			Hastings silty clay loam	Udic Argiustolls	3-7%, eroded	
			Deroin silty clay loam	Mollic Hapludalfs	11-30%, severely eroded	
HU16	2016	T.9N-R.7W., Sec 4, SW ¼, E ½	Hastings silt loam	Udic Argiustolls	0-1%	1.9-3.8%
			Crete silt loam	Udertic Argiustolls	0-1%	
			Hastings silty clay loam	Udic Argiustolls	7-11%, eroded	
			Hastings silty clay loam	Udic Argiustolls	3-7%, eroded	
KR16	2016	T.16N-R.1E., Sec 21, NW ¼, S ½	Brocksburg sandy loam	Pachic Argiustolls	0-2%	0.6-1.7%
AR17	2017	T.14N-R.9E., Sec 20, SW ¼, W ½	Yutan silty clay loam	Mollic Hapludalfs	2-6%, eroded	1.9-4.7%
			Filbert silt loam	Vertic Argialbolls	0-1%	
			Tomek silt loam	Pachic Argiudolls	0-2%	
HU17	2017	T.9N-R.8W, Sec 1, NE ¼, N ½	Hastings silt loam	Udic Argiustolls	0-1%	2.2-4.4%
			Hastings silt loam	Udic Argiustolls	1-3%	
JA17	2017	T.16N-R.4W, Sec 7, SE ¼, S ½	Thurman loamy fine sand	Udorthentic Haplustolls	2-6%	0.9-3.1%
			Loretto-Thurman complex	Udic Argiustolls	1-3%	
			Thurman loamy fine sand	Udorthentic Haplustolls	2-6%, eroded	
KR17	2017	T.16N-R.1E., Sec 16, SW ¼, S ½	Thurman loamy fine sand	Udorthentic Haplustolls	2-6%	0.7-2.0%
			Brocksburg sandy loam	Pachic Argiustolls	0-2%	

† Soil organic matter content (%). 25 soil samples per site at 20-cm depth.

Table 2.2. Producer management practices for all fields.

Field ID	Tillage†	Previous Crop	Planting Date	Hybrid	Seeding Rate	Producer Field N Rate	Harvest Date
					seeds·ha^{-1}	kg·ha^{-1}	
AR16	NT	Soybean	5/5/16	Pioneer 1197AM	76,600	195	10/15/16
CA16	NT	Maize	5/19/16	Golden Harvest G07B39-311A	74,130	245	10/20/16
HU16	ST	Maize	5/6/16	Pioneer 1105AM	81,540	245	10/11/16
KR16	NT	Soybean	4/24/16	Pioneer 33D53AM	79,070	188	10/15/16
AR17	NT	Soybean	4/25/17	DeKalb 62-98	81,510	202	10/16/17
HU17	ST	Maize	4/25/17	Pioneer 1306WHR	83,030	235	10/18/17
JA17	NT	Soybean	5/5/17	Pioneer 1690	74,100	163	10/17/17
KR17	NT	Soybean	4/23/17	Pioneer 1498	80,560	244	10/17/17

† NT: no-till; ST: strip-till

Table 2.3. Nitrogen management practices, plot design information, and field characteristics for all fields.

Field ID	Base N Application			In-Season N Application			Elevation Difference (m)	Plot Width (m)	Number of Treatment Blocks	Mean yield at EONR§
	Date	Crop Growth Stage†	Source‡	Date	Crop Growth Stage†	Source‡				
AR16	3/17/16	Pre-plant	Anhydrous ammonia	6/24/16	V9	28% UAN	4.4	6.1	10	14.5
CA16	6/6/16	V2	28% UAN	7/19/16	VT	28% UAN	20.0	6.1	13	11.3
HU16	6/17/16	V5	28% UAN	7/11/16	V13	28% UAN	8.5	9.1	15	15.0
KR16	6/7/16	V5	32% UAN	6/24/16	V10	32% UAN	4.8	6.1	16	12.8
AR17	6/1/17	V4	28% UAN	6/23/17	V11	28% UAN	4.0	6.1	12	14.3
HU17	6/8/17	V4	28% UAN	7/5/17	V13	28% UAN	5.1	4.6	14	16.4
JA17	6/2/17	V3	30% UAN	6/28/17	V11	32% UAN	7.0	6.1	16	17.9
KR17	6/2/17	V4	32% UAN	6/29/17	V11	32% UAN	2.9	6.1	16	14.0

† Number of collared leaves

‡ UAN = urea-ammonium nitrate solution

§ EONR = economic optimum nitrogen rate

Table 2.4. Yield response to N rate models for all treatment blocks.

Field	Rep	Quadratic Model			N Rate at Maximum Yield	Maximum Yield	EONR	Yield at EONR	ESS	TSS	RMSE	r^2
		a	b	c	kg·ha^{-1}	Mg·ha^{-1}	kg·ha^{-1}	Mg·ha^{-1}			Mg·ha^{-1}	
AR16	1	.	.	.	.	14.64	.	.	.	.	.	.
	2	.	.	.	.	15.47	.	.	.	.	.	.
	3	7.62	0.0708	-0.000190	186	14.22	165	14.13	0.8437	4.1215	0.46	0.80
	4	.	.	.	.	15.65	.	.	.	.	.	.
	5	.	.	.	.	15.37	.	.	.	.	.	.
	6	12.36	0.0060	.	.	14.71	.	.	0.5938	2.1356	0.39	0.72
	7	.	.	.	.	16.12	.	.	.	.	.	.
	8	7.75	0.0663	-0.000150	221	15.08	193	14.96	0.4014	6.0149	0.32	0.93
	9	10.80	0.0142	.	.	15.13	.	.	1.8721	8.9568	0.68	0.79
	10	11.66	0.0108	.	.	15.26	.	.	2.6992	6.6448	0.82	0.59
CA16	1	4.68	0.0534	-0.000090	297	12.60	251	12.41	0.3526	43.7206	0.30	0.99
	2	5.93	0.0784	-0.000310	126	10.89	113	10.83	2.3703	22.1658	0.77	0.89
	3	.	.	.	.	11.81	.	.	.	.	.	.
	4	8.08	0.0247	-0.000040	309	11.89	205	11.47	2.0394	12.7057	0.71	0.84
	5	7.16	0.0539	-0.000180	150	11.20	127	11.10	1.9798	16.0279	0.70	0.88
	6	9.07	0.0342	-0.000140	122	11.16	93	11.04	0.013	3.5955	0.06	1.00
	7	8.96	0.0087	.	.	11.77	.	.	3.1934	7.3633	0.89	0.57
	8	4.46	0.0811	-0.000250	162	11.04	146	10.97	0.8628	34.7939	0.46	0.98
	9*	6.03	0.0402	-0.000077	262	11.31	208	11.08	0.61762	19.9682	0.45	0.97
	10	8.16	0.1613	-0.002000	40	11.41	38	11.41	1.7113	10.5345	0.76	0.84
	11	7.47	0.1788	-0.002000	45	11.47	43	11.46	0.8806	14.1845	0.54	0.94
	12*	7.94	0.0215	.	.	12.16	.	.	1.1609	15.7735	0.62	0.93
	13*	.	.	.	.	12.36	.	.	.	.	.	.

Field	Rep	Quadratic Model			N Rate at Maximum Yield	Maximum Yield	EONR	Yield at EONR	ESS	TSS	RMSE	r^2
		a	b	c	kg·ha^{-1}	Mg·ha^{-1}	kg·ha^{-1}	Mg·ha^{-1}			Mg·ha^{-1}	
HU16	1	.	.	.	.	15.41	.	.	.	.	.	.
	2*	.	.	.	.	16.37	.	.	.	.	.	.
	3	10.69	0.0853	-0.000400	107	15.24	96	15.19	0.9345	17.5419	0.48	0.95
	4	9.61	0.2064	-0.002000	52	14.94	50	14.93	4.1492	27.7987	1.18	0.85
	5	.	.	.	.	16.36	.	.	.	.	.	.
	6	8.75	0.0680	-0.000240	142	13.57	124	13.50	0.6612	19.1305	0.41	0.97
	7	6.95	0.1042	-0.000390	134	13.91	123	13.87	4.6773	43.4414	1.08	0.89
	8	.	.	.	.	16.80	.	.	.	.	.	.
	9	.	.	.	.	16.08	.	.	.	.	.	.
	10	.	.	.	.	16.75	.	.	.	.	.	.
	11	13.64	0.0069	.	.	15.43	.	.	0.6615	3.2831	0.41	0.80
	12	.	.	.	.	16.15	.	.	.	.	.	.
	13	.	.	.	.	17.25	.	.	.	.	.	.
	14	8.92	0.1268	-0.000550	115	16.23	108	16.20	1.0734	43.4645	0.52	0.98
	15	11.02	0.0437	-0.000090	243	16.32	197	16.14	3.6349	26.3294	0.95	0.86
KR16	1	10.79	0.0438	-0.000093	235	15.94	191	15.75	0.7916	21.6562	0.51	0.96
	2*	9.55	0.0725	-0.000261	139	14.58	123	14.51	0.9382	20.2023	0.56	0.95
	3	7.91	0.0260	.	.	14.84	.	.	3.4606	42.3802	0.93	0.92
	4*	6.63	0.0479	-0.000115	208	11.60	172	11.45	1.4561	20.0069	0.70	0.93
	5	6.85	0.0625	-0.000130	240	14.36	209	14.23	1.2979	44.4320	0.57	0.97
	6*	8.64	0.0210	.	.	15.94	.	.	3.3670	27.6042	1.06	0.88
	7*	7.77	0.0614	-0.000126	244	15.27	211	15.14	0.2056	43.4994	0.26	1.00
	8	4.75	0.0783	-0.000170	230	13.77	206	13.67	8.2636	70.4994	1.44	0.88
	9	5.75	0.0259	.	.	12.60	.	.	3.5806	38.3504	0.95	0.91
	10	4.51	0.0610	-0.000120	254	12.26	220	12.12	4.2810	51.7127	1.03	0.92

Field	Rep	Quadratic Model			N Rate at Maximum Yield	Maximum Yield	EONR	Yield at EONR	ESS	TSS	RMSE	r^2
		a	b	c	kg·ha^{-1}	Mg·ha^{-1}	kg·ha^{-1}	Mg·ha^{-1}			Mg·ha^{-1}	
	11*	5.54	0.0425	-0.000079	268	11.23	216	11.01	1.5708	23.4229	0.72	0.93
	12	4.82	0.0676	-0.000190	178	10.83	156	10.74	0.3797	27.7944	0.31	0.99
	13	4.87	0.0370	-0.000080	231	9.15	180	8.93	0.1627	16.8716	0.20	0.99
	14	4.11	0.0803	-0.000220	183	11.44	164	11.36	0.6818	44.9332	0.41	0.98
	15	5.94	0.0706	-0.000200	177	12.17	156	12.09	1.9986	32.0714	0.71	0.94
	16	7.89	0.0540	-0.000090	300	15.99	254	15.80	1.1970	52.8749	0.55	0.98
AR17	1	No	Data									
	2	No	Data									
	3	No	Data									
	4	12.37	0.0199	.	.	19.20	.	.	8.0707	28.5921	1.42	0.72
	5	10.45	0.0178	.	.	15.86	.	.	11.0927	29.2539	1.67	0.62
	6*	11.72	0.0294	-0.000078	189	14.50	136	14.28	0.6216	6.7372	0.46	0.91
	7	9.94	0.0965	-0.000530	91	14.33	83	14.30	0.6183	16.233	0.39	0.96
	8	13.43	0.0089	.	.	16.46	.	.	1.7349	5.4478	0.66	0.68
	9*	14.92	0.0057	.	.	18.55	.	.	0.8814	2.7174	0.54	0.68
	10	9.78	0.0631	-0.000200	158	14.76	137	14.67	1.4802	20.435	0.61	0.93
	11*	10.43	0.1169	-0.000954	61	14.01	57	13.99	0.0180	10.2597	0.08	1.00
	12*	11.33	0.0143	.	.	16.14	.	.	2.3382	11.0691	0.88	0.79
HU17	1	12.12	0.0641	-0.000220	146	16.79	127	16.71	1.8507	18.8236	0.68	0.90
	2	11.18	0.2247	-0.002113	53	17.15	51	17.14	1.4497	31.1586	0.70	0.95
	3	12.44	0.1829	-0.002000	46	16.63	44	16.62	0.1657	14.7368	0.24	0.99
	4	11.52	0.0728	-0.000230	158	17.28	140	17.21	1.6951	27.5593	0.65	0.94
	5	12.44	0.0567	-0.000160	177	17.46	151	17.36	0.4600	20.6385	0.34	0.98
	6	10.82	0.1594	-0.000993	80	17.22	76	17.20	0.5260	33.5889	0.42	0.98
	7*	12.70	0.0739	-0.000379	98	16.30	87	16.26	1.0516	10.8076	0.59	0.90

Field	Rep	Quadratic Model			N Rate at Maximum Yield	Maximum Yield	EONR	Yield at EONR	ESS	TSS	RMSE	r^2
		a	b	c	kg·ha^{-1}	Mg·ha^{-1}	kg·ha^{-1}	Mg·ha^{-1}			Mg·ha^{-1}	
	8	12.04	0.1615	-0.002000	40	15.30	38	15.29	0.9157	9.7751	0.55	0.91
	9	8.28	0.1617	-0.000870	93	15.79	88	15.77	1.7769	49.2821	0.67	0.96
	10	11.83	0.0414	-0.000120	173	15.40	138	15.26	1.6166	13.0564	0.64	0.88
	11*	7.24	0.0943	-0.000260	181	15.78	165	15.71	0.7276	53.3193	0.49	0.99
	12	12.32	0.0588	-0.000200	147	16.64	126	16.56	0.1457	15.2115	0.19	0.99
	13*	13.57	0.0532	-0.000242	110	16.49	93	16.42	0.4287	6.8331	0.38	0.94
	14	8.14	0.1029	-0.000330	156	16.16	143	16.11	2.0891	54.9824	0.72	0.96
JA17	1	14.12	0.0134	.	.	17.91	.	.	3.8036	11.5934	0.98	0.67
	2	13.42	0.0239	.	.	21.47	.	.	6.2859	31.6302	1.25	0.80
	3	.	.	.	.	18.19	.	.	.	.	.	.
	4	14.92	0.0310	.	.	24.01	.	.	1.2394	45.2830	0.56	0.97
	5	.	.	.	.	18.72	.	.	.	.	.	.
	6	.	.	.	.	18.87	.	.	.	.	.	.
	7	15.75	0.0181	.	.	20.88	.	.	11.2172	26.6296	1.67	0.58
	8	.	.	.	.	21.44	.	.	.	.	.	.
	9	.	.	.	.	20.95	.	.	.	.	.	.
	10	12.02	0.0243	.	.	18.19	.	.	10.5658	37.4477	1.63	0.72
	11	9.25	0.0688	-0.000148	233	17.27	205	17.15	2.7426	31.6184	0.96	0.91
	12	11.68	0.0653	-0.000150	218	18.79	190	18.67	0.9702	20.8846	0.49	0.95
	13	.	.	.	.	18.43	.	.	.	.	.	.
	14*	.	.	.	.	21.39	.	.	.	.	.	.
	15	14.69	0.0151	.	.	18.47	.	.	3.4298	13.4622	0.93	0.75
	16	10.53	0.0155	.	.	14.79	.	.	3.5929	14.1226	0.95	0.75
KR17	1	8.51	0.0560	-0.000140	200	14.11	170	13.99	1.6953	16.5799	0.65	0.90
	2	7.32	0.1072	-0.000370	145	15.08	134	15.04	3.7628	27.4803	0.97	0.86

Field	Rep	Quadratic Model			N Rate at Maximum Yield	Maximum Yield	EONR	Yield at EONR	ESS	TSS	RMSE	r^2
	3	7.31	0.0722	-0.000210	172	13.52	152	13.43	0.4683	17.2993	0.34	0.97
	4	5.94	0.0956	-0.000320	149	13.08	136	13.03	0.9839	20.9229	0.50	0.95
	5	8.36	0.0549	-0.000160	172	13.07	146	12.96	1.0600	10.3011	0.51	0.90
	6	6.16	0.1105	-0.000430	128	13.26	119	13.22	0.9852	19.1401	0.50	0.95
	7	6.16	0.0878	-0.000280	157	13.04	142	12.98	1.8028	21.2045	0.67	0.91
	8	10.83	0.0126	.	.	14.55	.	.	2.4176	10.6158	0.78	0.77
	9	8.26	0.0424	-0.000090	236	13.25	190	13.06	1.2454	12.6892	0.56	0.90
	10	11.88	0.0150	.	.	16.31	.	.	4.3697	17.2803	1.05	0.75
	11	9.84	0.0646	-0.000160	202	16.36	176	16.25	4.3923	26.0778	1.05	0.83
	12	12.66	0.0338	-0.000060	282	17.42	213	17.14	1.0193	11.8296	0.50	0.91
	13	8.95	0.0561	-0.000160	175	13.87	149	13.76	1.2012	12.5816	0.55	0.90
	14	10.19	0.0159	.	.	14.95	.	.	3.0219	16.4045	0.87	0.82
	15	.	.	.	.	11.77	.	.	.	.	.	.
	16	8.40	0.0638	-0.000230	139	12.82	121	12.75	1.2089	8.8998	0.55	0.86

*One outlier observation removed

Table 2.5. Pearson correlation coefficients of soil and topographic variables to check plot yield and in-season NDRE measurements across all fields (Global Approach) (n = 108; for SOM n = 92).

			Apparent Electrical Conductivity		Soil Optical Reflectance		Landscape	
	Yield	**NDRE**	**EC_s**	**EC_d**	**SR_{soil}**	**SOM**	**$Elev_{rel}$**	**Slope**
Yield	1							
NDRE	0.67***	1						
EC_s	-0.01	-0.09	1					
EC_d	0.03	-0.13	0.94***	1				
SR_{soil}	-0.10	-0.14	-0.34***	-0.30**	1			
SOM	-0.04	0.04	0.65***	0.71***	-0.04	1		
$Elev_{rel}$	-0.17	-0.21*	0.52***	0.45***	-0.31**	0.22*	1	
Slope	-0.19	-0.25*	0.45***	0.33***	-0.38***	-0.07	0.65***	1

* Statistical significance at P < 0.05.
** Statistical significance at P < 0.01.
*** Statistical significance at P < 0.001.

Table 2.6. Pearson correlation coefficients of soil and topographic variables to in-season NDRE measurements for all nonzero plots across all fields (Global Approach) (n = 552; for SOM n = 472).

		Apparent Electrical Conductivity		Soil Optical Reflectance		Landscape	
	NDRE	**EC_s**	**EC_d**	**SR_{soil}**	**SOM**	**$Elev_{rel}$**	**Slope**
NDRE	1						
EC_s	-0.03	1					
EC_d	-0.05	0.95***	1				
SR_{soil}	-0.14***	-0.33***	-0.25***	1			
SOM	0.17***	0.64***	0.72***	0.00	1		
$Elev_{rel}$	-0.11*	0.58***	0.50***	-0.29***	0.24***	1	
Slope	-0.14**	0.46***	0.35***	-0.35***	-0.06	0.63***	1

* Statistical significance at P < 0.05.
** Statistical significance at P < 0.01.
*** Statistical significance at P < 0.001.

Table 2.7. Pearson correlation coefficients of soil and topographic variables to check plot yield and NDRE for all site-years (Field-Specific Approach). Bold data indicate select variables used in management zone delineation.

	Crop	N Rate		Electrical Conductivity		Soil Optical Reflectance		Landscape	
Field	**Parameter**	**kg·ha^{-1}**	***n***	**EC_s**	**EC_d**	**SR_{soil}**	**SOM**	**$Elev_{rel}$**	**Slope**
AR16	NDRE	84	60	**-0.66*****	**-0.61*****	0.25	0.43**	-0.56***	-0.34**
	Yield	84	10	**0.46**	**0.41**	-0.30	-0.40	0.28	0.21
CA16	NDRE	56	65	0.07	-0.06	0.01	0.06	**0.23**	-0.15
	NDRE	0	13	0.55	0.41	-0.20	0.36	**0.60***	-0.32
	Yield	0	13	0.43	0.41	0.30	-0.12	**0.43**	-0.18
HU16	NDRE	56	75	**-0.60*****	**-0.57*****	0.38***	0.41***	0.35**	-0.35**
	NDRE	0	12	**-0.63***	**-0.78****	0.44	0.52	0.51	-0.52
	Yield	0	12	**-0.64***	**-0.80****	0.42	0.51	0.46	-0.44
KR16	NDRE	56	80	**0.69*****	**0.66*****	-0.55***	-	0.14	0.05
	NDRE	0	16	**0.83*****	**0.67****	-0.65**	-	0.15	-0.17
	Yield	0	16	**0.91*****	**0.72****	-0.74**	-	0.22	-0.08
AR17	NDRE	56	52	-0.22	-0.18	-0.08	**0.16**	**-0.12**	0.14
	NDRE	0	11	-0.40	-0.27	0.44	**0.30**	**-0.77****	-0.23
	Yield	0	11	-0.55	-0.35	-0.24	**0.62***	**-0.36**	-0.36
HU17	NDRE	56	70	**-0.57*****	-0.34**	0.12	**0.68*****	-0.39**	-0.63***
	NDRE	0	14	**-0.79*****	-0.62*	-0.07	**0.73****	-0.40	-0.56*
	Yield	0	14	**-0.79*****	-0.56*	0.07	**0.73****	-0.21	-0.64*
JA17	NDRE	56	80	0.35**	0.18	-0.49***	**0.50*****	-0.14	-0.18
	NDRE	39	16	0.40	0.31	-0.47	**0.47**	-0.30	-0.45
	Yield	39	16	0.19	0.27	0.07	**-0.02**	-0.20	-0.15
KR17	NDRE	80	80	**0.45*****	**0.26***	-0.30**	0.44***	0.12	-0.36**
	NDRE	24	16	**0.53***	**0.46**	-0.52*	0.50*	-0.14	-0.54*
	Yield	24	16	**0.85*****	**0.84*****	-0.08	-0.03	0.42	0.22

* Statistical significance at $P < 0.05$.

** Statistical significance at $P < 0.01$.

*** Statistical significance at $P < 0.001$.

Table 2.8. Soil chemical properties for delineated MZ. Soil samples were collected from the 0 to 20 cm depth. Statistically different MZ are indicated with the appropriate significance level indicator.

Field	MZ	*n*	pH	Mehlich-III P	SOM	CEC
				$mg \cdot kg^{-1}$	$g \cdot g^{-1}$	$cmol_c \cdot kg^{-1}$
AR16	1	14	6.01	67.6*	3.99	16.7**
	2	11	6.08	29.9*	3.84	20.8**
CA16	1	15	5.94	24.4	3.10	20.5
	2	10	5.98	22.7	2.81	18.4
HU16	1	11	5.79*	46.9	3.17**	14.6**
	2	14	6.07*	55.1	2.69**	18.2**
KR16	1	4	5.98	155.0	1.40**	7.3**
	2	14	5.59	65.6	0.81**	4.4**
AR17	1	19	6.47	14.8	3.05	18.9
	2	6	6.62	7.7	2.78	21.4
HU17	1	15	6.01	23.8	3.41	17.6**
	2	10	6.28	14.8	3.22	19.8**
JA17	1	13	6.05	45.3	1.80**	10.2**
	2	12	6.08	44.3	1.06**	6.7**
KR17	1	9	6.74	17.1	1.38	8.0
	2	16	6.72	25.3	1.08	6.1

*Statistical significance at $p < 0.05$.
**Statistical significance at $p < 0.01$.

Table 2.9. Yield response to N rate models by zone. Fields HU16 and JA17 did not have any blocks fitting a quadratic-plateau function in one of their zones, so comparisons could not be made.

Field	Zone	Quadratic Model			N Rate at Max Yield	Max Yield	EONR	Yield at EONR	ESS	TSS	RMSE	r^2	Difference Between Zones†
		a	b	c	kg·ha^{-1}	Mg·ha^{-1}	kg·ha^{-1}	Mg·ha^{-1}					
AR16	1	7.75	0.0663	-0.000154	216	14.90	189	14.79	0.4015	6.0149	0.32	0.93	NS
	2	7.62	0.0708	-0.000188	188	14.27	166	14.18	0.8437	4.1215	0.46	0.80	
CA16	1	7.02	0.0918	-0.000519	88	11.08	80	11.05	0.0394	13.2782	0.10	1.00	NS
	2	6.23	0.0496	-0.000117	212	11.48	176	11.33	1.0882	22.9005	0.52	0.95	
HU16	1	.	.	.	.	.	.	.	.	.	.	.	-
	2	9.78	0.0921	-0.000396	116	15.14	106	15.10	0.0777	23.1395	0.14	1.00	
KR16	1	10.79	0.0438	-0.000093	235	15.93	191	15.75	0.7916	21.6562	0.44	0.96	***
	2	5.88	0.0552	-0.000116	238	12.44	202	12.29	0.0376	34.7155	0.10	1.00	
AR17	1	10.84	0.0606	-0.000253	120	14.47	103	14.40	0.2593	10.7858	0.25	0.98	NS
	2	10.17	0.0659	-0.000253	130	14.46	114	14.39	0.5071	15.1901	0.36	0.97	
HU17	1	12.11	0.1027	-0.000586	88	16.61	81	16.58	0.0447	16.2871	0.11	1.00	**
	2	9.68	0.0874	-0.000302	145	16.00	131	15.94	0.7416	33.5209	0.43	0.98	
JA17	1	10.47	0.0669	-0.000150	223	17.94	196	17.83	1.3068	25.5128	0.57	0.95	-
	2	.	.	.	.	.	.	.	.	.	.	.	
KR17	1	10.39	0.0539	-0.000135	199	15.76	169	15.63	0.7065	14.8252	0.42	0.95	***
	2	7.43	0.0750	-0.000236	159	13.37	141	13.30	0.3099	15.2573	0.28	0.98	

† NS: Not significant at $\alpha = 0.05$.

** Statistical significance at $p < 0.01$.

*** Statistical significance at $p < 0.001$.

CHAPTER 3: EVALUATING THE POTENTIAL OF AN INTEGRATED MANAGEMENT ZONE-CANOPY SENSOR APPROACH FOR IMPROVED NITROGEN MANAGEMENT IN MAIZE

ABSTRACT

Active crop canopy sensors and soil-based management zones (MZ) are tools that can be used to direct variable-rate, in-season nitrogen (N) fertilizer applications in maize (*Zea mays* L.). Some have suggested the integration of these two methods may improve performance of sensor-based N application algorithms through increased N use efficiency (NUE) and profitability. The objectives of this research study were to (1) test a sensor-based N application algorithm compared to uniform N management in a variety of soil conditions and (2) evaluate the potential of an integrated MZ- and sensor-based N management approach compared to sensor-based N management alone. Research was carried out on eight irrigated maize fields in east central Nebraska during the 2016 and 2017 growing seasons. Three N treatments were applied in field-length strips in a RCBD with 6 replications per field. Canopy reflectance and yield data were collected, and partial factor productivity of N was calculated for each treatment. Sensor-based application resulted in significantly increased NUE compared to uniform N management in six of eight fields. Marginal net return was significantly increased in four of eight fields. Management zones delineated using field-specific soil and topographic variables accurately characterized spatial variability in in-season N status in four of eight fields. Integrating MZ with a sensor-based approach has the potential to further increase NUE and economic return in fields with high spatial variability in soils and topography. Future research should

seek to modify current sensor algorithms to allow for incorporation of MZ and validate this practice compared to sensor-based N management.

Abbreviations: EC_a, apparent electrical conductivity; EONR, economic optimum nitrogen rate; MZ, management zones; NDRE, normalized difference red edge; NIR, near-infrared; NUE, nitrogen use efficiency; RE, red edge; RMSE, root mean square error; SI, sufficiency index; SOM, soil organic matter.

INTRODUCTION

As the most widely grown crop in the US and the largest user of nitrogen (N) fertilizer (Morris et al., 2018), maize is often the target of environmental impact policies where N is concerned (Snyder, 2012). Fertilizer N use in cereal production is historically inefficient, with estimates of maize N use efficiency (NUE) ranging from 35 to 75% (Morris et al., 2018). Applied N fertilizer that is not taken up by the crop is subject to numerous loss mechanisms, including denitrification, volatilization, and leaching (Cassman et al., 2002). Low NUE over time has resulted in severe environmental consequences in several regions of the US.

Low NUE in maize production can be attributed to three major factors: (1) poor synchrony between soil N supply and crop demand (Shanahan et al., 2008), (2) applying uniform rates of fertilizer N to spatially variable landscapes, and (3) failure to account for temporal variability in crop response to N. Collectively, these three factors make accurate estimation of EONR difficult for many fields. Innovative N management strategies that can account for these factors are needed to increase NUE and mitigate detrimental environmental impacts.

Delineating fields into management zones (MZ) is one method for managing within-field variability to increase NUE. Management zones are regions of a field with homogenous soil and landscape attributes, resulting in similar yield-limiting factors and corresponding uniform levels of crop inputs (Doerge, 1999). Myriad approaches to MZ delineation have been developed in the last 25 years (Khosla et al., 2010). Some common attributes that have been used—either individually or in combination—for MZ delineation include soil apparent electrical conductivity (EC_a) (Kitchen et al., 1999;

Fleming et al., 2004), yield maps (Flowers et al., 2005), imagery (Schepers et al., 2004), topography (Fraisse et al., 2001), and soil survey maps (Franzen et al., 2002). The classification methods used to delineate MZ are also numerous. Among them is a free software program called Management Zone Analyst (MZA) (University of Missouri, USDA-ARS, Columbia, MO), which uses a fuzzy *c*-means (or *k*-means) algorithm for clustering (Fridgen et al., 2004).

While managing N through the use of MZ often improves efficiency compared to uniform field management by helping to characterize the spatial variability in soil physical and chemical properties, MZ are often inconsistent in characterizing the spatial variability in crop N requirement because of the effect of temporal variability on crop N response (Shanahan et al., 2008). In a five-year study in Nebraska, Schepers et al. (2004) found temporal variability to greatly affect MZ, and the use of MZ to direct variable N application would have been appropriate in only three of five years. They concluded that a static, soil-based MZ approach alone is likely inadequate for directing variable applications of N due to the inability to account for temporal variability.

One tool with the potential to manage all three factors causing low NUE is crop canopy sensing. This strategy is known as a reactive approach to N fertilizer management because the sensors can identify and correct N stress that has already occurred during the growing season (Ping et al., 2008). Rather than using indirect measures of growing condition from the soil or from atmospheric conditions, canopy sensors use the crop itself as a bio-indicator to assess crop N status and direct real-time, variable-rate, in-season applications of N fertilizer (Adamchuk et al., 2011). Canopy sensors have been used successfully to direct in-season variable-rate N fertilizer applications in several crops,

including maize (Holland and Schepers, 2010), wheat (Solie et al., 2012), cotton (Oliveira et al., 2013), rice (Tubaña et al., 2012), and sugarcane (Amaral et al., 2015).

Active crop canopy sensors emit modulated light in two or more wavelengths in the visible (400-700 nm) and near-infrared (NIR) (750-1400 nm) regions of the electromagnetic spectrum, and measure the reflectance from the crop canopy with photodetectors. Reflectance in these wavelengths is combined into vegetation indices, which are well correlated with chlorophyll content and N sufficiency (Walburg et al., 1982). In order to assess crop N status, canopy reflectance of plants yet to be fertilized is compared to reflectance from plants receiving an adequate amount of N fertilizer such that N is not a limiting factor (Shanahan et al., 2008). This N-sufficient reference is used to calculate a ratio known as the Sufficiency Index (SI) (Peterson et al., 1993). Essentially, lower SI values signify that unfertilized plants are more deficient, and so will require more N fertilizer to achieve their yield potential (Shanahan et al., 2008).

Numerous algorithms have been developed to convert sensor reflectance data into an in-season N fertilizer application rate (Scharf et al., 2011; Solie et al., 2012; Franzen et al., 2014). Holland and Schepers (2010) developed a generalized N application algorithm for use with crop canopy sensors. The algorithm uses an estimated optimum N rate (N_{OPT}) along with the calculated SI to control the yield response model. It also allows for incorporating economics into the N_{OPT} term and accounts for fertilizer N already applied as well as any N credits.

The use of these systems to direct variable-rate, in-season N fertilizer applications in cereal cropping systems has resulted in positive environmental and economic returns (Kitchen et al., 2010; Roberts et al., 2010). However, crop canopy sensors and their

corresponding algorithms are not without their limitations. With no direct knowledge of the soil and topographic characteristics underneath the growing crop, the sensor cannot accurately predict how spatial variability may affect future N mineralization or losses that are not expressed in the crop at the time of sensing. This lack of soil-based information has resulted in poor algorithm performance in certain subfield regions due to local spatial variability (Ferguson, unpublished data, 2015). Researchers agree that refinements are needed in order to account for additional management, soil, and climatic factors (Shanahan et al., 2008), combining both anticipatory and reactive decision-making (Ping et al., 2008). Schepers et al. (2004) and others (Holland and Schepers, 2010; Solari et al., 2008) have suggested combining MZ and in-season crop canopy sensing to better predict the EONR throughout the field and achieve greater NUE.

Roberts et al. (2012) experimented with an integrated MZ and canopy sensor approach on six irrigated fields in Nebraska, USA and found potential for this integrated approach to increase NUE and economic return over current management practices, particularly in silt loam fields with eroded slopes. However, they believed further research was needed to further refine current algorithms and explore how to best integrate the two N management strategies. The objectives of this research study were to (1) test a sensor-based N application algorithm compared to uniform N management in a variety of soil conditions and (2) evaluate the potential of an integrated MZ- and sensor-based N management approach compared to sensor-based N management alone.

MATERIALS AND METHODS

Research Fields

Experiments were conducted on eight maize fields, all center-pivot irrigated, during the 2016 (Fields AR16, CA16, HU16, and KR16) and 2017 (Fields AR17, HU17, JA17, and KR17) growing seasons. Fields were located in east central Nebraska, USA (Fig. 3.1). Fields AR16, KR16, AR17, HU17, and KR17 were relatively flat (< 5 m of relief), while there were substantial differences in elevation (~7-20 m) and topography for Fields CA16, HU16, and JA17. The sites were grouped into four classifications based on soil texture and topography: sandy loam, relatively level (KR16 and KR17), silt loam, relatively level (AR16, AR17, HU17), silt loam, eroded slopes (CA16 and HU16), and sandy loam, eroded slopes (JA17). One to four soil series were represented at each site (Table 3.1).

Experimental Treatments

Tillage practices, crop rotation, hybrid selection, planting date, seeding rate, irrigation, and other field management decisions and operations were managed by individual producers (Table 3.2). The eight fields in the study were part of a larger three-year study of 54 fields that compared a commercially-available active-sensor system to producer-chosen N rates. Results for the eight fields with additional small plot N treatments (Chapter 2) were used to compare an integrated MZ-sensor approach to sensor-based application alone and to uniform N management.

There were three N application treatments:

1. ~84 kg·ha^{-1} early season base rate + sensor-based variable-rate N (Sensor)
2. Producer-selected uniform N rate (Uniform)

3. High-N reference (N Ref)

Nitrogen rate and application timing for Treatment 2 were decided by individual producers. Treatment 3 provided a non-limiting area for implementation of the sensor algorithm, receiving 252 or 280 kg $N \cdot ha^{-1}$. Nitrogen rates and timing for each field are shown in Table 3.3. The experimental design consisted of field-length strips in a RCBD with four replications of Treatments 1 and 2 and two replications of Treatment 3. Treatment strips were 8, 12, or 16 rows wide, depending on the width of the producers' equipment (Table 3.2). An experimental design map for Field HU16 is shown in Figure 3.2, and treatment maps for all fields can be located in Appendix 1.

Sensor-based N application was carried out using a commercially-available, on-the-go active crop canopy sensing system called OptRx (Ag Leader Technology, Ames, IA). Four OptRx sensors were mounted on the front of a Hagie DTS 10 high-clearance applicator (Hagie Manufacturing Co., Clarion, IA) approximately 0.3 to 0.6 m above the crop canopy. The sensors were positioned over rows 4, 7, 9, and 12 for the 16-row strips. For the 8-row and 12-row studies, only two sensors were utilized. They were positioned over rows 5 and 7 for the 12-row studies and over rows 3 and 5 for the 8-row study. Nitrogen fertilizer was applied with a high-clearance applicator (Hagie DTS 10, Hagie Manufacturing Co., Clarion, IA), and the fertilizer was applied through a straight stream nozzle between each row. Flow rate was controlled with a pulse-width modulation spray rate controller (PinPoint, Capstan Ag Systems, Topeka, KS).

Sensor reflectance in the red-edge (RE; 730 nm) and NIR (780 nm) wavelengths was used to calculate the normalized difference red edge (NDRE) vegetation index using the following equation (Gitelson and Merzylak, 1994):

$$NDRE = \frac{NIR_{780} - RE_{730}}{NIR_{780} + RE_{730}} \quad [3.1]$$

The NDRE values were then related to a reference value of plants receiving an adequate amount of N fertilizer such that N is not a limiting factor. These NDRE values are used to calculate a Sufficiency Index (SI) with the following equation (Peterson et al., 1993):

$$SI = \frac{VI_{Target}}{VI_{Reference}} \quad [3.2]$$

where

$0 \leq SI \leq 1$

VI_{Target} = vegetation index of target crop

$VI_{Reference}$ = vegetation index of high-N reference

The OptRx system uses a virtual-reference approach to determine the value for $VI_{Reference}$. This statistical approach involves driving over a portion of the field for five minutes, observing a wide range of plant vigor and N status. The 95th percentile value is selected from a histogram of NDRE values, and this value is used as $VI_{Reference}$ to generate the SI (Holland and Schepers, 2013).

Nitrogen rate was determined using the OptRx algorithm controlled by the Ag Leader monitor in the high-clearance applicator. This algorithm is a slightly modified version of the Holland and Schepers algorithm and takes the following form (Holland and Schepers, 2010):

$$N_{APP} = (N_{OPT} - N_{PreFert} - N_{CRD}) \cdot \sqrt{\frac{(1-SI)}{\Delta SI}} \quad [3.3]$$

where

N_{APP} = N application rate

N_{OPT} = the EONR or the maximum N rate prescribed by producers

$N_{PreFert}$ = the sum of fertilizer N applied before sensor-based N application

N_{CRD} = N credit for previous crop, NO_3^- in irrigation water, manure application, etc.

SI = Sufficiency Index of target crop

$\Delta SI = 1 - SI(0)$; the difference between $SI = 1$ and the *y*-intercept of the N response curve; set to default of 0.7

The N_{OPT} term was calculated using Maize-N (NUtech Ventures, Lincoln, NE), a simulation model for estimating EONR for maize. Maize-N uses N uptake efficiency, expected yield response, grain and fertilizer prices, and soil N mineralization to estimate EONR (Setiyono et al., 2011). To avoid double-counting of N credits, only nitrate in irrigation water was used for the N_{CRD} term. Minimum and maximum N rates of 34 and 336 kg N·ha^{-1} were implemented to place limits on the sensor algorithm when necessary.

Nitrogen source for all sensor-based treatments was either 28 or 32% urea ammonium nitrate (UAN) solution (Table 3.3). Nitrogen fertilizer was applied simultaneously with sensing using the high-clearance applicator, with the fertilizer applied through a straight stream nozzle between each row. Fertilizer application data were collected with a flowmeter at a rate of 1 Hz. Fifteen m of data points were removed from each end of the field for each pass.

Field Data Collection

Soil Data

Spatial soil data collected for each field included soil apparent electrical conductivity (EC_a) and soil optical reflectance (red and NIR bands). These attributes were

collected for each field prior to planting (except for Field HU17, for which data were collected following harvest) using a Veris MSP3 on-the-go soil sensing platform (Veris Technologies, Inc., Salina, KS). The MSP3 instrument uses two arrays of coulter-electrode pairs to measure soil EC_a at depths of 0 to 0.3 m (shallow EC—EC_s) and 0 to 0.9 m (deep EC—EC_d) simultaneously. The MSP3 also measures soil optical reflectance with an active optical sensor located ~5 cm deep in the soil measuring in red and near-infrared (NIR) wavelengths. The simple ratio (SR_{soil}) $\left(\frac{NIR}{Red}\right)$ was calculated from the reflectance readings. 25 soil samples were collected to a depth of 20 cm across the range of EC_{sh} and reflectance values for the field, and results were used by Veris Technologies to calibrate the optical reflectance readings to estimate soil organic matter (SOM). A global positioning system (GPS) receiver was mounted on the MSP3 sensor to log geographic coordinates as the instrument made parallel passes ~18 m apart throughout the field.

Elevation for each field as 2-m Digital Elevation Model grids was retrieved from the Nebraska Department of Natural Resources (NeDNR) LiDAR Repository (NeDNR, 2010). Elevation data for the experimental sites was collected in 2009 (Fields CA16, HU16, and HU17) and 2010 (Fields AR16, KR16, AR17, JA17, and KR17). Relative elevation ($Elev_{rel}$) was calculated for each field by subtracting all grids by the minimum elevation within the field. Slope was calculated using the Spatial Analyst package in ArcMap 10.4 (ESRI, Redlands, CA). Summary statistics for the spatial data can be found in Appendix 1.

All spatial data were projected into the Universal Transverse Mercator (UTM) Zone 14N (NAD83 Datum) projection. To obtain values of each data layer for the entire

field study, ordinary kriging was used to interpolate each layer (EC_s, EC_d, SR_{soil}, OM, $Elev_{rel}$, and Slope). Interpolation was conducted using the Geostatistical Analyst package in ArcMap 10.4.

Crop Response Data

In addition to the four OptRx active canopy sensors directing the sensor-based N fertilizer application, canopy reflectance was measured with an additional OptRx sensor and logged with a GeoSCOUT X data logger (Holland Scientific, Lincoln, NE). The NDRE vegetation index was calculated from this reflectance data. This sensor was also mounted to the front of the high-clearance applicator approximately 0.3-0.6 m above the crop canopy. The sensor was positioned over either of the center two rows of each strip in the nadir view. Canopy reflectance measurements were collected at a rate of 1 Hz while the vehicle traveled at a speed of ~3 to 5 $m \cdot sec^{-1}$.

Yield Data

Each field was harvested at physiological maturity by the producer using a harvester equipped with a differential GPS and a yield monitor. Yield monitors were calibrated by each producer prior to harvest. Raw yield data files were imported into SMS Advanced (Ag Leader Technology, Ames, IA) and then loaded to Yield Editor (v. 2.0.7. USDA-ARS, Columbia, MO) for cleaning (Sudduth and Drummond, 2007). Fifteen m of yield data points were removed from each end of the field for each pass. Harvested weight was adjusted to a standard moisture of 155 $g \cdot kg^{-1}$. To compare NUE between the sensor-based approach and uniform N management, the partial factor productivity of applied N (PFP_N) was calculated, where PFP_N = kg grain $\cdot$ kg N $applied^{-1}$.

Whole Field Treatment Effects

Average treatment effects on NDRE, N rate, grain yield, PFP_N, and marginal net return were first evaluated for each field using values for field-length treatment strips. Maize and N fertilizer prices of \$120.07·Mg^{-1} (\$3.05·bu^{-1}) and \$0.99·kg N^{-1} (\$0.45·lb N^{-1}) were used in the analysis. Analysis of variance (PROC GLIMMIX, SAS 9.4, SAS Institute Inc., Cary, NC) was used to evaluate treatment effects, and provide least significant difference (LSD) values to separate treatment means at a significance level of 0.05.

Management Zone Delineation

In order to explore the relationships between the measured soil and crop variables, a Pearson correlation analysis was conducted using the methods described in Chapter 2. Using Global (all fields combined) and Field-Specific approaches, the two variables with the highest significant correlation ($p < 0.05$ and $R > 0.50$) to either NDRE or check yield for each field were selected as input variables for clustering in Management Zone Analyst (MZA) 1.0.1 (USDA-ARS and University of Missouri, Columbia, MO) (Fridgen et al., 2004). To increase the number of observations for clustering and to increase the overall spatial area of the MZ, all soil and landscape data collected from the plots as well as adjacent to them were used as inputs into MZA, resulting in a total area of 12-30 ha. In the software, Mahalanobis distance was selected as the measure of similarity except when variables with identical units were used. In these instances Euclidean distance was chosen.

Two indices are calculated by MZA to help determine the optimum number of classes. The Normalized Classification Entropy (NCE) quantifies the disorganization created by dividing data into classes (Lark and Stafford, 1997). The Fuzziness Performance Index (FPI) determines the amount of membership sharing (fuzziness) among classes (Odeh et al., 1992). Class number is optimized when both NCE and FPI are minimized, meaning a low degree of membership sharing and low disorganization from the clustering process (Fridgen et al., 2004).

Evaluation of Treatment Differences by Zone

After evaluating treatment differences by strip and delineating MZ, treatments were then evaluated by MZ for each field. To accomplish this, field-length treatment strips were divided into square grids with length and width equal to the width of each treatment strip (Table 3.2). Nitrogen rate, yield, NDRE, and PFP_N values were averaged within each polygon, and zonal differences were determined using a t-test, LSD calculations, and treatment mean groupings.

RESULTS AND DISCUSSION

Treatment Effects on Yield and PFP_N

Nitrogen rates and yield response to N are presented for each field in Figs. 3.3 and 3.4 and in Table 3.4. Growing conditions were good for both 2016 and 2017, with an overall average yield of 14.1 $Mg \cdot ha^{-1}$ for the high-N reference treatment. The N rate prescribed by the active sensing system was significantly lower than the producer-chosen uniform rate in five of eight fields, averaging 66 kg $N \cdot ha^{-1}$ lower. Yield for the sensor treatment was also significantly lower than the uniform treatment in all five of those fields, by an average of 0.67 $Mg \cdot ha^{-1}$. For the remaining three fields (KR16, AR17, JA17), the sensor-based N rate was either not significantly different or significantly higher than the uniform rate. This resulted in significantly increased yield for the Sensor treatment for these three fields with an average increase of 0.80 $Mg \cdot ha^{-1}$.

When comparing PFP_N for the sensor and uniform treatments, the sensor-based strategy resulted in a significantly higher PFP_N in six of eight fields (Figs. 3.5 and 3.6; Table 3.4). Among these six were the five fields that produced a lower N rate and a lower yield using the sensor-based approach. The sixth field (Field KR16) had the same amount of N applied, but the sensor treatment increased yield by 1.6 $Mg \cdot ha^{-1}$ compared to the uniform treatment. This result can be attributed to the timing of N application. The uniform rate was applied in split applications, but all were completed before V5. The sensor treatment was not applied until V10. The coarse-textured soil on this field is very prone to nitrate leaching. By applying fertilizer later in the growing season, more N was able to be recovered by the crop, resulting in increased yield for the sensor-based approach. These results indicate that in-season, sensor-based application has the potential

to increase NUE compared to uniform application, primarily through substantially decreasing N applied with only a slight reduction in yield as was found by Roberts et al. (2010).

In order for variable-rate, sensor-based N application to be adopted by crop producers, economic benefits need to be shown compared to conventional management practices (Swinton and Lowenberg-DeBoer, 1998). An analysis of marginal net return between treatments is shown in Table 3.4. A comparison of marginal net return for the sensor and uniform treatments produced mixed results. Profitability was increased in four of eight fields when using the sensor-based approach, decreased in three of eight fields, and there was no significant difference in Field AR16. Of the four fields with increased marginal net return, the increase came from higher yields in two fields (KR16 and JA17) and from decreased N fertilizer in the other two fields (CA16 and HU17).

For the fields with decreased marginal net return, two of them (HU16 and KR17) came from decreases in yield and the other (AR17) came from a large increase in applied N fertilizer with only a slight increase in yield. Fields HU16 and KR17 had higher than normal base rates (122 and 178 kg $N \cdot ha^{-1}$, respectively), while the other six fields had base rates ranging from 78 to 91 kg $N \cdot ha^{-1}$ (Table 3.3). This increased base rate likely resulted in higher SI values for the sensor treatment during in-season application and correspondingly low N rates applied. In the case of these two fields, the N rates were too low to maintain yield, and profitability was decreased compared to the uniform rate.

Future research should investigate the optimal timing of sensor-based N application as well as the base rate required to sustain the crop until in-season application under different soil and climatic conditions. Soil N mineralization varies significantly

with latitude, SOM content, and annual precipitation (Liu, et al., 2017). Therefore, appropriate base N rate recommendations are likely to vary by region and even by field. When N fertilizer application occurs before any N stress is realized, either by applying too early in the crop life cycle or by applying too high a base rate, the recommended N rate will likely be too low. Conversely, applying N fertilizer after the crop is experiencing significant N stress will negatively impact yield. The optimal window for sensor-based N fertilizer application appears to be much narrower than that currently recommended by Ag Leader, between the V5 and VT growth stages.

An alternative to a recommended growth stage window or growing degree day calculation could be identifying a threshold SI value above which it is too early for N fertilizer application. In addition, a range of SI could establish the appropriate window for in-season application that would be much narrower than a window that relies on crop growth stage. Obtaining the SI for a field prior to N fertilizer application would not necessarily require driving over the field multiple times with a vehicle-mounted active sensor but could come from a handheld crop sensor, a chlorophyll meter, or even from unmanned aerial, manned aerial, or satellite imagery.

Management Zone Delineation

Fields were clustered into soil-based MZ using MZA in order to compare treatment performance between MZ within each field. For the Global Approach, there was no significant correlation of any soil or topographic variable to check yield and only weak correlations to NDRE, so no variable was chosen to cluster MZ in the Global Approach (Tables 3.5 and 3.6). Correlations were subsequently evaluated on a field-by-field basis (Field-Specific Approach). Results from this analysis are found in Table 3.7.

Two clustering variables were chosen for each field, except for Fields CA16 and JA17, where only one variable was used. Shallow EC_a was chosen as a clustering variable in five of eight fields, and EC_d was chosen as a clustering variable in four of eight fields. Soil organic matter was chosen in three of eight fields, and $Elev_{rel}$ was selected in two of eight fields.

Results from MZA were evaluated using two indices calculated by MZA—NCE and FPI. Class number is optimized when both NCE and FPI are minimized (Fridgen et al., 2004). The FPI indicated that optimal clustering occurred with five MZ in two of six fields, with three MZ in two of six fields, and with two MZ in four of six fields (Fig. 3.7). For NCE, optimal clustering occurred with two MZ for all eight fields (Fig. 3.7). To simplify analysis, each field was clustered into two MZ.

A map of delineated MZ for Field HU17 is presented in Fig. 3.8. Classification maps for all fields are included in Appendix 1. For all sites, Zone 1 consisted of more productive soils with higher SOM content while Zone 2 classified the less productive areas of the field. For the sandy level fields (KR16 and KR17), Zone 1 contained soils with higher soil EC_a and corresponding higher SOM content. The fields with eroded slopes (CA16, HU16, JA17) had more productive areas in the level, upland positions of the landscape, while Zone 2 areas were associated with steep slopes and drainage areas, and lower SOM, with conditions less suitable for growth. Silt loam level fields (AR16, AR17, HU17) had more productive Zone 1 areas associated with lower soil EC_a in slight depressions.

Management Zone Validation

Normalized Difference Red Edge Index

Previous research has shown NDRE to be a good measure of in-season crop N status (Li et al., 2014), and it was consequently used for to verify that crop response to N is consistently affected by MZ. The results of this analysis are shown in Figs. 3.9 and 3.10. Only two fields (HU16 and KR16) had significantly higher NDRE values for Zone 1 versus Zone 2 across all N treatments. When looking at the Sensor treatment only, NDRE values were significantly higher in Zone 1 than in Zone 2 in four fields (CA16, HU16, KR16, and JA17). Though not always statistically significant, NDRE values were consistently greater for Zone 1 for all treatments in seven of eight fields. Field AR16 had an inconsistent zonal response (Fig. 3.9). This can be attributed to a lack of variability in this field, which was very level with similar soil texture across the field. These results suggest that these delineated MZ based on field-specific variables can properly characterize differences in crop response to N.

Yield

Yield response to N was also used to validate MZ delineation for the two MZ (Figs. 3.11 and 3.12). Across all treatments, yield was significantly higher ($p < 0.05$) in Zone 1 than in Zone 2 in five of eight fields (AR16, HU16, KR16, HU17, and KR17). Yield was higher—though not always significantly higher—for Zone 1 compared to Zone 2 across all treatments and sites, excluding the N Ref treatment in Field AR17. These results indicate that areas classified in Zone 1 were likely more productive and able to provide higher amounts of mineralized N than Zone 2 areas.

The lack of differences between MZ for Field AR17 can be attributed to the general lack of spatial variability in this field and high SOM levels throughout the field. Field JA17 was a very highly variable field in terms of both soils and topography. Just

two delineated MZ using only one attribute (SOM) was likely not enough to capture the high variability present in the field. For Field CA16, all but the Uniform treatment showed a significant difference, and this treatment still resulted in a yield increase for Zone 1 of 0.7 $Mg \cdot ha^{-1}$ ($p = 0.09$).

Nitrogen Use Efficiency

Across all treatments, PFP_N was generally higher in Zone 1 than in Zone 2 in seven of eight fields, however it was only significantly higher ($p < 0.05$) for all treatments in two fields (HU16 and KR16) (Figs. 3.13 and 3.14). When looking at the Sensor treatment only, PFP_N was significantly higher ($p < 0.05$) in Zone 1 than Zone 2 in six of eight fields. Fields AR16 and AR17, which did not show a statistically significant difference between zones in any of the treatments, were the least variable of all fields studied. They had the highest SOM levels of any site (Table 3.1) and had little variability in topography (Table 3.3). These low PFP_N values for Zone 2 were a result of low N sufficiency at the time of sensing and in-season N application, which resulted in excessively high N rates in areas with inherently lower yield potential. Increased PFP_N may be realized in these areas by modifying the sensor-based algorithm with a separate NDRE reference value for each zone to account for differences in soils and expected productivity. Future research should validate this approach in a field setting.

CONCLUSIONS

This study compared in-season, sensor-based N application to producer-selected uniform N management in eight fields with varying soil and topographic conditions in east central Nebraska. The sensor-based treatment resulted in significantly increased PFP_N compared to the uniform treatment in six of eight fields. The increase came from drastically decreasing N rate while slightly decreasing yield in five of the fields, and maintaining the same N rate while increasing yield in the sixth field. These results indicate that in-season, sensor-based application has the potential to increase NUE compared to uniform N application, primarily through decreasing applied N with a slight or no reduction in grain yield.

Results from MZ delineation showed that MZ accurately characterized spatial differences in N status, measured as NDRE, for the sensor-based treatment in four of eight fields. Though not always statistically significant, NDRE values were consistently greater for the more productive Zone 1 soils in seven of eight fields. Yield was higher for Zone 1 compared to Zone 2 across both sensor-based and uniform treatments for all sites, and this difference was statistically significant in five of eight fields. For the sensor-based treatment, PFP_N was significantly higher for Zone 1 than Zone 2 in six of eight fields. These results indicate that further increases in NUE may be achieved by incorporating soil-based MZ into sensor-based algorithms, particularly in fields with high variability in soils and topography. Integration may not prove successful in fields with little field variability when compared to sensor-based N application alone or to uniform N management.

REFERENCES

Adamchuk, V.I., R.A. Viscarra Rossel, K.A. Sudduth, and P.S. Lammers. 2011. Sensor fusion for precision agriculture. In: Thomas, C. (Ed.), *Sensor Fusion—Foundation and Applications.* (pp. 27-40). Rijeka, Croatia: InTech.

Amaral, L.R., J.P. Molin, and J.S. Schepers. 2015. Algorithm for variable-rate nitrogen application in sugarcane based on active crop canopy sensor. Agron. J. 107:1513-1523.

Cassman, K.G., A.R. Dobermann, and D.T. Walters. 2002. Agroecosystems, nitrogen-use efficiency, and nitrogen management. Ambio. 31:132-140.

Doerge, T. 1999. Defining management zones for precision farming. Crop Insight. 8:21. Pioneer Hi-Bred International, Inc.

Fleming, K.L., D.F. Heermann, and D.G. Westfall. 2004. Evaluating soil color with farmer input and apparent soil electrical conductivity for management zone delineation. Agron J. 96:1581-1587.

Flowers, M., R. Weisz, and J.G. White. 2005. Yield-based management zones and grid sampling strategies: Describing soil test and nutrient variability. Agron. J. 97:968-982.

Fraisse, C.W., K.A. Sudduth, and N.R. Kitchen. 2001. Delineation of site-specific management zones by unsupervised classification of topographic attributes and soil electrical conductivity. Transactions of the ASAE. 44:155-166.

Franzen, D.W., D.H. Hopkins, M.D. Sweeney, M.K. Ulmer, and A.D. Halvorson. 2002. Evaluation of soil survey scale for zone development of site-specific nitrogen management. Agron J. 94:381-389.

Franzen, D., L.K. Sharma, and H. Bu. 2014. Active optical sensor algorithms for corn yield prediction and a corn side-dress nitrogen rate aid. NDSU Circ. SF1176-5, North Dakota State Univ. Ext. Serv., Fargo, ND.

Fridgen, J.J., N.R. Kitchen, K.A. Sudduth, S.T. Drummond, W.J. Wiebold, and C.W. Fraisse. 2004. Management Zone Analyst (MZA): Software for subfield management zone delineation. Agron. J. 96:100-108.

Gitelson, A.A., and M.N. Merzlyak. 1994. Quantitative estimation of chlorophyll-a using reflectance spectra: Experiments with autumn chestnut and maple leaves. J. Photochem. Photobiol. 22:247-252.

Holland, K.H., and J.S. Schepers. 2010. Derivation of a variable rate nitrogen application model for in-season fertilization of corn. Agron. J. 102:1415-1424.

Holland, K.H., and J.S. Schepers. 2013. Use of a virtual-reference concept to interpret active crop canopy sensor data. Precis. Agric. 14:71-85.

Khosla, R., D.G. Westfall, R.M. Reich, J.S. Mahal, and W.J. Gangloff. 2010. Spatial variation and site-specific management zones. *In* M.A. Oliver (Ed.), *Geostatistical applications in precision agriculture* (pp. 195-219). New York, NY: Springer.

Kitchen, N.R., K.A. Sudduth, and S.T. Drummond. 1999. Soil electrical conductivity as a crop productivity measure for claypan soils. J. Prod. Agric. 12:607-617.

Kitchen, N.R., K.A. Sudduth, S.T. Drummond, P.C. Scharf, H.L. Palm, D.F. Roberts, and E.D. Vories. 2010. Ground-based canopy reflectance sensing for variable-rate nitrogen corn fertilization. Agron. J. 102:71-84.

Lark, R.M., and J.V. Stafford. 1997. Classification as a first step in the interpretation of temporal and spatial variation of crop yield. Annals Appl. Biol. 130:111-121.

Li, F., Y. Miao, G. Feng, F. Yuan, S. Yue, X. Gao, Y. Liu, B. Liu, S. Ustin, X. Chen. 2014. Improving estimation of summer maize nitrogen status with red edge-based spectral vegetation indices. Field Crops Res. 157:111-123.

Liu, Y., C. Wang, N. He, X. Wen, Y. Gao, S. Li, S. Niu, K. Butterbach-Bahl, Y. Luo, and G. Yu. 2017. A global synthesis of the rate and temperature sensitivity of soil nitrogen mineralization: latitudinal patterns and mechanisms. Glob. Chang. Biol. 23:455-464.

Morris, T.F., T.S. Murrell, D.B. Beegle, J.J. Camberato, R.B. Ferguson, J. Grove, Q. Ketterings, P.M. Kyveryga, C.A.M. Laboski, J.M. McGrath, J.J. Meisinger, J. Melkonian, B.N. Moebius-Clune, E.D. Nafziger, D. Osmond, J.E. Sawyer, P.C. Scharf, W. Smith, J.T. Spargo, H.M. van Es, and H. Yang. 2018. Strengths and limitations of nitrogen rate recommendations for corn and opportunities for improvement. Agron. J. 110: 1-37.

Nebraska Department of Natural Resources. 2010. Elevation data. URL: https://dnr.nebraska.gov/data/elevation-data.

Odeh, I.O.A., A.B. McBratney, and D.J. Chittleborough. 1992. Soil pattern recognition with fuzzy c-means: application to classification and soil-landform interrelationships. Soil Sci. Soc. Am. J. 56:505-516.

Oliveira, L.F., P.C. Scharf, E.D. Vories, S.T. Drummond, D. Dunn, W.G. Stevens, K.F. Bronson, N.R. Benson, V.C. Hubbard, and A.S. Jones. 2013. Calibrating canopy

reflectance sensors to predict optimal mid-season nitrogen rate for cotton. Soil Sci. Soc. Am. J. 77:173-183.

Peterson, T.A., T.M. Blackmer, D.D. Francis, and J.S. Schepers. 1993. Using a chlorophyll meter to improve N management. NebGuide G93-1171-A. Coop. Ext. Serv., Univ. of Nebraska, Lincoln.

Ping, J.L., R. B. Ferguson, and A. Dobermann. 2008. Site-specific nitrogen and plant density management in irrigated maize. Agron. J. 100:1193-1204.

Roberts, D.F. 2009. An integrated crop- and soil-based strategy for variable-rate nitrogen management in corn. PhD dissertation, Univ. Nebraska, Lincoln.

Roberts, D.F., R.B. Ferguson, N.R. Kitchen, V.I. Adamchuk, and J.F. Shanahan. 2012. Relationships between soil-based management zones and canopy sensing for corn nitrogen management. Agron. J. 104:119-129. doi:10.2134/agronj2011.0044

Roberts, D.F., N.R. Kitchen, P.C. Scharf, and K.A. Sudduth. 2010. Will variable-rate nitrogen fertilization using corn canopy reflectance sensing deliver environmental benefits? Agron. J. 102:85-95.

Scharf, P.C., D.K. Shannon, H.L. Palm, K.A. Sudduth, S.T. Drummond, N.R. Kitchen, L.J. Mueller, V.C. Hubbard, and L.F. Oliveira. 2011. Sensor-based nitrogen applications out-performed producer-chosen rates for corn in on-farm demonstrations. Agron J. 103:1683-1691.

Schepers, A.R., J.F. Shanahan, M.A. Liebig, J.S. Schepers, S.H. Johnson, and A. Luchiari, Jr. 2004. Appropriateness of management zones for characterizing spatial variability of soil properties and irrigated corn yields across years. Agron. J. 96:195-203.

Setiyono, T.D., H. Yang, D.T. Walters, A. Dobermann, R.B. Ferguson, D.F. Roberts, D.J. Lyon, D.E. Clay, and K.G. Cassman. 2011. Maize-N: a decision tool for nitrogen management in maize. Agron. J. 103:1276-1283.

Shanahan, J.F., N.R. Kitchen, W.R. Raun, and J.S. Schepers. 2008. Responsive in-season nitrogen management for cereals. Comput. Electron. Agric. 61:51-62.

Snyder, C.S. 2012. Are Midwest corn farmers over-applying fertilizer N? Better Crops Plant Food 96:3-4.

Solari, F., J. Shanahan, R. Ferguson, J. Schepers, and A. Gitelson. 2008. Active sensor reflectance measurements of corn nitrogen status and yield potential. Agron. J. 100:571-579.

Solie, J.B., A.D. Monroe, W.R. Raun, and M.L. Stone. 2012. Generalized algorithm for variable-rate nitrogen application in cereal grains. Agron. J. 104:378-387.

Sudduth, K.A., and S.T. Drummond. 2007. Yield editor: Software for removing errors from crop yield maps. Agron. J. 99:1471-1482.

Swinton, S.M., and J. Lowenberg-DeBoer. 1998. Evaluating the profitability of site-specific farming. J. Prod. Agric. 11:439-446.

Tubaña, B.S., D.L. Harrell, T. Walker, J. Teboh, J. Lofton and Y. Kanke. 2012. In-season canopy reflectance-based estimation of rice yield response to nitrogen. Agron. J. 104:1604-1611.

Walburg, G., M.E. Bauer, C.S.T. Daughtry, and T.L. Housley. 1982. Effects of nitrogen nutrition on the growth, yield, and reflectance characteristics of corn canopies. Agron. J. 74:677-683.

FIGURES AND TABLES

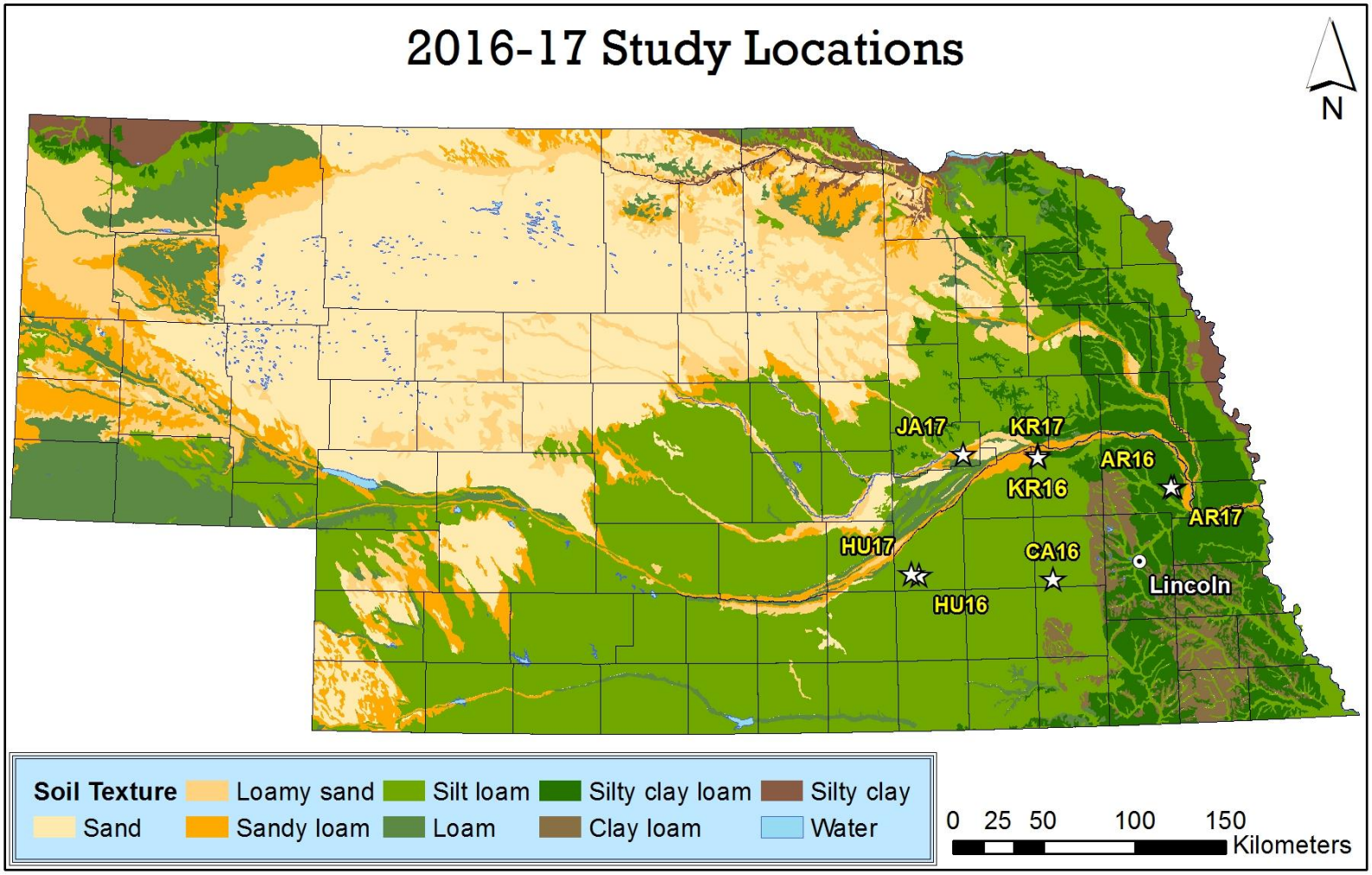

Fig 3.1. Study site locations within the state of Nebraska. Surface soil texture also shown.

Fig. 3.2. Experimental design of field-length treatments and small plots in Field HU16.

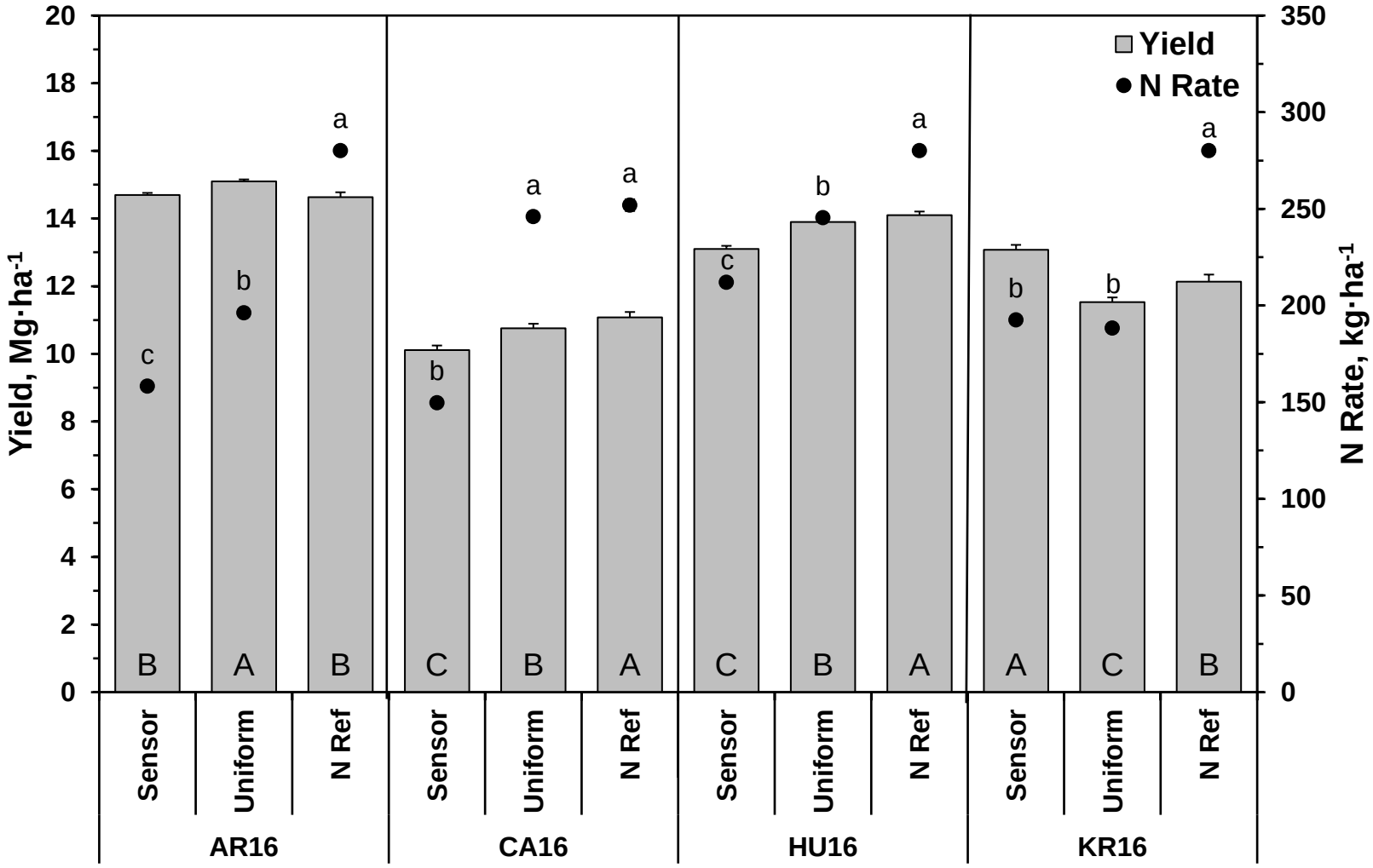

Fig. 3.3. Nitrogen rate and yield for each treatment for the 2016 fields. Treatment mean groupings are indicated for yield (uppercase letters) and N rate (lowercase letters) for each field. Bars with the same letter are not significantly different. Error bars indicate standard error for each treatment.

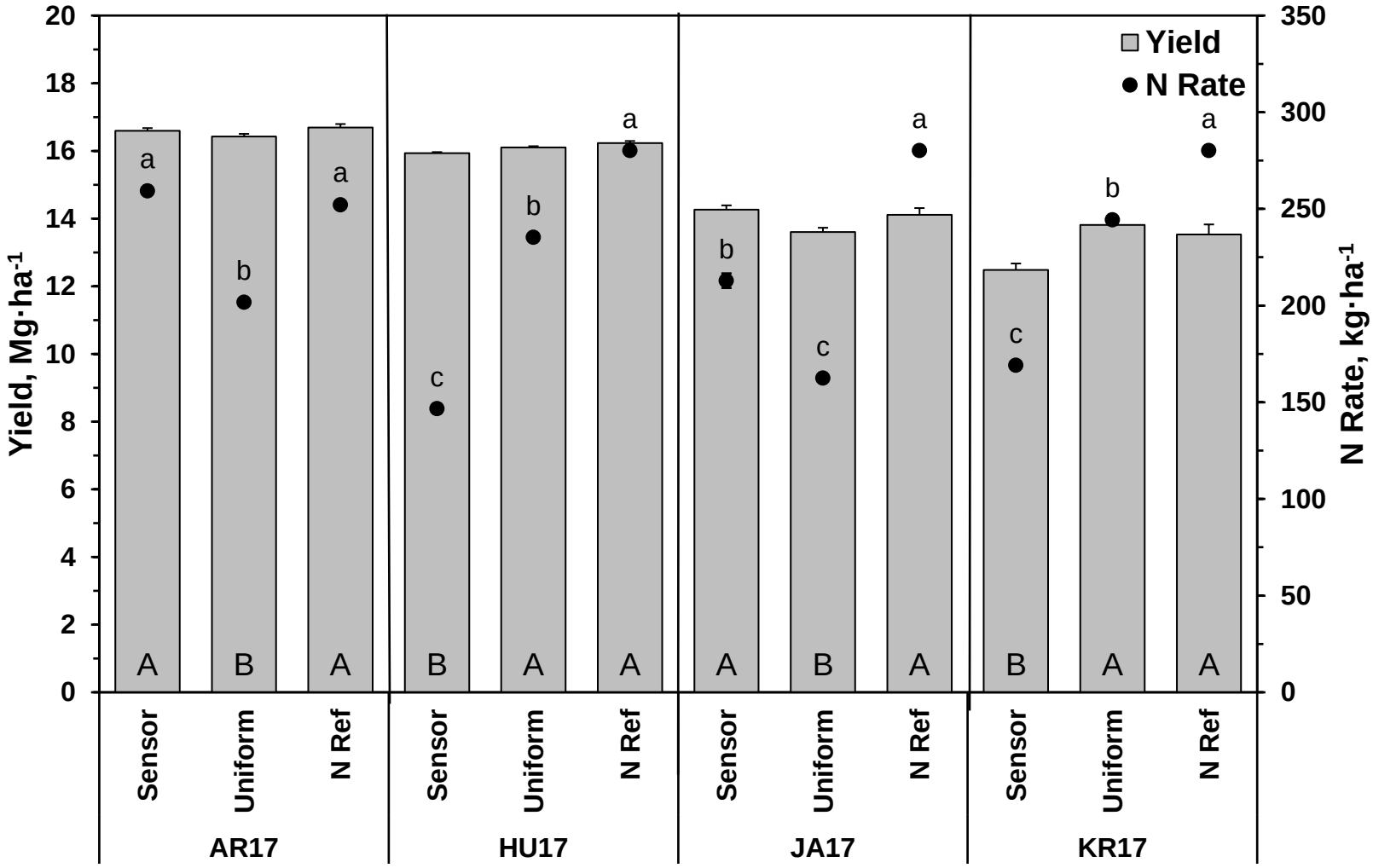

Fig. 3.4. Nitrogen rate and yield for each treatment for the 2017 fields. Treatment mean groupings are indicated for yield (uppercase letters) and N rate (lowercase letters) for each field. Bars with the same letter are not significantly different. Error bars indicate standard error for each treatment.

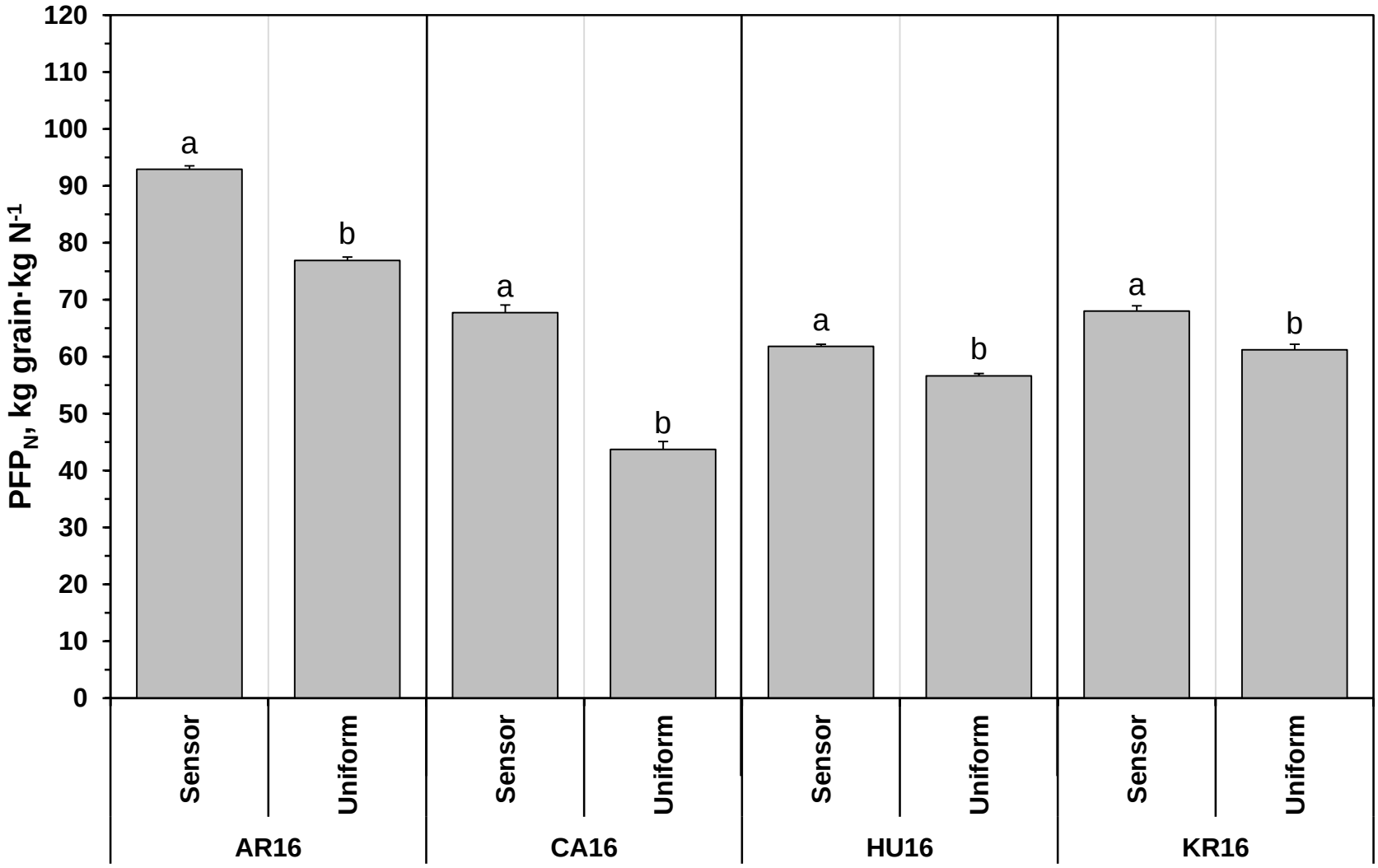

Fig. 3.5. Partial factor productivity of nitrogen (PFP_N) for each treatment for the 2016 fields. Treatment mean groupings are indicated for each field. Bars with the same letter are not significantly different. Error bars indicate standard error for each treatment.

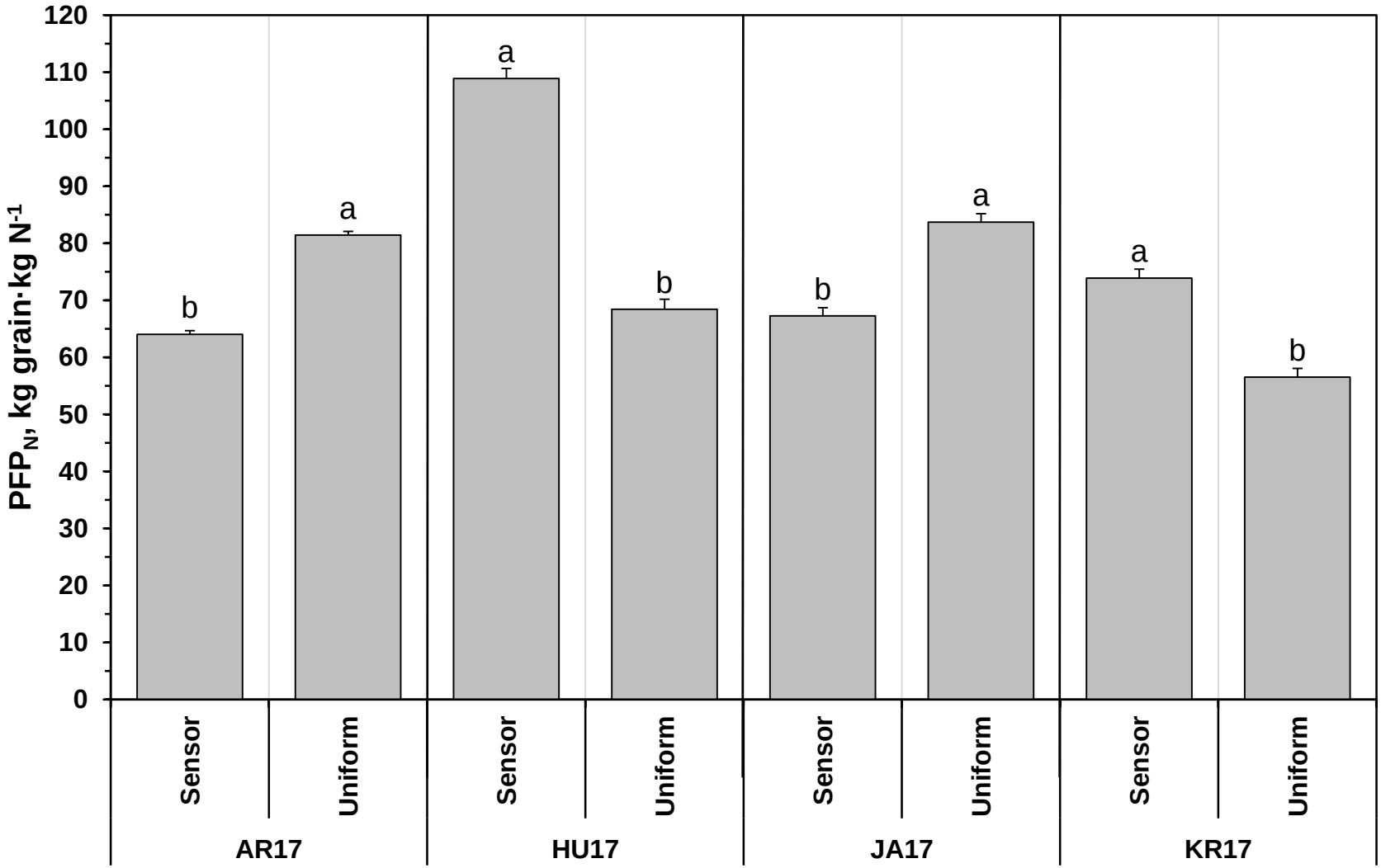

Fig. 3.6. Partial factor productivity of nitrogen (PFP_N) for each treatment for the 2017 fields. Treatment mean groupings are indicated for each field. Bars with the same letter are not significantly different. Error bars indicate standard error for each treatment.

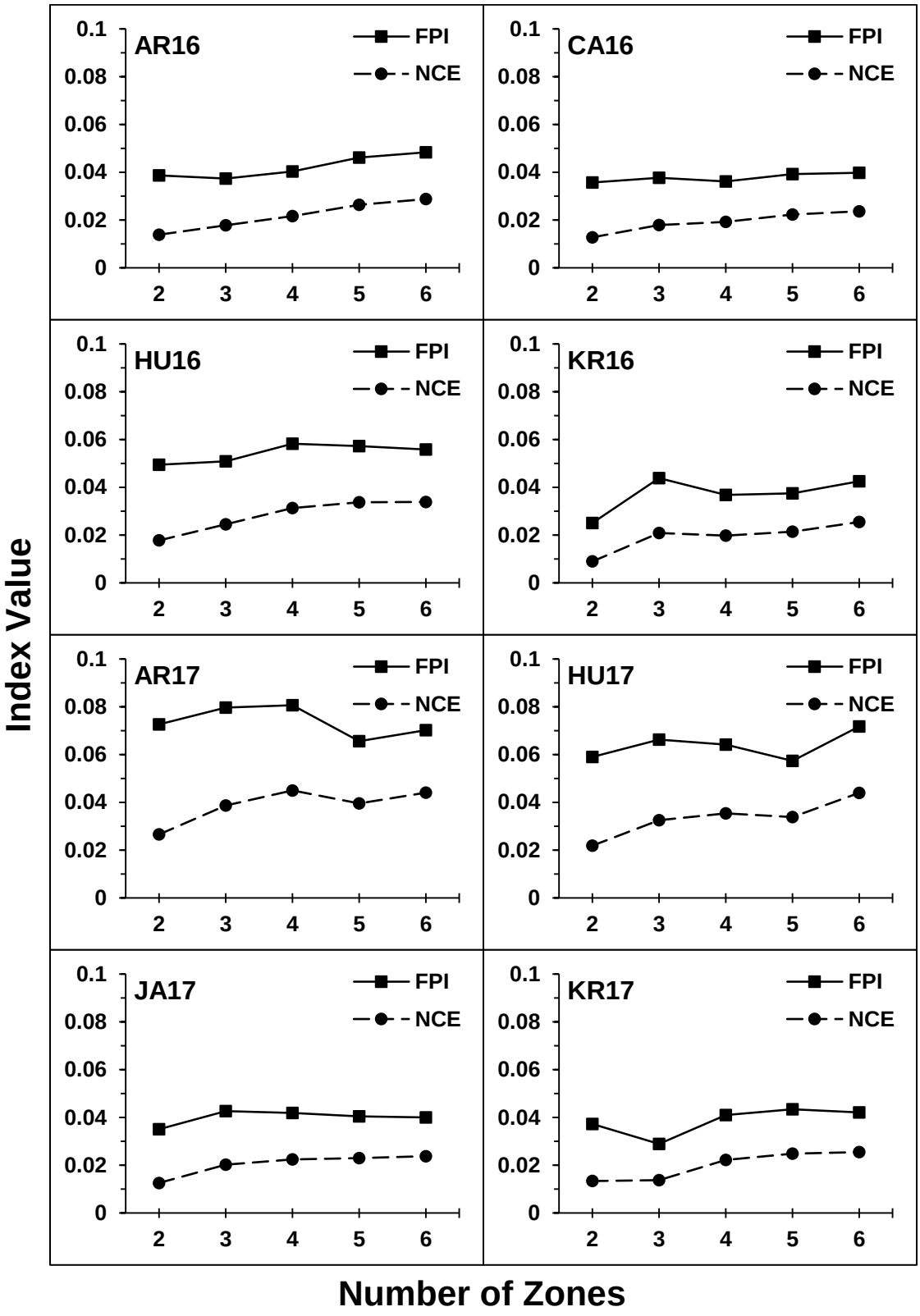

Fig 3.7. FPI and NCE values calculated in MZA for all fields.

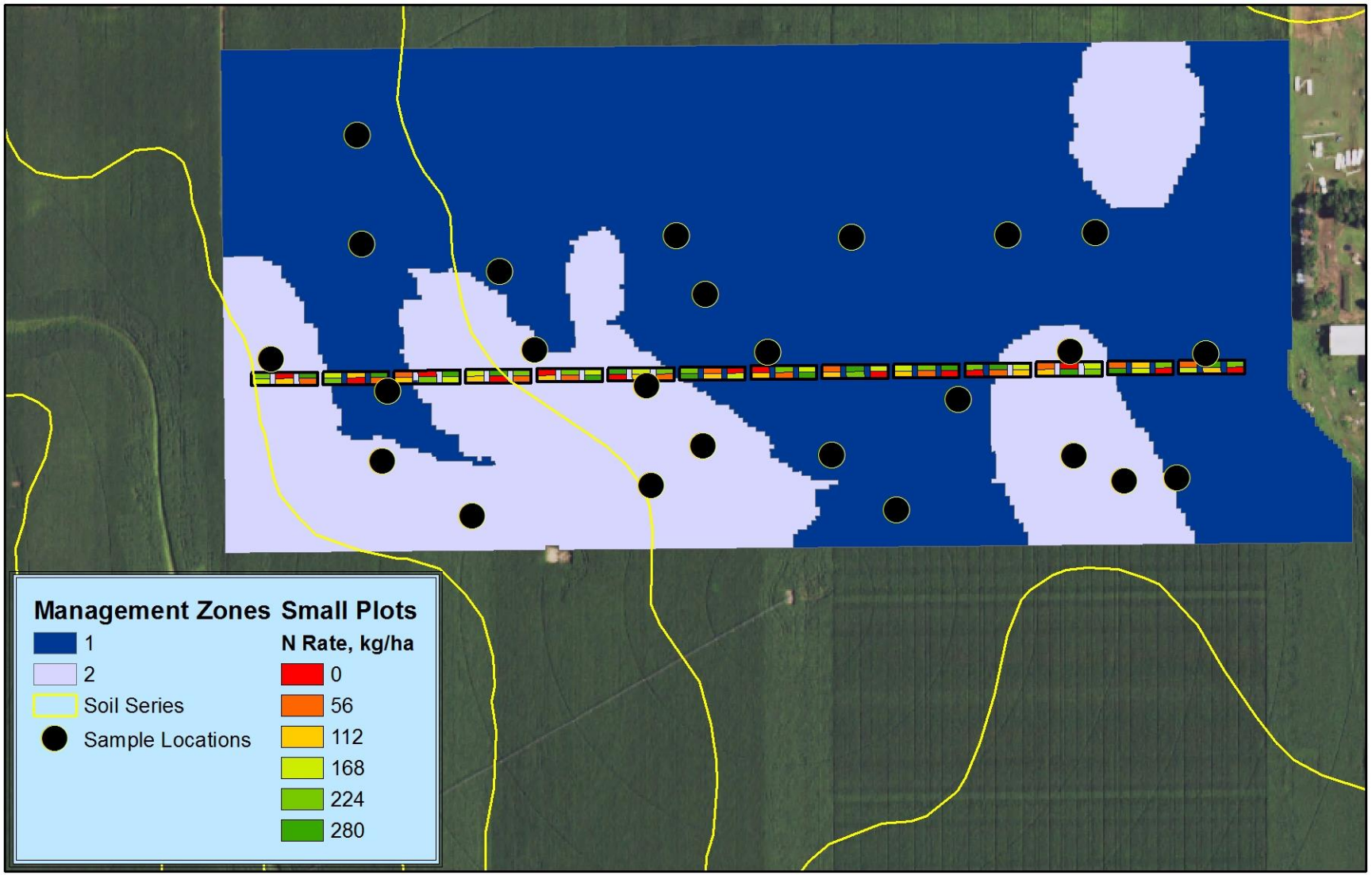

Fig. 3.8. Management zone delineation for Field HU17 using EC_s and SOM.

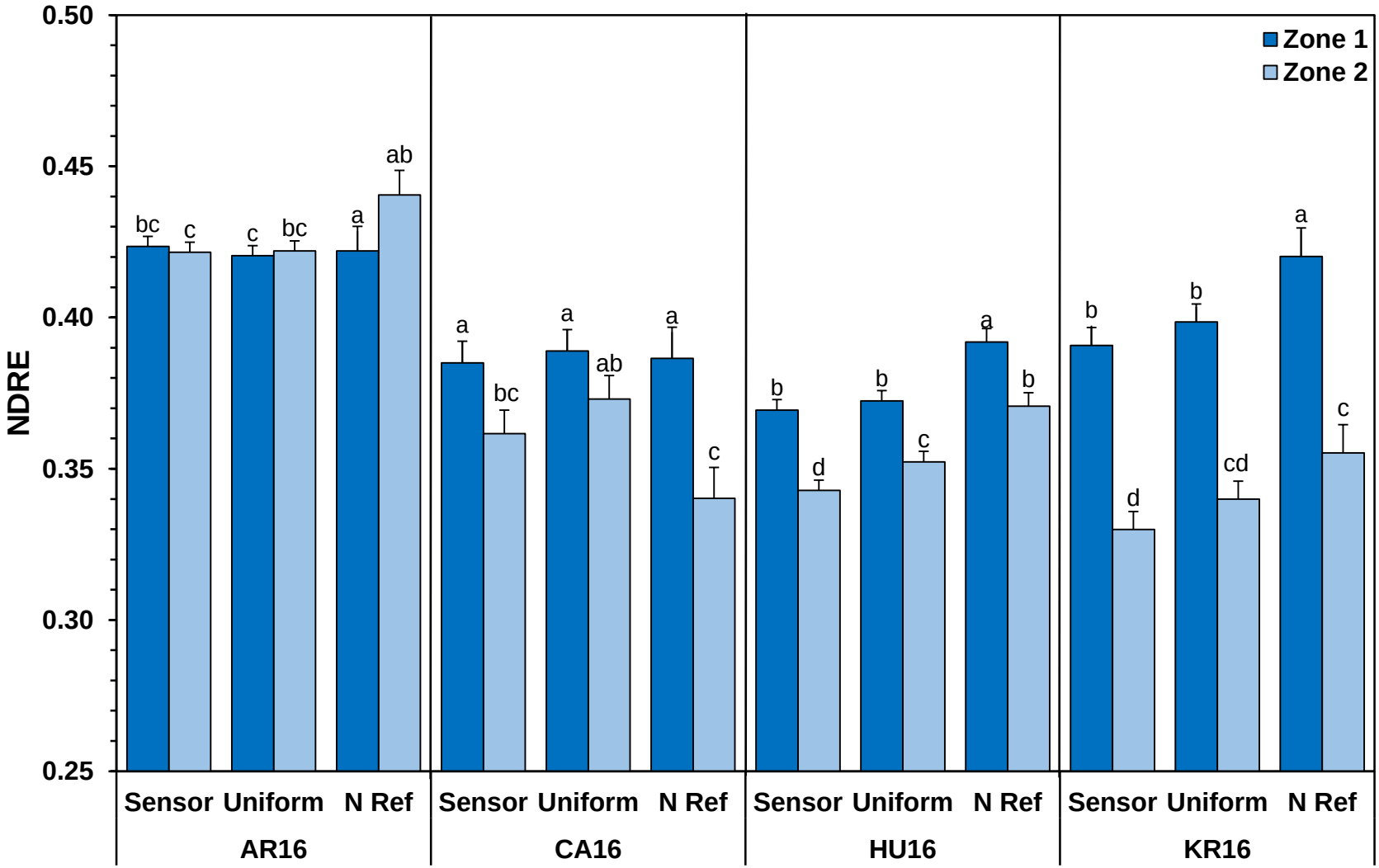

Fig. 3.9. NDRE by treatment by MZ for the 2016 fields. Treatment mean groupings are indicated for each field. Bars with the same letter are not significantly different. Error bars indicate standard error for each treatment.

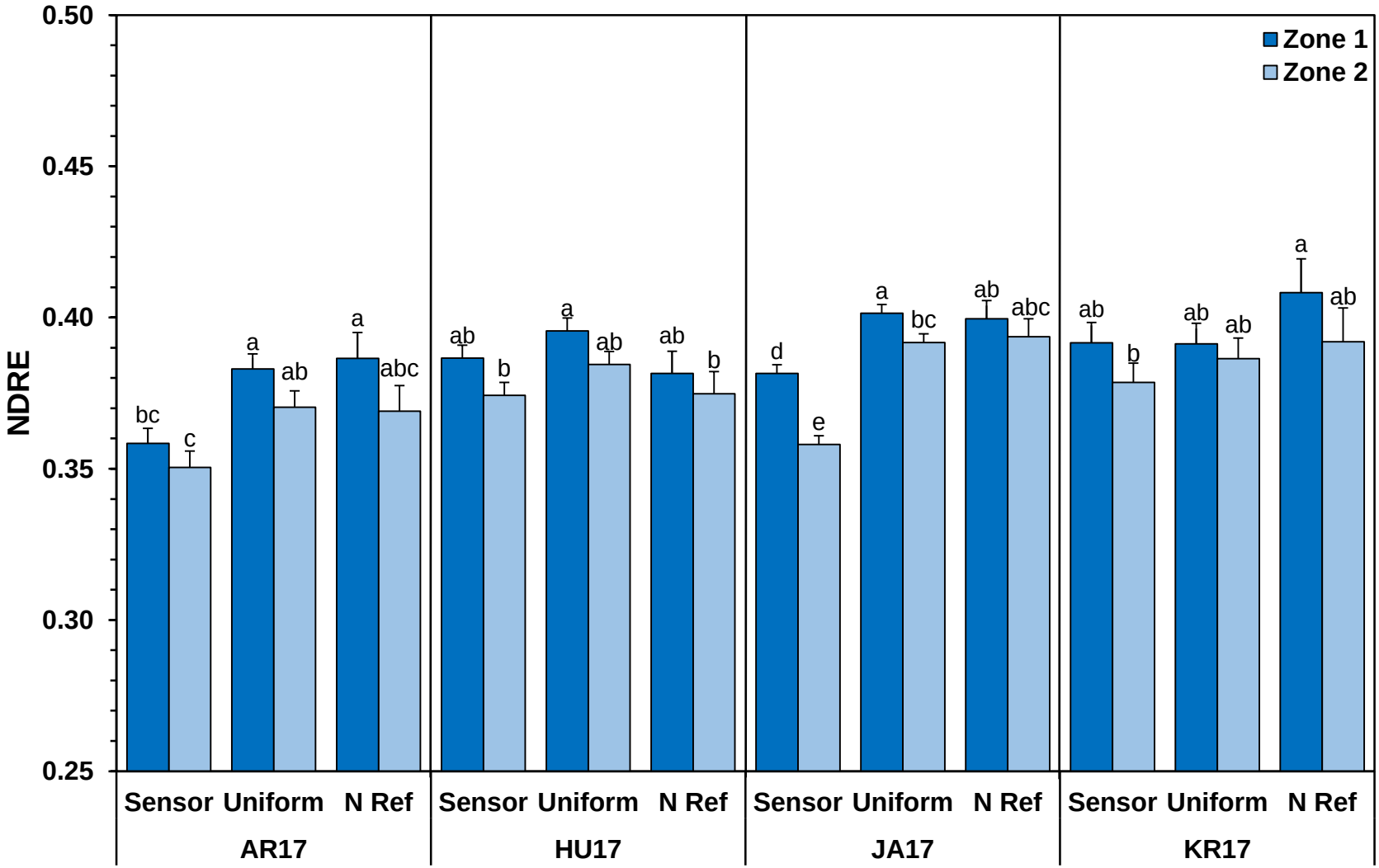

Fig. 3.10. NDRE by treatment by MZ for the 2017 fields. Treatment mean groupings are indicated for each field. Bars with the same letter are not significantly different. Error bars indicate standard error for each treatment.

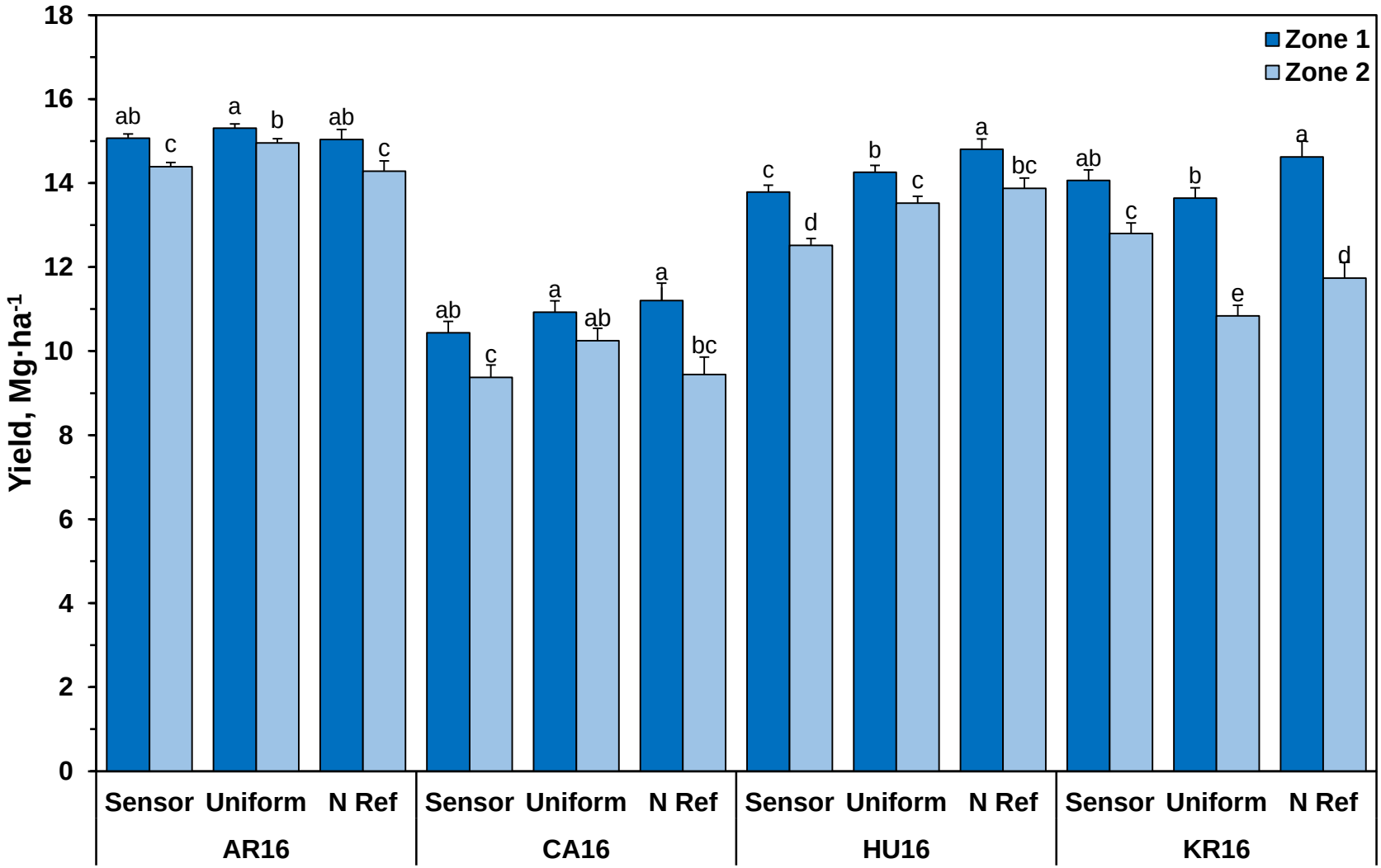

Fig. 3.11. Yield by treatment by MZ for the 2016 fields. Treatment mean groupings are indicated for each field. Bars with the same letter are not significantly different. Error bars indicate standard error for each treatment.

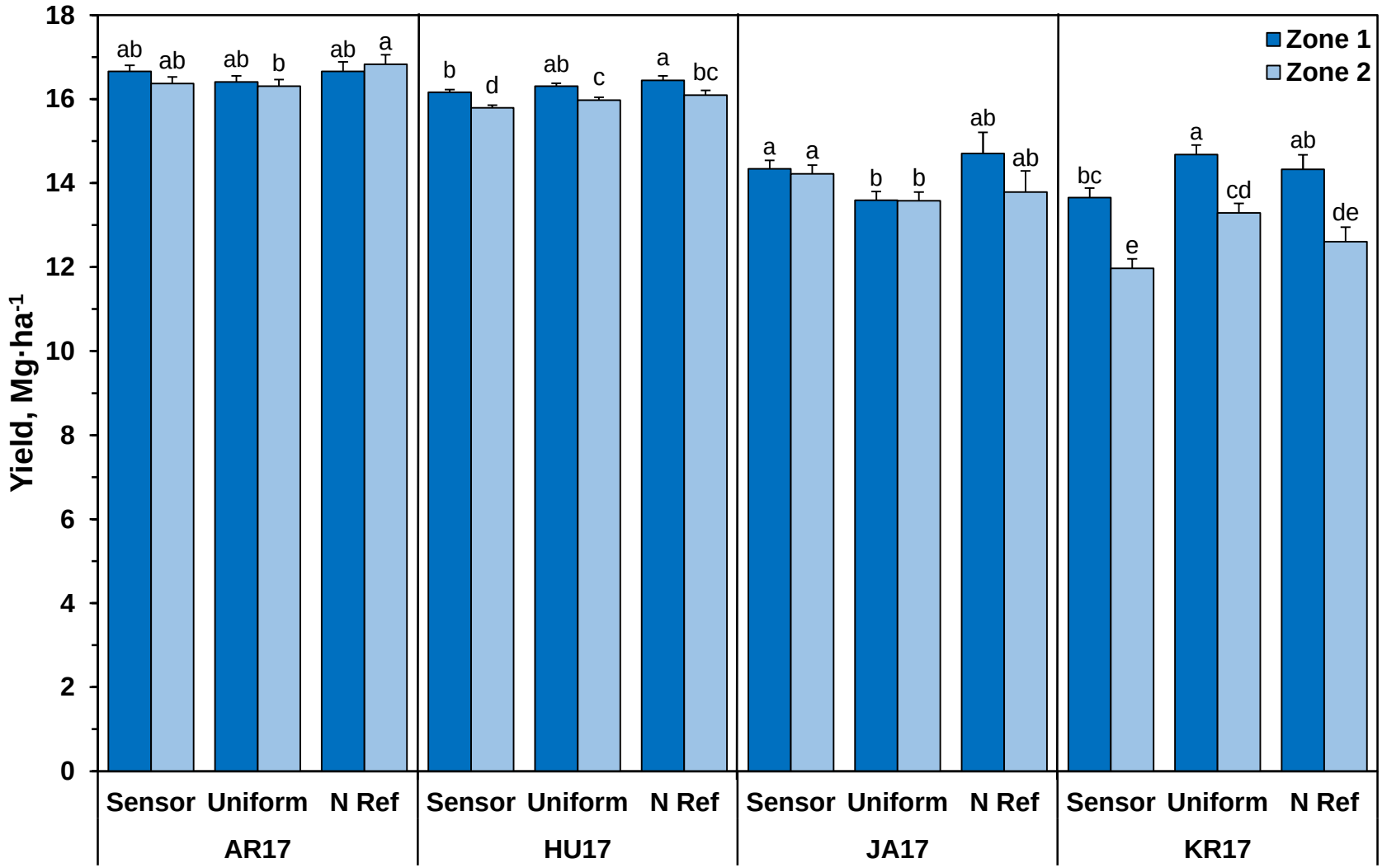

Fig. 3.12. Yield by treatment by MZ for the 2017 fields. Treatment mean groupings are indicated for each field. Bars with the same letter are not significantly different. Error bars indicate standard error for each treatment.

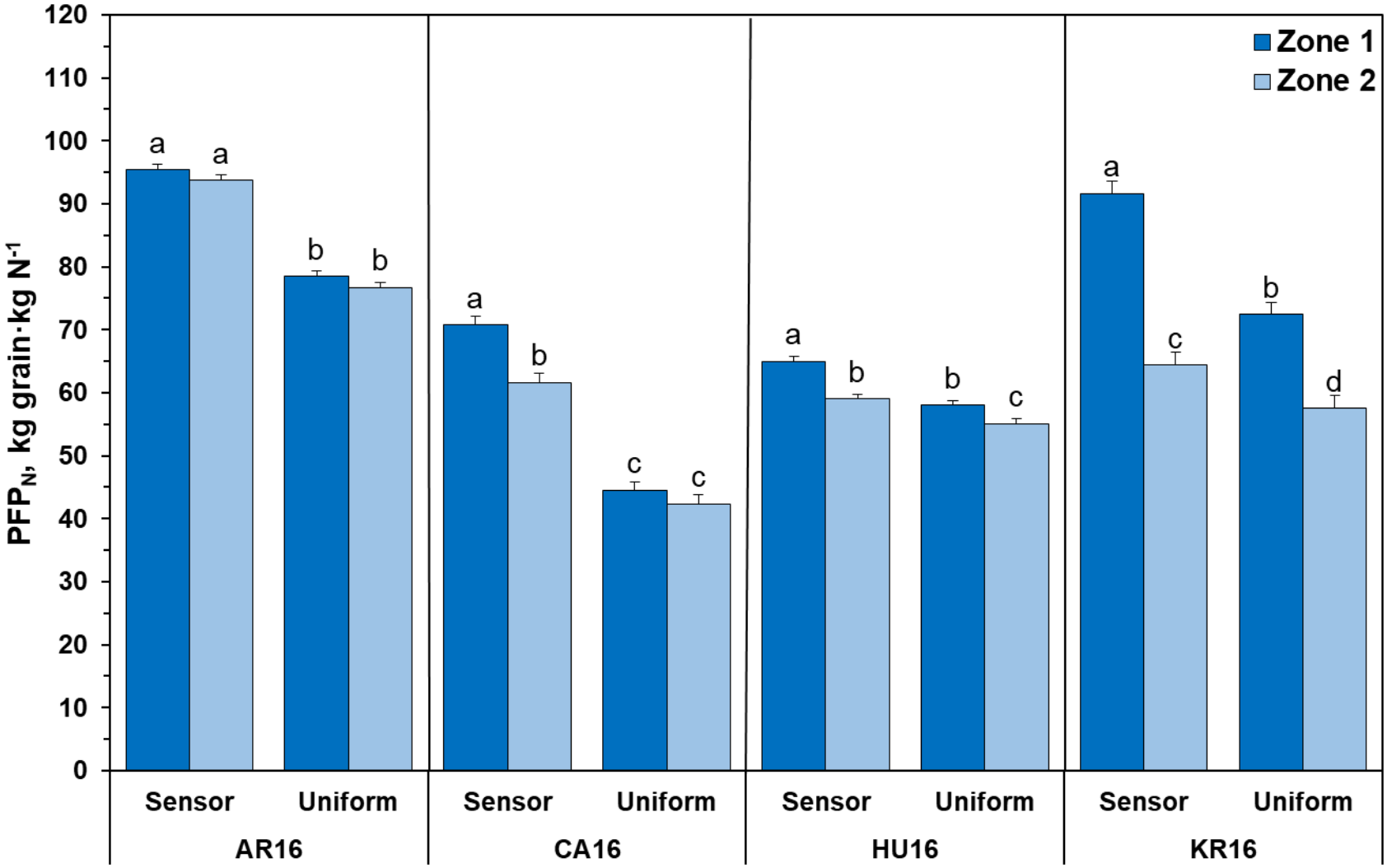

Fig. 3.13. Partial factor productivity of nitrogen (PFP_N) by treatment by MZ for the 2017 fields. Treatment mean groupings are indicated for each field. Bars with the same letter are not significantly different. Error bars indicate standard error for each treatment.

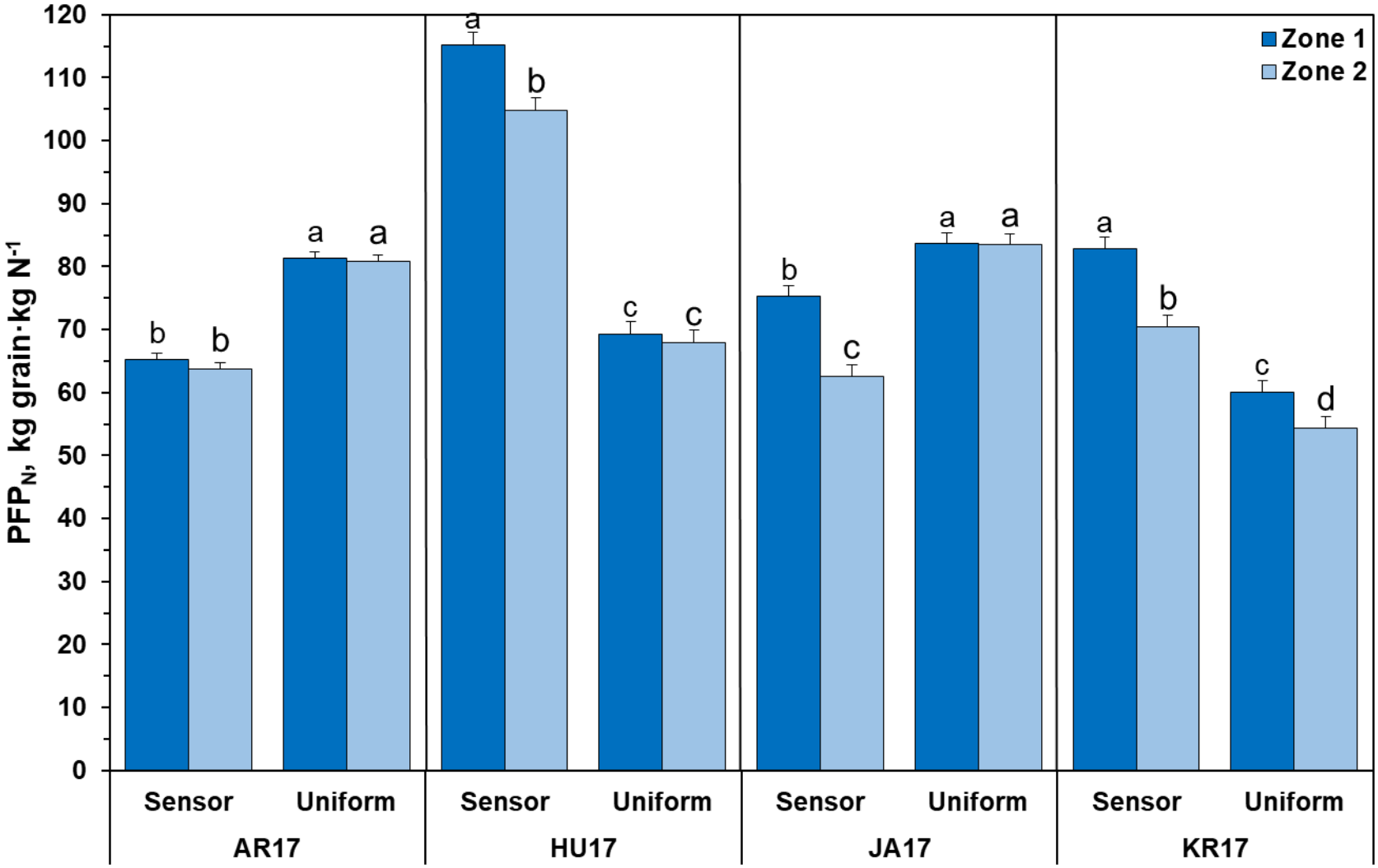

Fig. 3.14. Partial factor productivity of nitrogen (PFP_N) by treatment by MZ for the 2017 fields. Treatment mean groupings are indicated for each field. Bars with the same letter are not significantly different. Error bars indicate standard error for each treatment.

Table 3.1. Field location, soil series, and soil classification for all fields.

Field ID	Year	Legal Description	Soil Series	Soil Great Group	Slope	SOM Range†
AR16	2016	T.14N-R.9E., Sec 19, NW ¼, N ½	Filbert silt loam	Vertic Argialbolls	0-1%	2.9-5.0%
			Tomek silt loam	Pachic Argiudolls	0-2%	
			Yutan silty clay loam	Mollic Hapludalfs	2-6%, eroded	
CA16	2016	T.9N-R.2E., Sec 19, NW ¼, W ½, S ½	Deroin silty clay loam	Mollic Hapludalfs	6-11%, severely eroded	1.9-3.6%
			Hastings silty clay loam	Udic Argiustolls	3-7%, eroded	
			Deroin silty clay loam	Mollic Hapludalfs	11-30%, severely eroded	
HU16	2016	T.9N-R.7W., Sec 4, SW ¼, E ½	Hastings silt loam	Udic Argiustolls	0-1%	1.9-3.8%
			Crete silt loam	Udertic Argiustolls	0-1%	
			Hastings silty clay loam	Udic Argiustolls	7-11%, eroded	
			Hastings silty clay loam	Udic Argiustolls	3-7%, eroded	
KR16	2016	T.16N-R.1E., Sec 21, NW ¼, S ½	Brocksburg sandy loam	Pachic Argiustolls	0-2%	0.6-1.7%
AR17	2017	T.14N-R.9E., Sec 20, SW ¼, W ½	Yutan silty clay loam	Mollic Hapludalfs	2-6%, eroded	1.9-4.7%
			Filbert silt loam	Vertic Argialbolls	0-1%	
			Tomek silt loam	Pachic Argiudolls	0-2%	
HU17	2017	T.9N-R.8W, Sec 1, NE ¼, N ½	Hastings silt loam	Udic Argiustolls	0-1%	2.2-4.4%
			Hastings silt loam	Udic Argiustolls	1-3%	
JA17	2017	T.16N-R.4W, Sec 7, SE ¼, S ½	Thurman loamy fine sand	Udorthentic Haplustolls	2-6%	0.9-3.1%
			Loretto-Thurman complex	Udic Argiustolls	1-3%	
			Thurman loamy fine sand	Udorthentic Haplustolls	2-6%, eroded	
KR17	2017	T.16N-R.1E., Sec 16, SW ¼, S ½	Thurman loamy fine sand	Udorthentic Haplustolls	2-6%	0.7-2.0%
			Brocksburg sandy loam	Pachic Argiustolls	0-2%	

† Soil organic matter content (%). 25 soil samples per site at 20-cm depth.

Table 3.2. Producer management practices for all fields.

Field ID	Tillage†	Previous Crop	Planting Date	Hybrid	Seeding Rate	Strip Width	Harvest Date
					seeds·ha^{-1}	m	
AR16	NT	Soybean	5/5/16	Pioneer 1197AM	76,600	6.1	11/1/16
CA16	NT	Maize	5/19/16	Golden Harvest G07B39-311A	74,130	12.2	10/25/16
HU16	ST	Maize	5/6/16	Pioneer 1105AM	81,540	9.1	10/17/16
KR16	NT	Soybean	4/24/16	Pioneer 33D53AM	79,070	12.2	10/22/16
AR17	NT	Soybean	4/25/17	DeKalb 62-98	81,510	12.2	10/11/17
HU17	ST	Maize	4/25/17	Pioneer 1306WHR	83,030	9.1	10/30/17
JA17	NT	Soybean	5/5/17	Pioneer 1690	74,100	12.2	11/5/17
KR17	NT	Soybean	4/23/17	Pioneer 1498	80,560	12.2	10/17/17

† NT: no-till; ST: strip-till

Table 3.3. Nitrogen application information for all treatments for all fields.

Field ID	Base Rate Application				Sensor-Based Application				Producer Field N Rate	High-N Reference
	Date	Crop Growth Stage†	N Rate	Source‡	Date	Crop Growth Stage†	Average N Rate	Source‡		
			kg·ha^{-1}				kg·ha^{-1}		kg·ha^{-1}	kg·ha^{-1}
AR16	3/17/16	Pre-plant	84	Anhydrous ammonia	6/24/16	V9	158	28% UAN	196	252
CA16	6/6/16	V2	84	28% UAN	7/19/16	VT	150	28% UAN	246	252
HU16	6/24/16	V7	178	28% UAN	7/11/16	V13	212	28% UAN	245	280
KR16	5/4/16	Pre-emerge	82	32% UAN	6/24/16	V10	193	32% UAN	188	280
AR17	3/24/17	Pre-plant	84	Anhydrous ammonia	6/23/17	V11	259	28% UAN	202	252
HU17	6/7/17	V4	91	28% UAN	7/5/17	V13	147	28% UAN	235	280
JA17	5/9/17	Pre-emerge	78	30% UAN	6/28/17	V11	213	32% UAN	163	280
KR17	4/29/17	Pre-emerge	122	32% UAN	6/29/17	V11	169	32% UAN	244	280

† Number of collared leaves

‡ UAN = urea-ammonium nitrate solution

Table 3.4. Treatment effects on N applied, grain yield, partial factor productivity of nitrogen (PFP_N), and marginal net return. Treatment mean groupings were calculated separately for each field. Maize and N fertilizer prices of \$120.07·Mg^{-1} (\$3.05·bu^{-1}) and \$0.99·kg N^{-1} (\$0.45·lb N^{-1}) were used to calculate marginal net return.

Field	Treatment	N Applied (kg N·ha^{-1})	Sig*	Yield (Mg·ha^{-1})	Sig	PFP_N (kg grain · kg N^{-1})	Sig	Marginal Net Return (\$·ha^{-1})	Sig
AR16	Sensor	158	B	14.7	B	93	A	1,607.85	A
	Uniform	196	A	15.1	A	77	B	1,617.83	A
CA16	Sensor	150	B	10.1	B	68	A	1,065.74	A
	Uniform	246	A	10.8	A	44	B	1,047.38	B
HU16	Sensor	212	B	13.1	B	62	A	1,362.40	B
	Uniform	245	A	13.9	A	57	B	1,425.63	A
KR16	Sensor	193	A	13.1	A	68	A	1,379.45	A
	Uniform	188	A	11.5	B	61	B	1,197.11	B
AR17	Sensor	259	A	16.6	A	64	B	1,735.36	B
	Uniform	202	B	16.4	B	81	A	1,771.81	A
HU17	Sensor	147	B	15.9	B	109	A	1,767.09	A
	Uniform	235	A	16.1	A	68	B	1,700.09	B
JA17	Sensor	213	A	14.3	A	67	B	1,501.92	A
	Uniform	163	B	13.6	B	84	A	1,472.39	B
KR17	Sensor	169	B	12.5	B	74	A	1,330.94	B
	Uniform	244	A	13.8	A	57	B	1,415.56	A

* Treatments with the same letter not significantly different at $\alpha = 0.05$.

Table 3.5. Pearson correlation coefficients of soil and topographic variables to check plot yield and in-season NDRE measurements across all fields (Global Approach) (*n* = 108; for SOM *n* = 92).

			Apparent Electrical Conductivity		Soil Optical Reflectance		Landscape	
	Yield	**NDRE**	**EC_s**	**EC_d**	**SR_{soil}**	**SOM**	**$Elev_{rel}$**	**Slope**
Yield	1							
NDRE	0.67***	1						
EC_s	-0.01	-0.09	1					
EC_d	0.03	-0.13	0.94***	1				
SR_{soil}	-0.10	-0.14	-0.34***	-0.30**	1			
SOM	-0.04	0.04	0.65***	0.71***	-0.04	1		
$Elev_{rel}$	-0.17	-0.21*	0.52***	0.45***	-0.31**	0.22*	1	
Slope	-0.19	-0.25*	0.45***	0.33***	-0.38***	-0.07	0.65***	1

* Statistical significance at P < 0.05.
** Statistical significance at P < 0.01.
*** Statistical significance at P < 0.001.

Table 3.6. Pearson correlation coefficients of soil and topographic variables to in-season NDRE measurements for all nonzero plots across all fields (Global Approach) (*n* = 552; for SOM *n* = 472).

		Apparent Electrical Conductivity		Soil Optical Reflectance		Landscape	
	NDRE	**EC_s**	**EC_d**	**SR_{soil}**	**SOM**	**$Elev_{rel}$**	**Slope**
NDRE	1						
EC_s	-0.03	1					
EC_d	-0.05	0.95***	1				
SR_{soil}	-0.14***	-0.33***	-0.25***	1			
SOM	0.17***	0.64***	0.72***	0.00	1		
$Elev_{rel}$	-0.11*	0.58***	0.50***	-0.29***	0.24***	1	
Slope	-0.14**	0.46***	0.35***	-0.35***	-0.06	0.63***	1

* Statistical significance at P < 0.05.
** Statistical significance at P < 0.01.
*** Statistical significance at P < 0.001.

Table 3.7. Pearson correlation coefficients of soil and topographic variables to check plot yield and NDRE for all site-years (Field-Specific Approach). Bold data indicate select variables used in management zone delineation.

	Crop	N Rate		Electrical Conductivity		Soil Optical Reflectance		Landscape	
Field	**Parameter**	**kg·ha^{-1}**	***n***	**EC_s**	**EC_d**	**SR_{soil}**	**SOM**	**$Elev_{rel}$**	**Slope**
AR16	NDRE	84	60	**-0.66*****	**-0.61*****	0.25	0.43**	-0.56***	-0.34**
	Yield	84	10	**0.46**	**0.41**	-0.30	-0.40	0.28	0.21
CA16	NDRE	56	65	0.07	-0.06	0.01	0.06	**0.23**	-0.15
	NDRE	0	13	0.55	0.41	-0.20	0.36	**0.60***	-0.32
	Yield	0	13	0.43	0.41	0.30	-0.12	**0.43**	-0.18
HU16	NDRE	56	75	**-0.60*****	**-0.57*****	0.38***	0.41***	0.35**	-0.35**
	NDRE	0	12	**-0.63***	**-0.78****	0.44	0.52	0.51	-0.52
	Yield	0	12	**-0.64***	**-0.80****	0.42	0.51	0.46	-0.44
KR16	NDRE	56	80	**0.69*****	**0.66*****	-0.55***	-	0.14	0.05
	NDRE	0	16	**0.83*****	**0.67****	-0.65**	-	0.15	-0.17
	Yield	0	16	**0.91*****	**0.72****	-0.74**	-	0.22	-0.08
AR17	NDRE	56	52	-0.22	-0.18	-0.08	**0.16**	**-0.12**	0.14
	NDRE	0	11	-0.40	-0.27	0.44	**0.30**	**-0.77****	-0.23
	Yield	0	11	-0.55	-0.35	-0.24	**0.62***	**-0.36**	-0.36
HU17	NDRE	56	70	**-0.57*****	-0.34**	0.12	**0.68*****	-0.39**	-0.63***
	NDRE	0	14	**-0.79*****	-0.62*	-0.07	**0.73****	-0.40	-0.56*
	Yield	0	14	**-0.79*****	-0.56*	0.07	**0.73****	-0.21	-0.64*
JA17	NDRE	56	80	0.35**	0.18	-0.49***	**0.50*****	-0.14	-0.18
	NDRE	39	16	0.40	0.31	-0.47	**0.47**	-0.30	-0.45
	Yield	39	16	0.19	0.27	0.07	**-0.02**	-0.20	-0.15
KR17	NDRE	80	80	**0.45*****	**0.26***	-0.30**	0.44***	0.12	-0.36**
	NDRE	24	16	**0.53***	**0.46**	-0.52*	0.50*	-0.14	-0.54*
	Yield	24	16	**0.85*****	**0.84*****	-0.08	-0.03	0.42	0.22

* Statistical significance at $P < 0.05$.

** Statistical significance at $P < 0.01$.

*** Statistical significance at $P < 0.001$.

APPENDIX 1

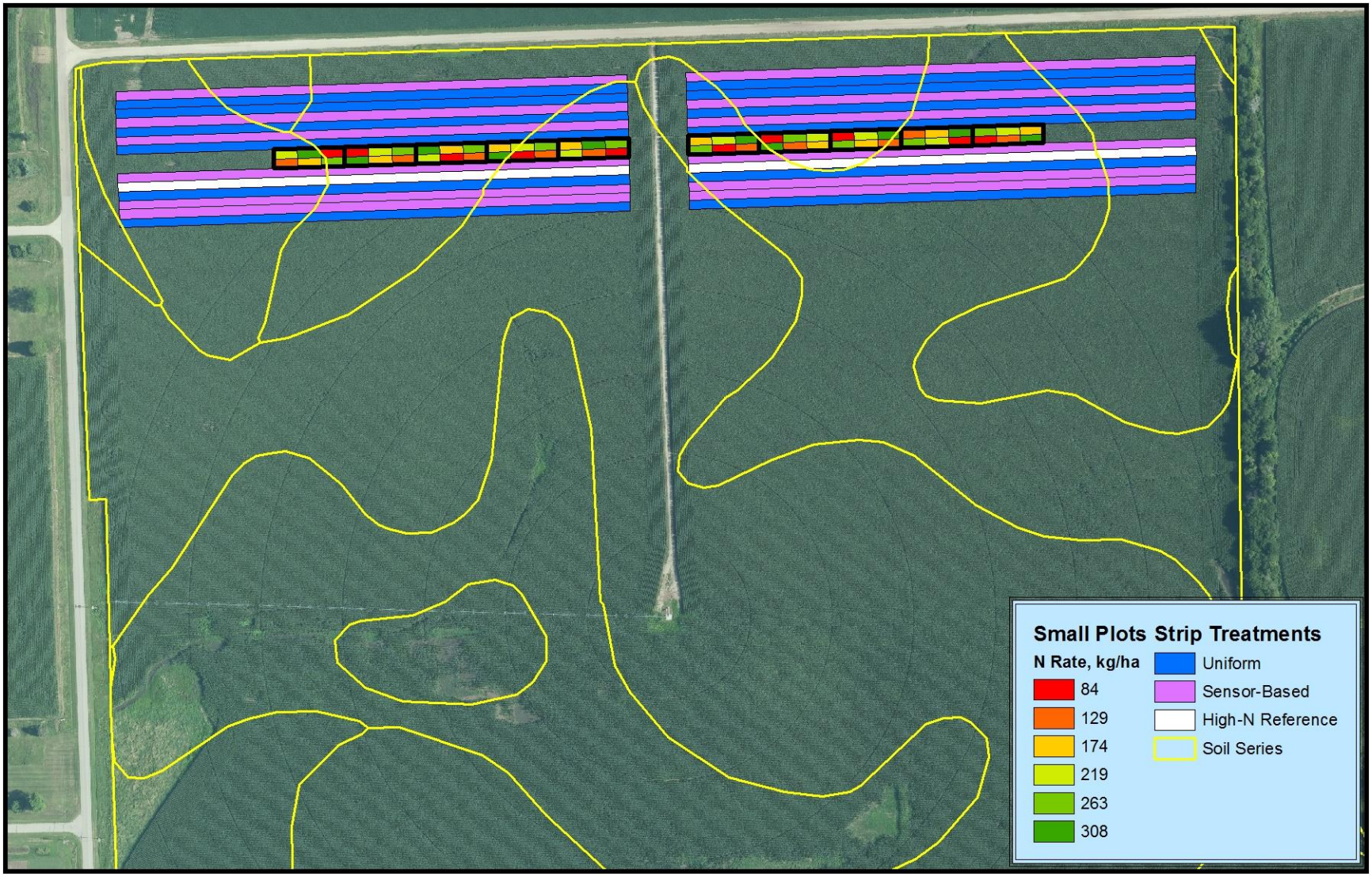

Fig. A1.1. Experimental design of field-length treatments and small plots in Field AR16.

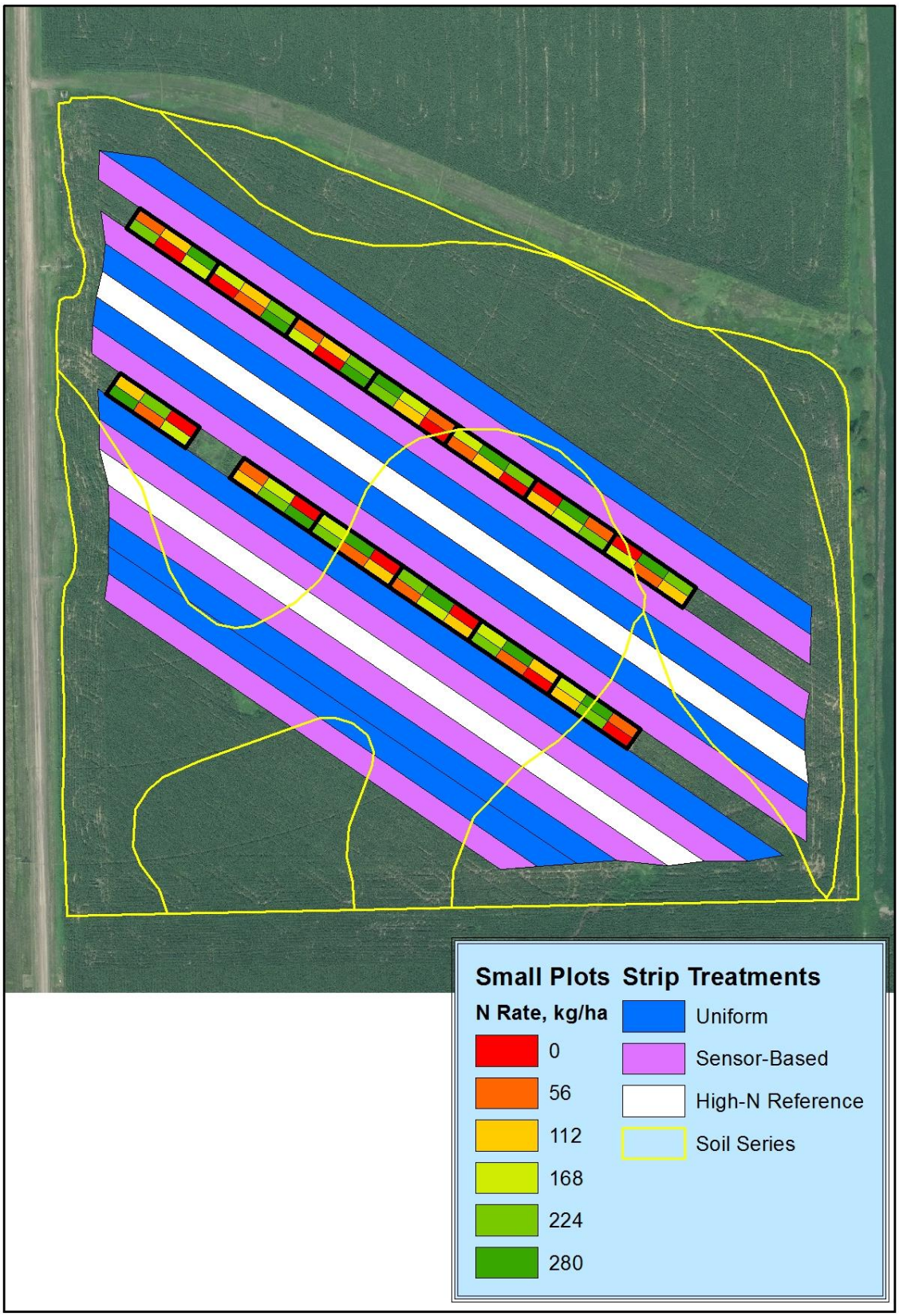

Fig. A1.2. Experimental design of field-length treatments and small plots in Field CA16.

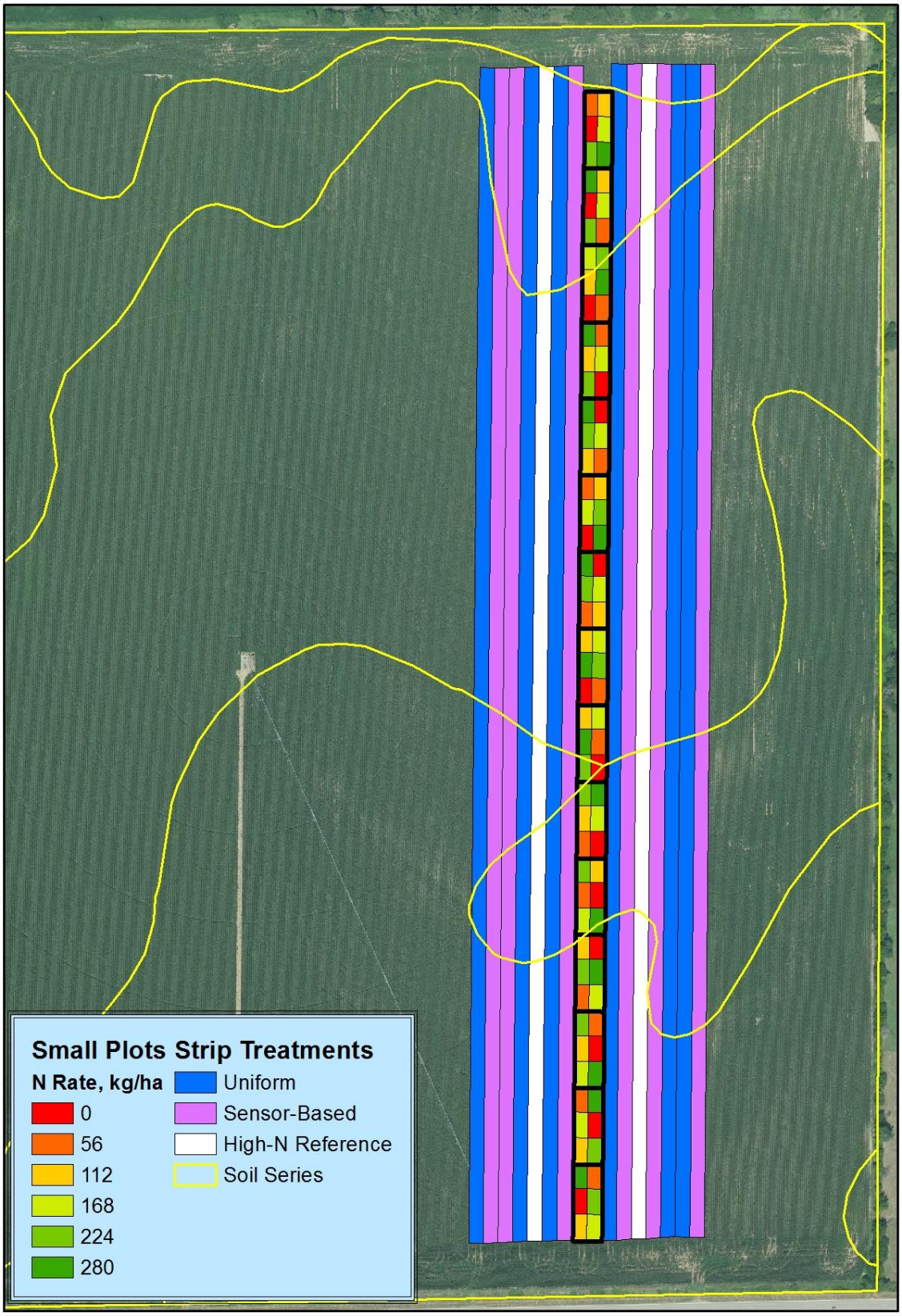

Fig. A1.3. Experimental design of field-length treatments and small plots in Field HU16.

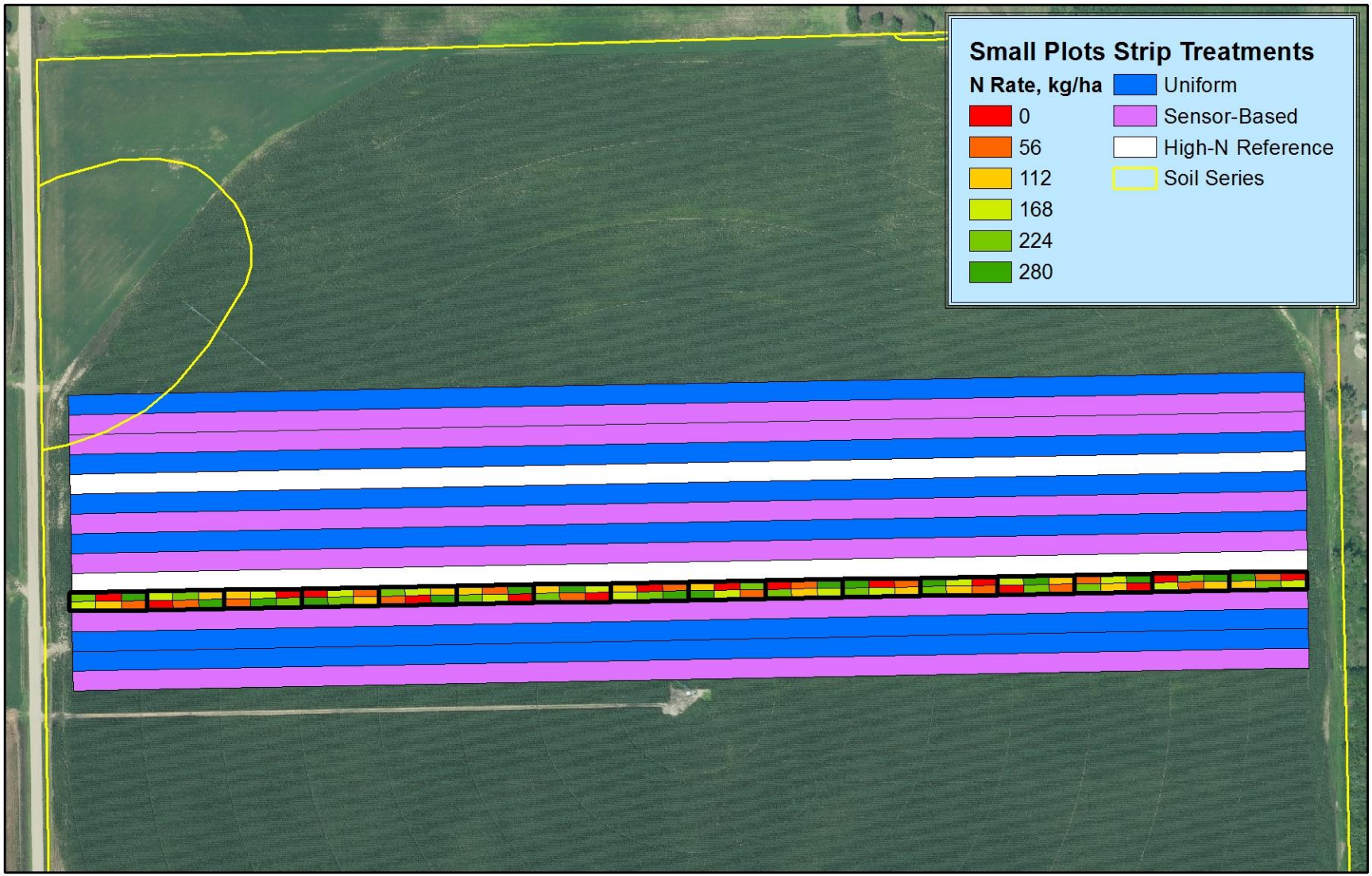

Fig. A1.4. Experimental design of field-length treatments and small plots in Field KR16.

Fig. A1.5. Experimental design of field-length treatments and small plots in Field AR17.

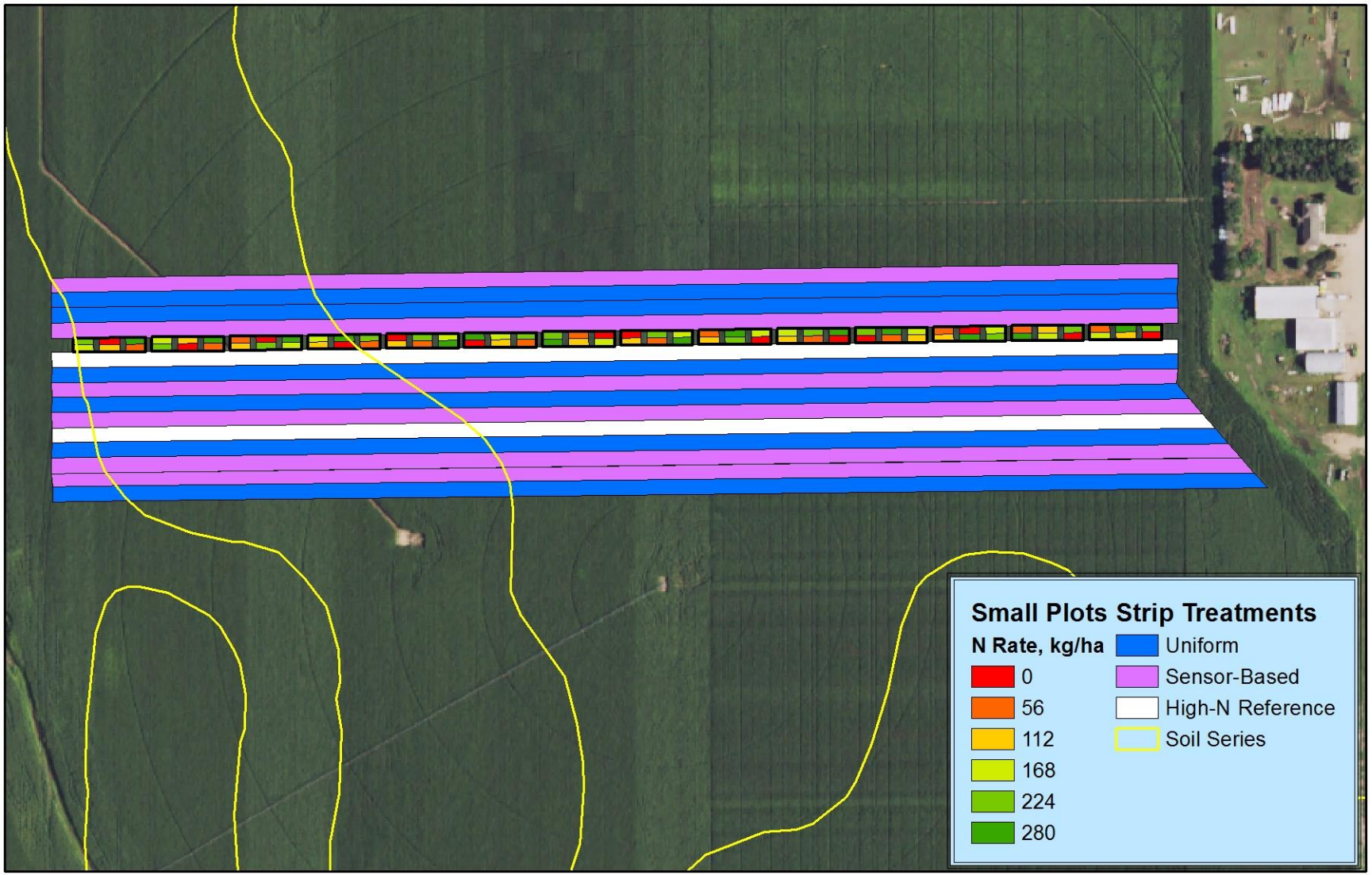

Fig. A1.6. Experimental design of field-length treatments and small plots in Field HU17.

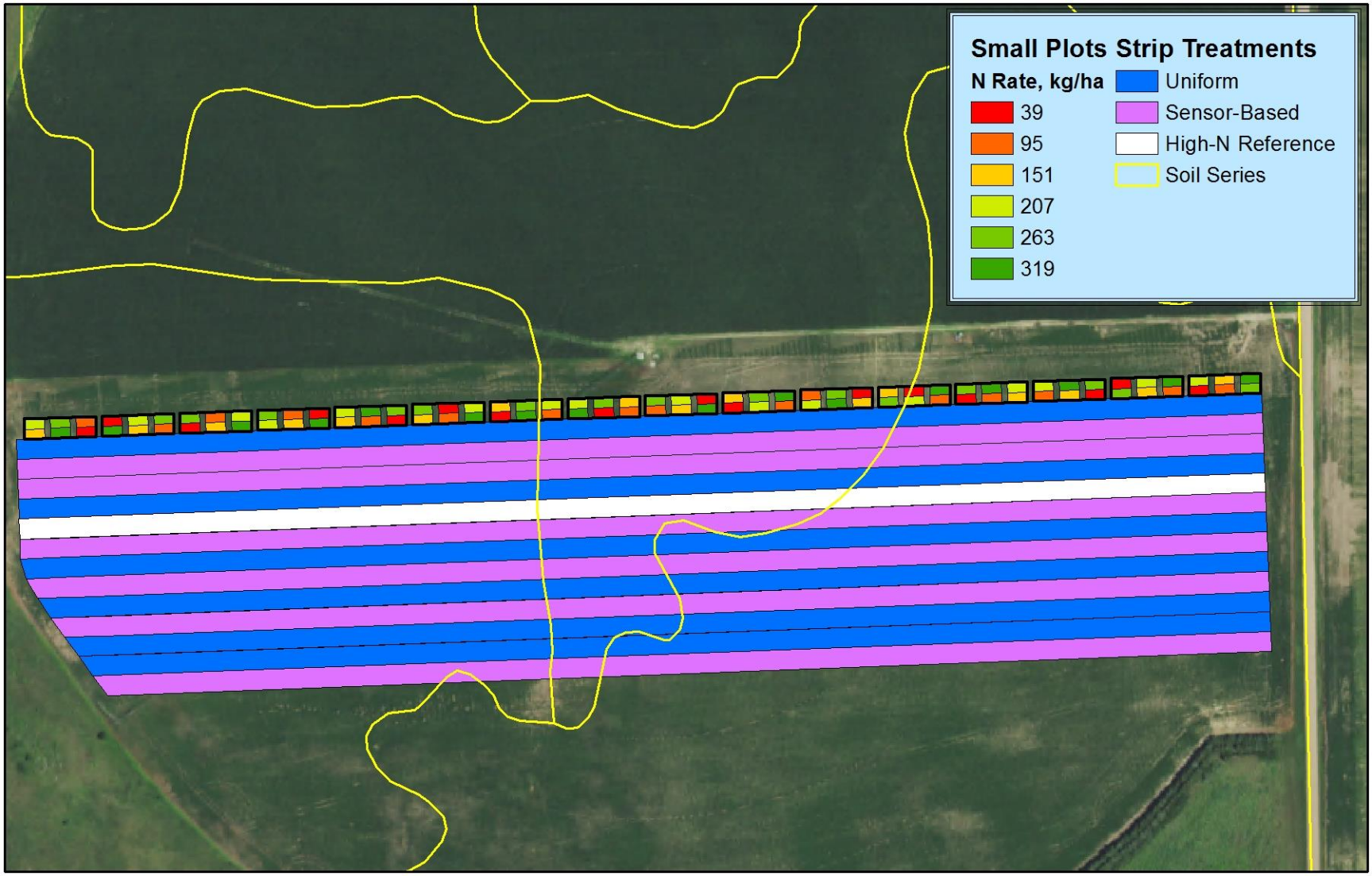

Fig. A1.7. Experimental design of field-length treatments and small plots in Field JA17.

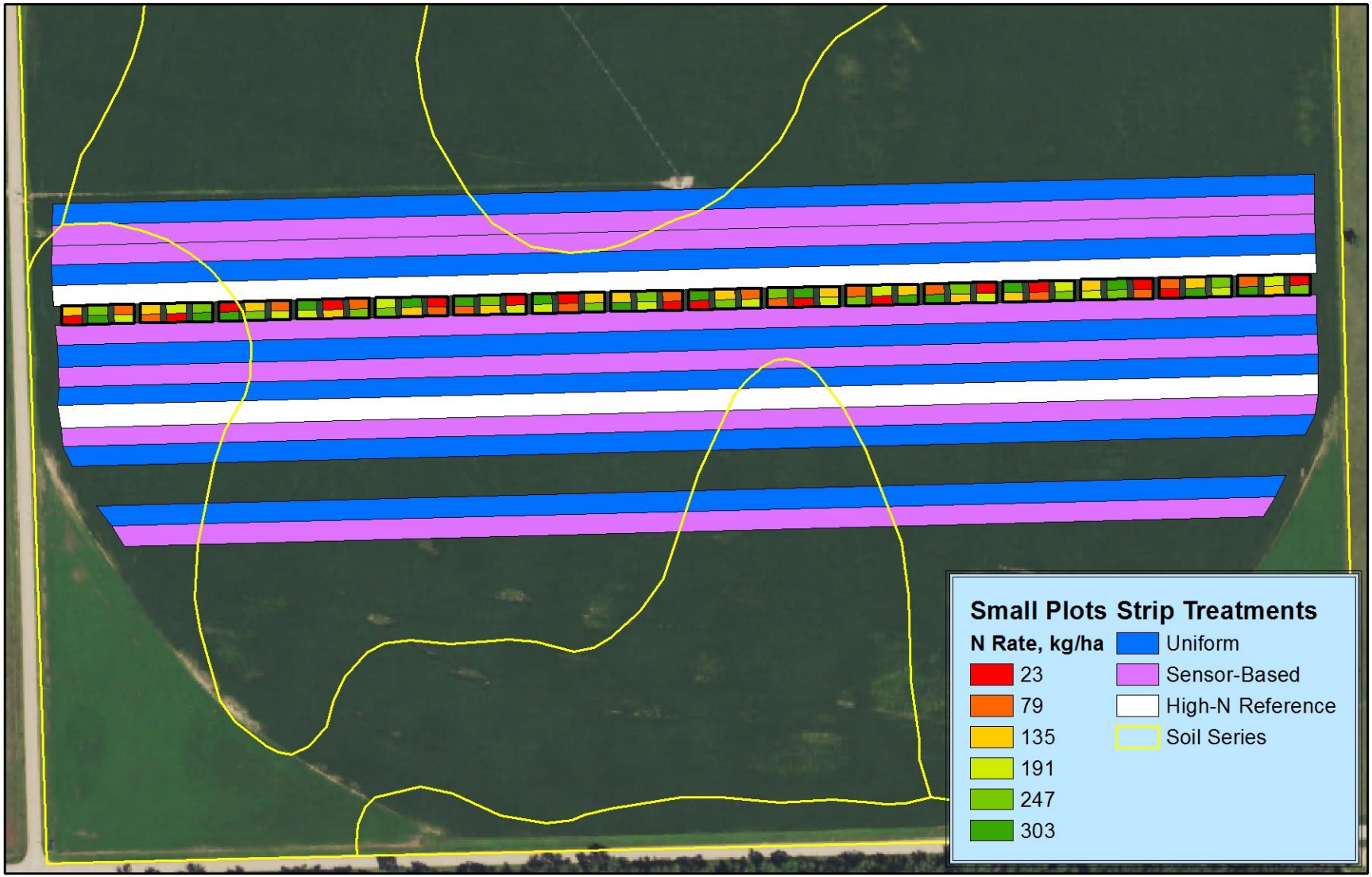

Fig. A1.8. Experimental design of field-length treatments and small plots in Field KR17.

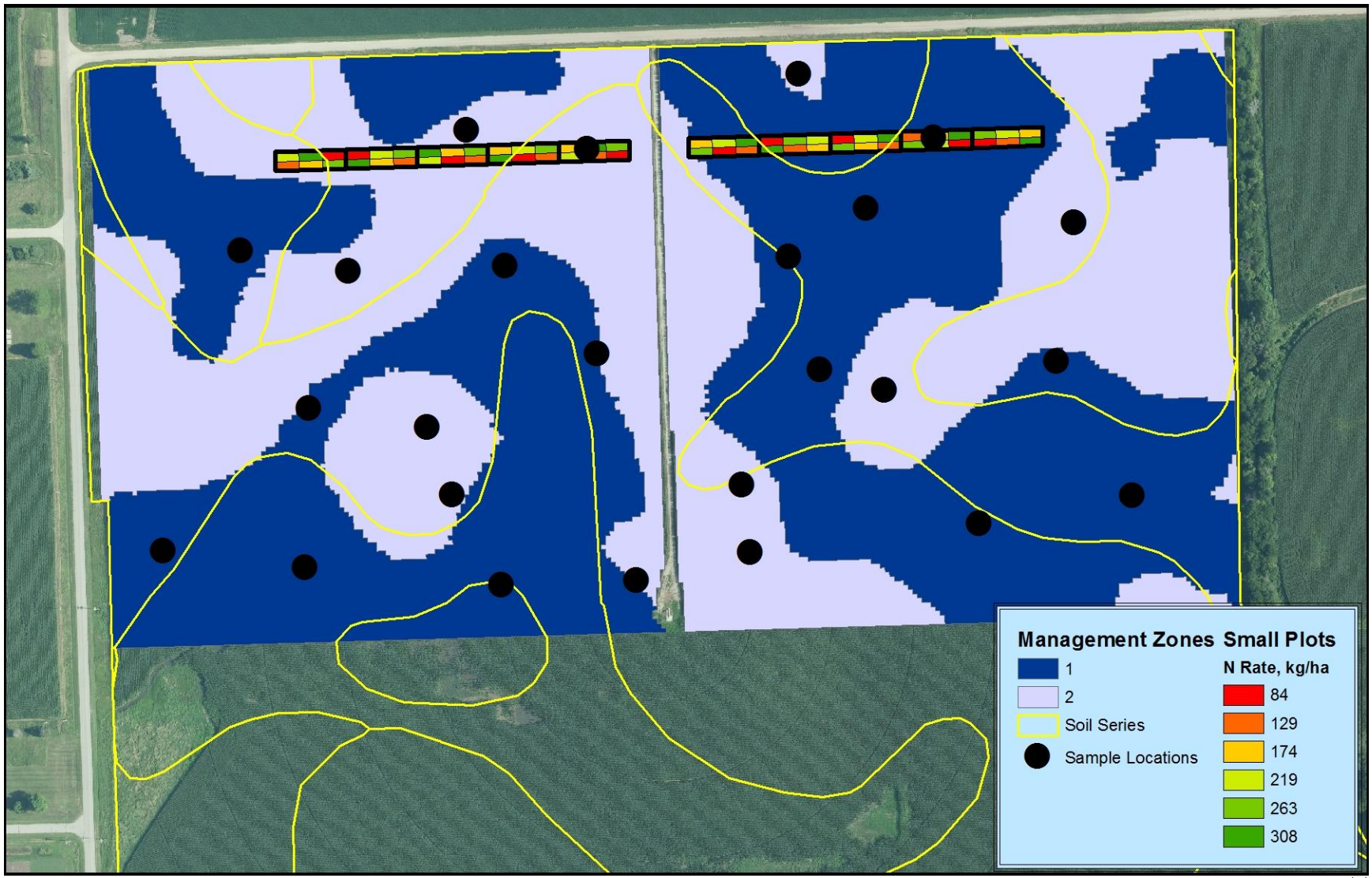

Fig. A1.9. Management zone delineation for Field AR16 using EC_s and EC_d.

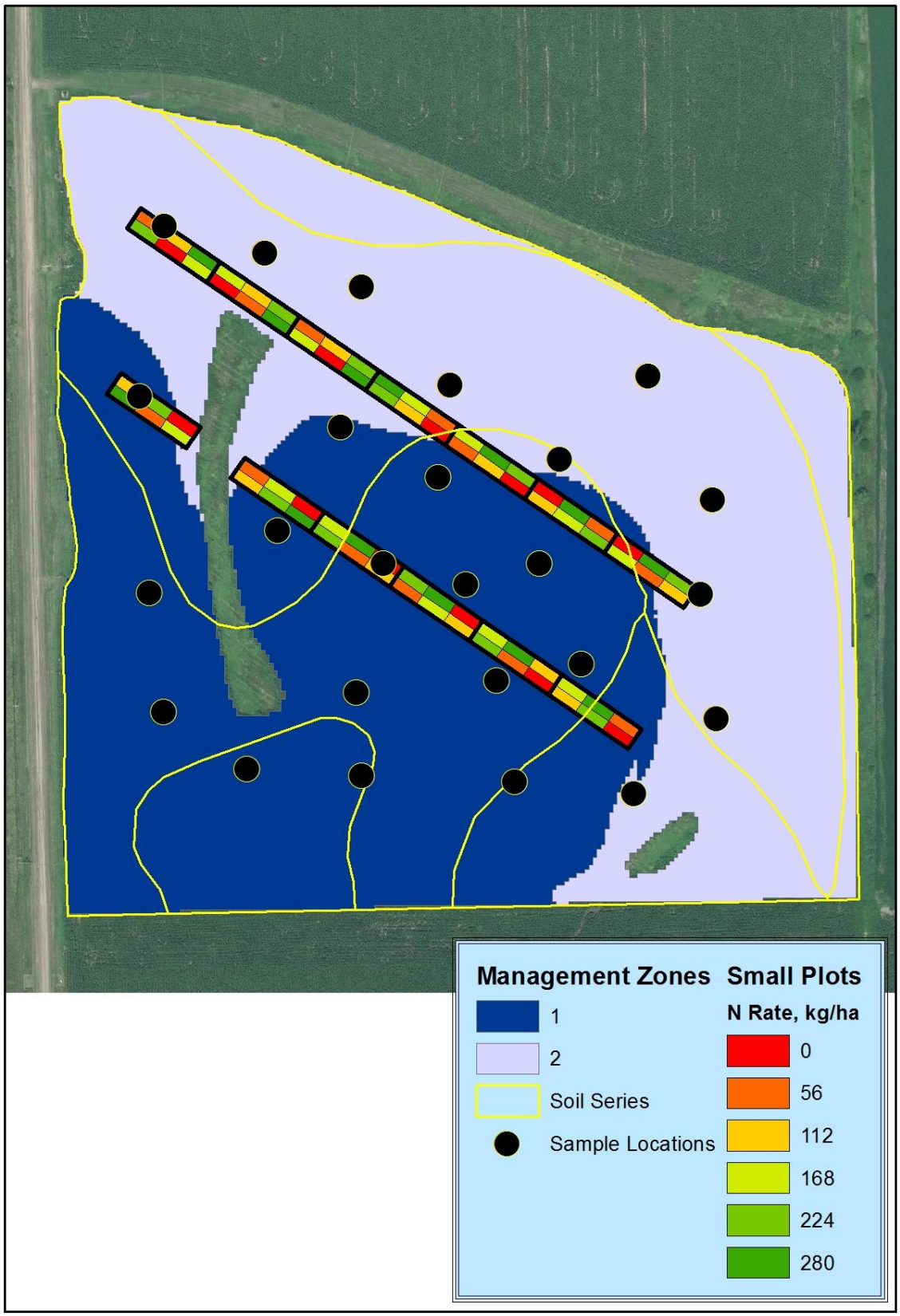

Fig. A1.10. MZ delineation for Field CA16 using $Elev_{rel}$.

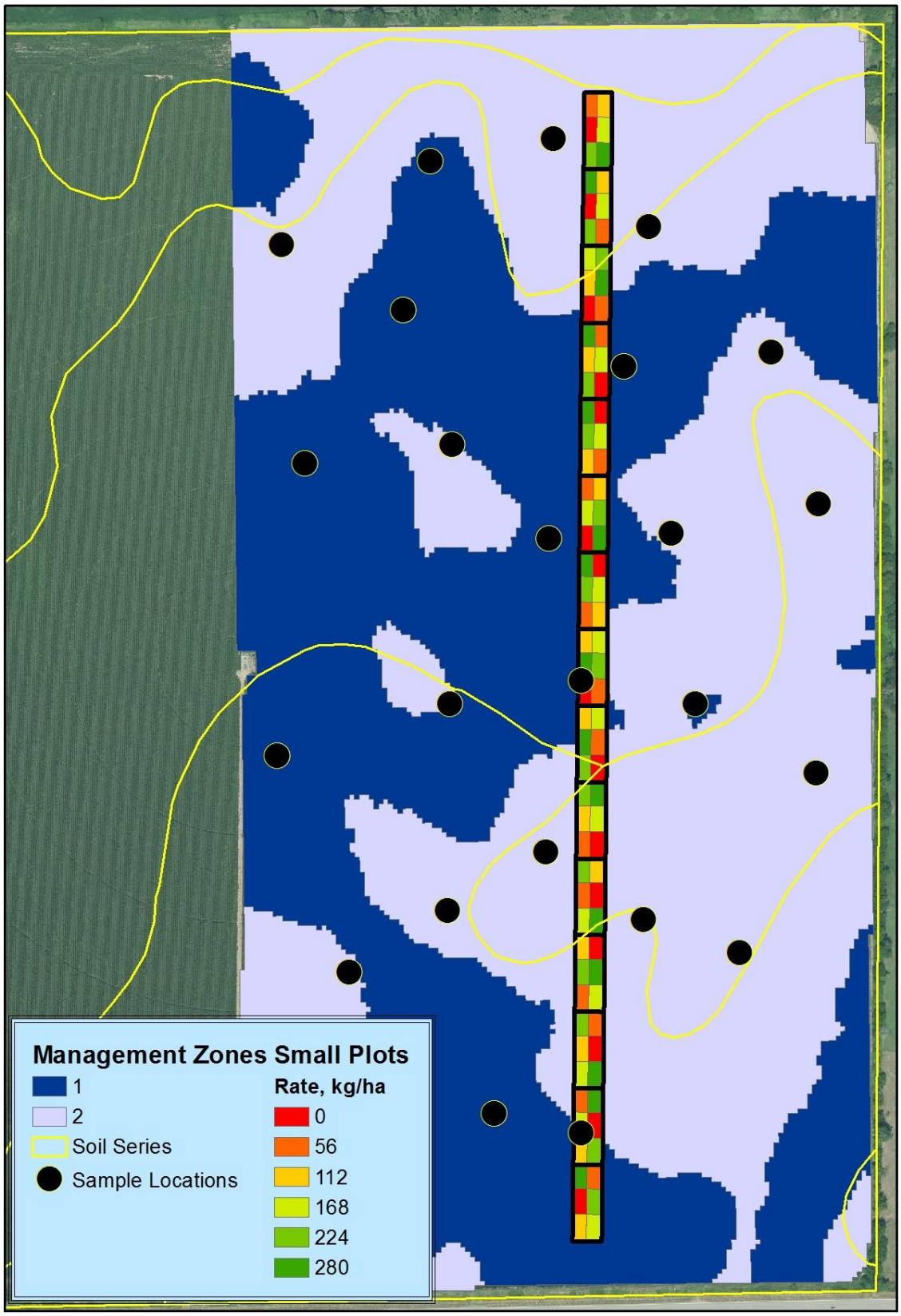

Fig. A1.11. MZ delineation for Field HU16 using EC_d and EC_s.

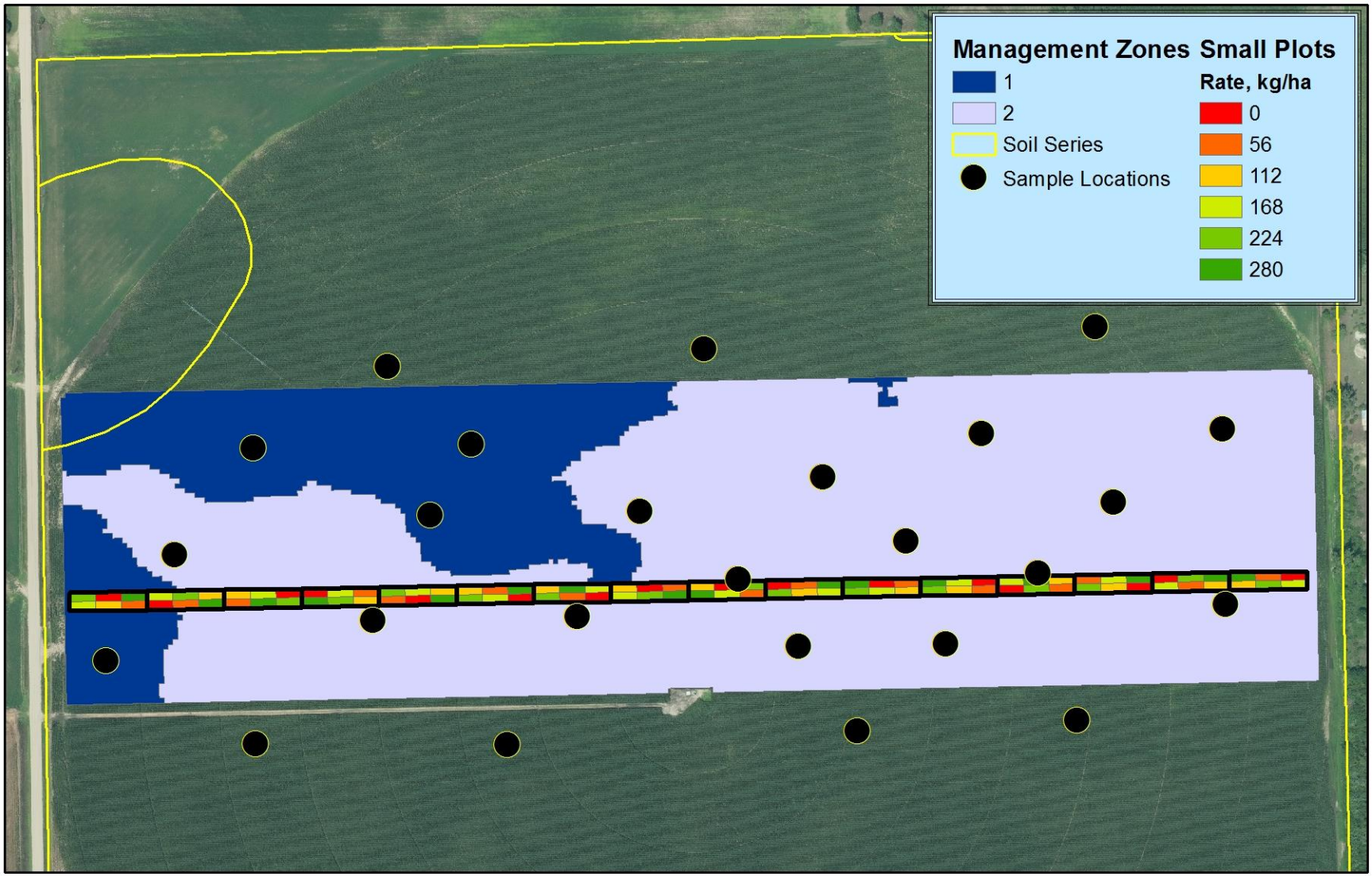

Fig A1.12. MZ delineation for Field KR16 using EC_s and EC_d.

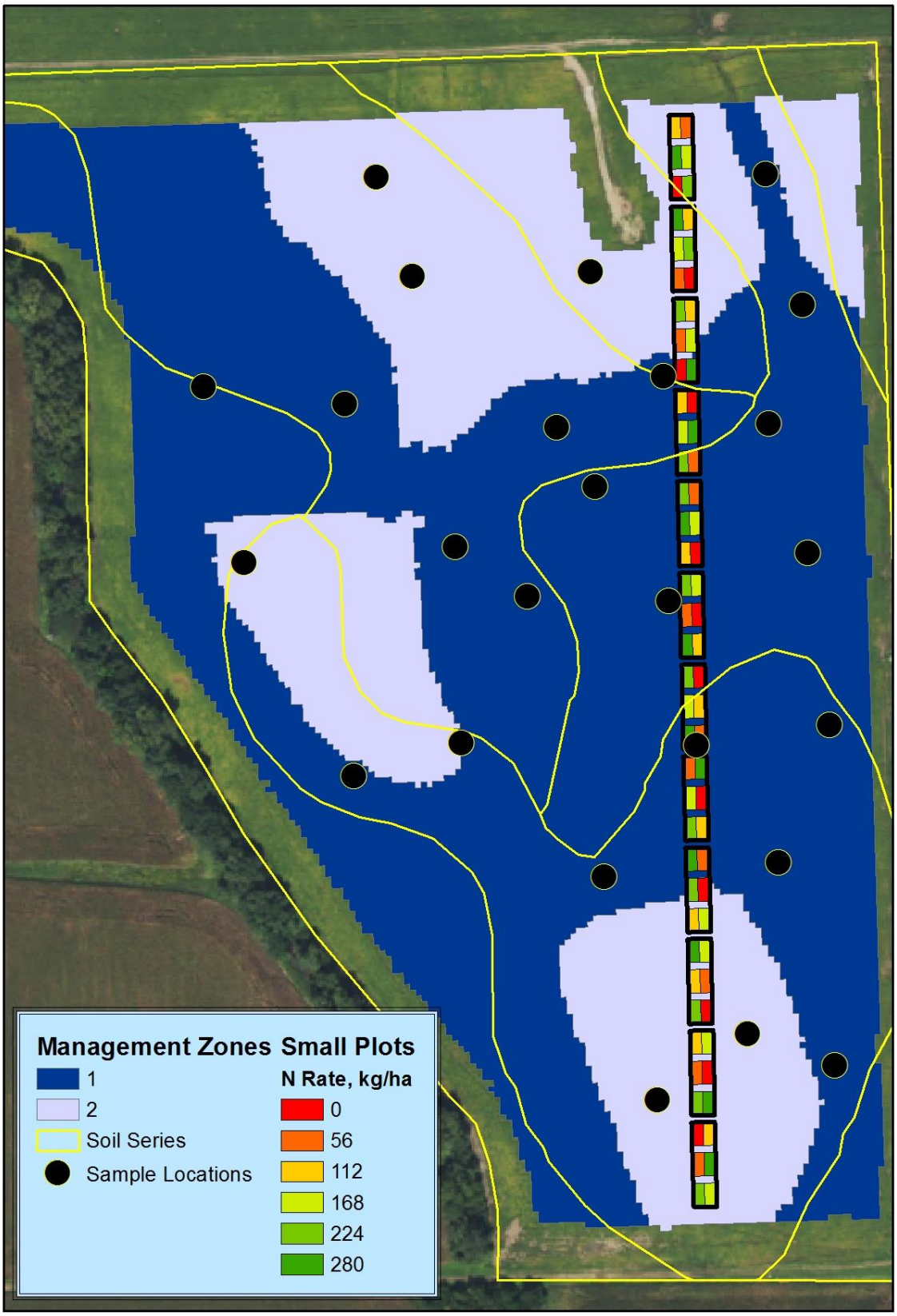

Fig. A1.13. MZ delineation for Field AR17 using $Elev_{rel}$ and SOM.

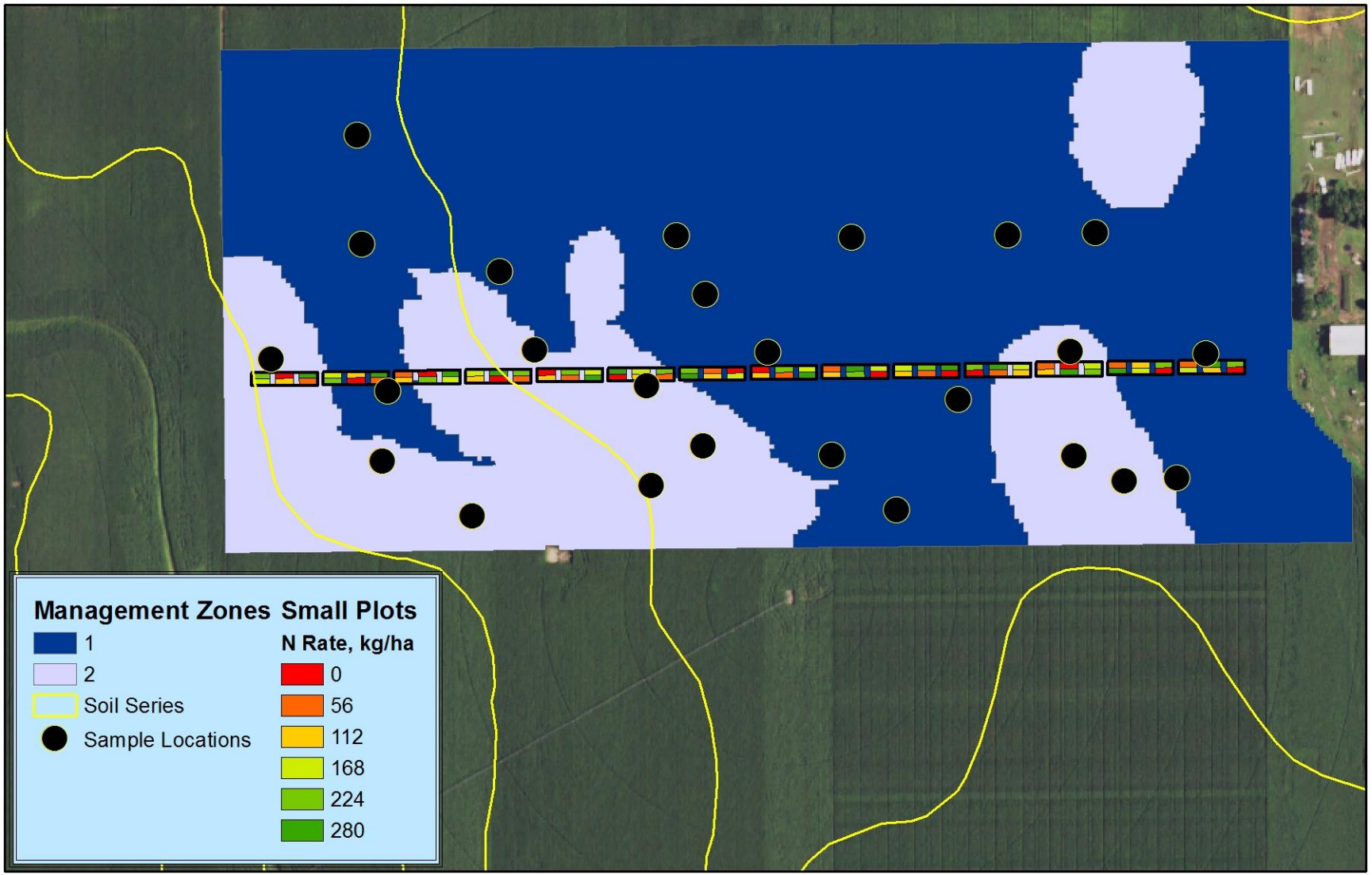

Fig. A1.14. MZ delineation for Field HU17 using EC_s and SOM.

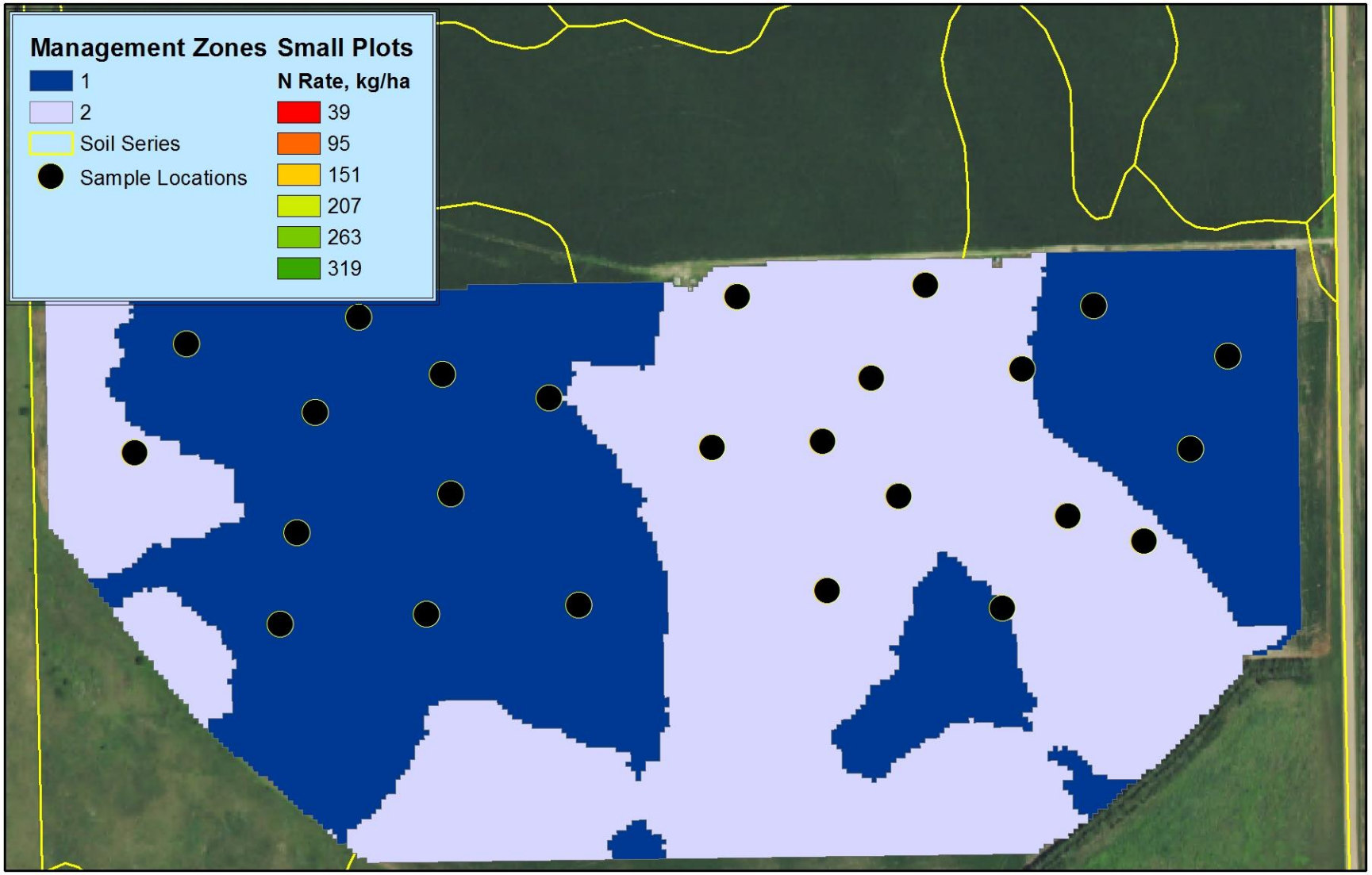

Fig. A1.15. MZ delineation for Field JA17 using SOM.

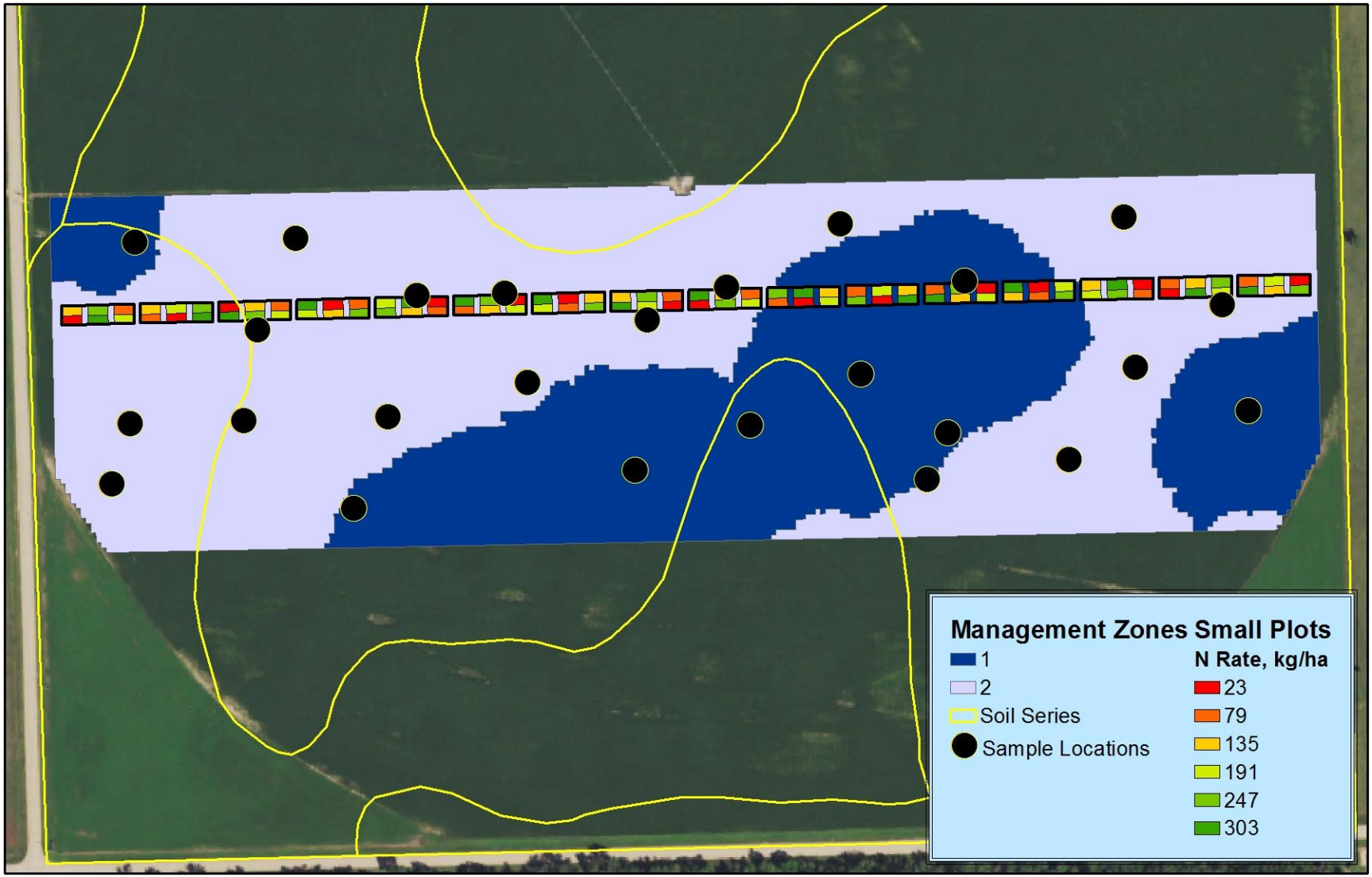

Fig A1.16. MZ delineation for Field KR17 using EC_s and EC_d.

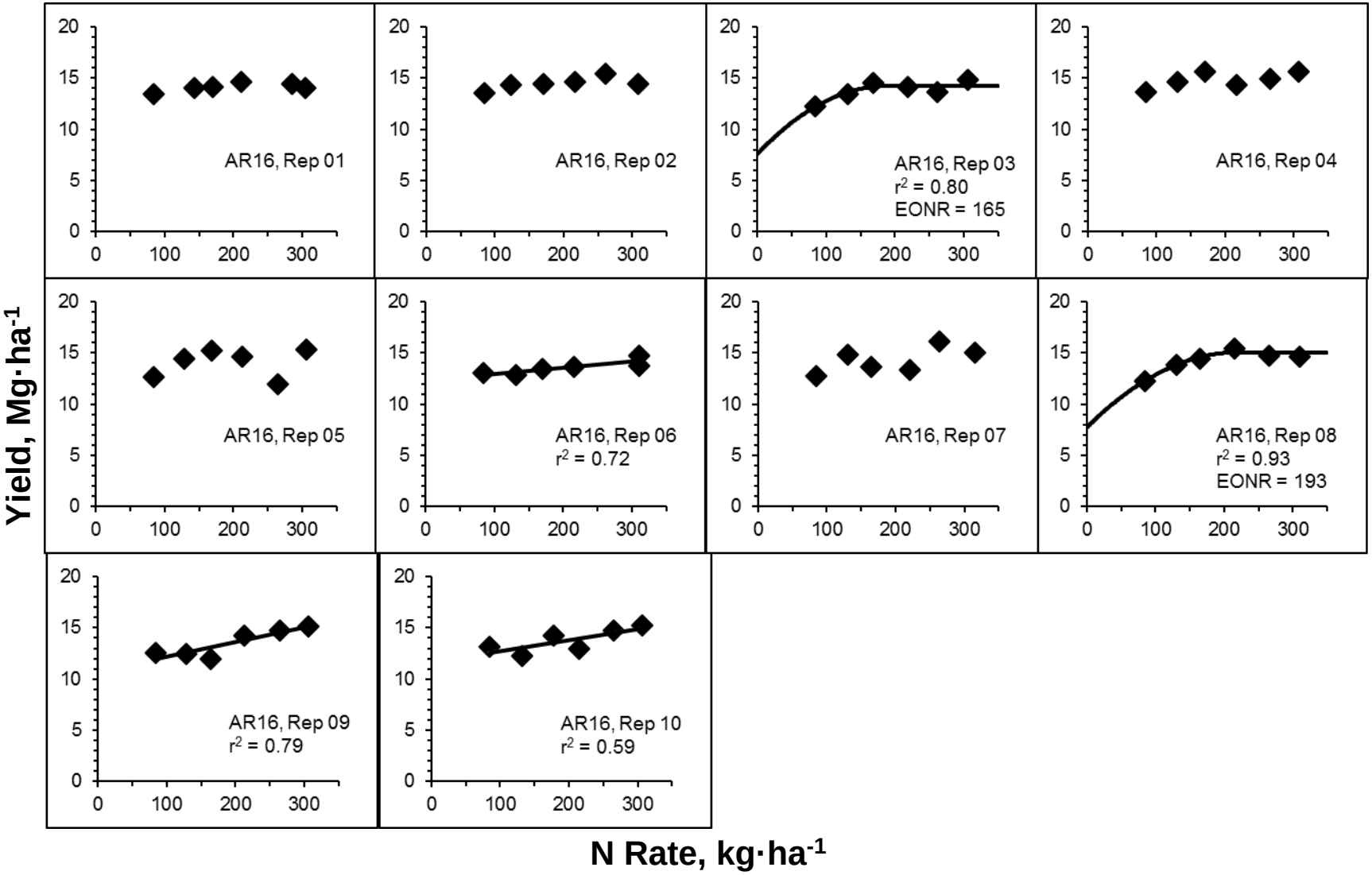

Fig. A1.17. Yield response to N rate models for treatment blocks in Field AR16.

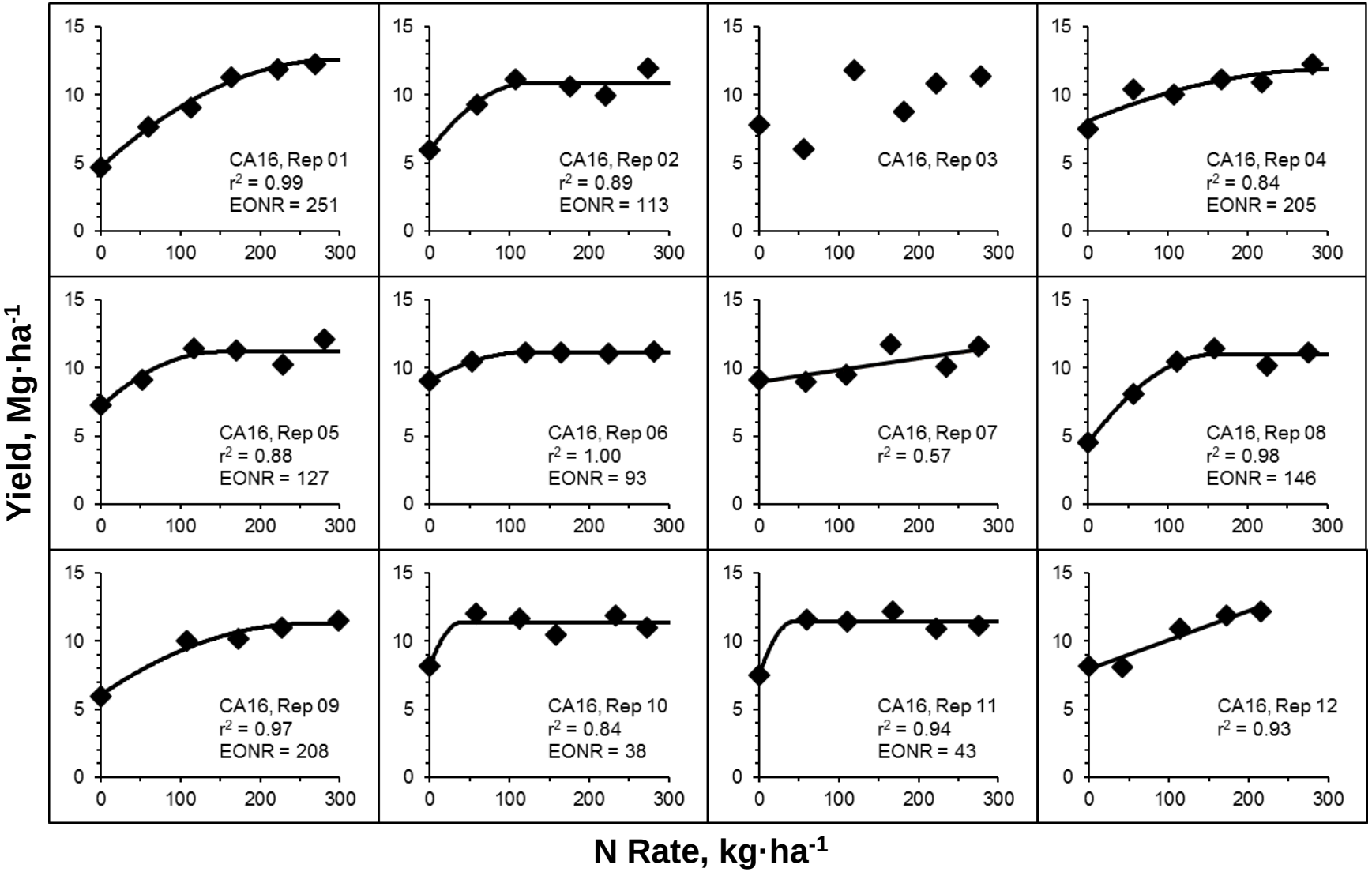

Fig. A1.18. Yield response to N rate models for treatment blocks in Field CA16.

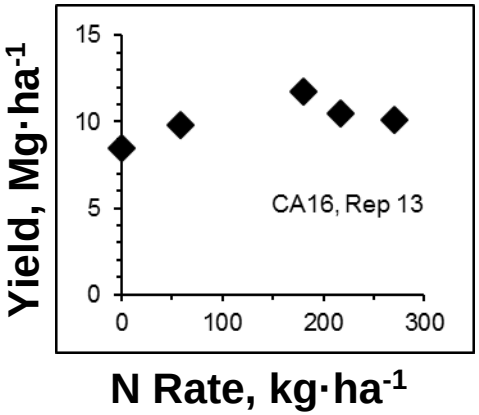

Fig. A1.18. Yield response to N rate models for treatment blocks in Field CA16.

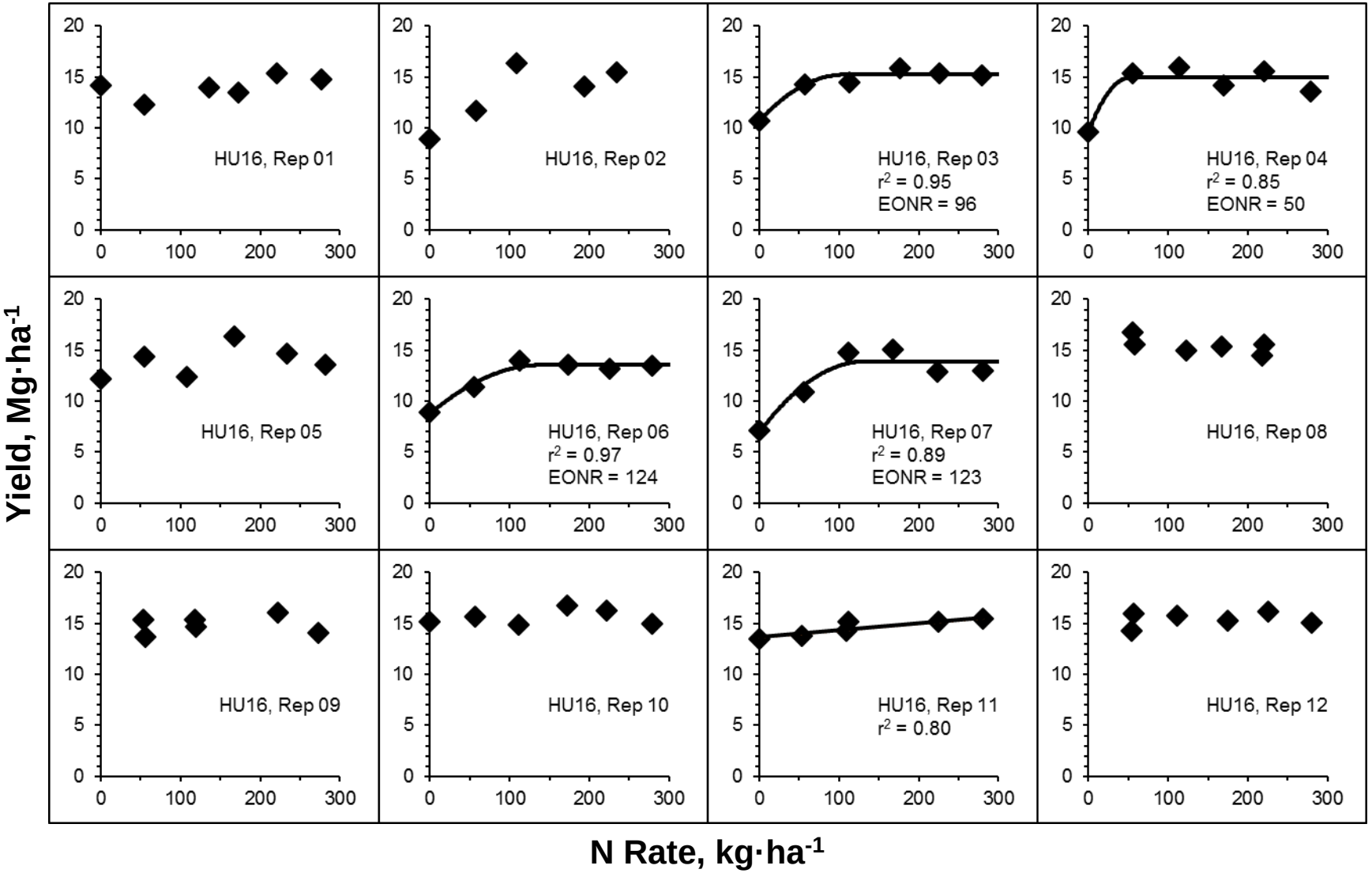

Fig. A1.19. Yield response to N rate models for treatment blocks in Field HU16.

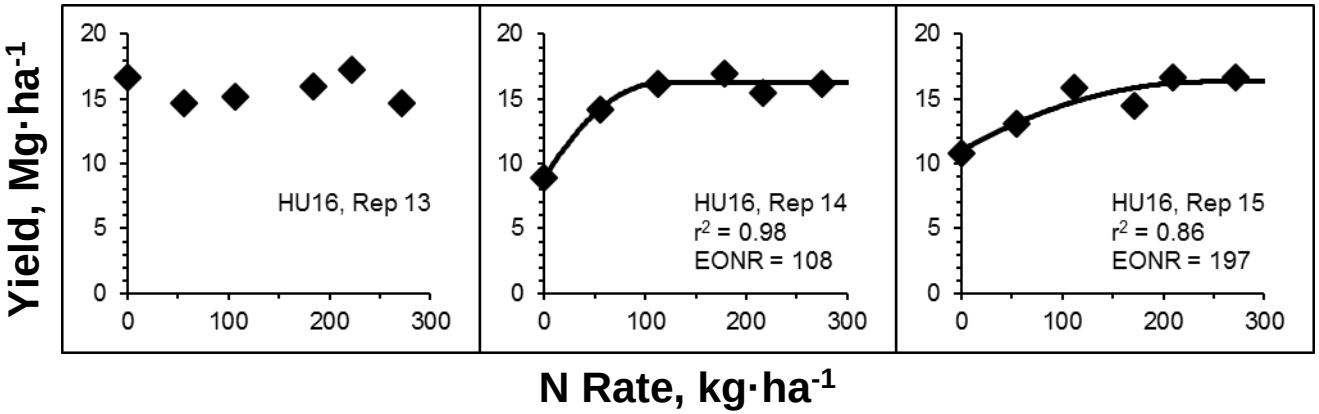

Fig. A1.19. Yield response to N rate models for treatment blocks in Field HU16.

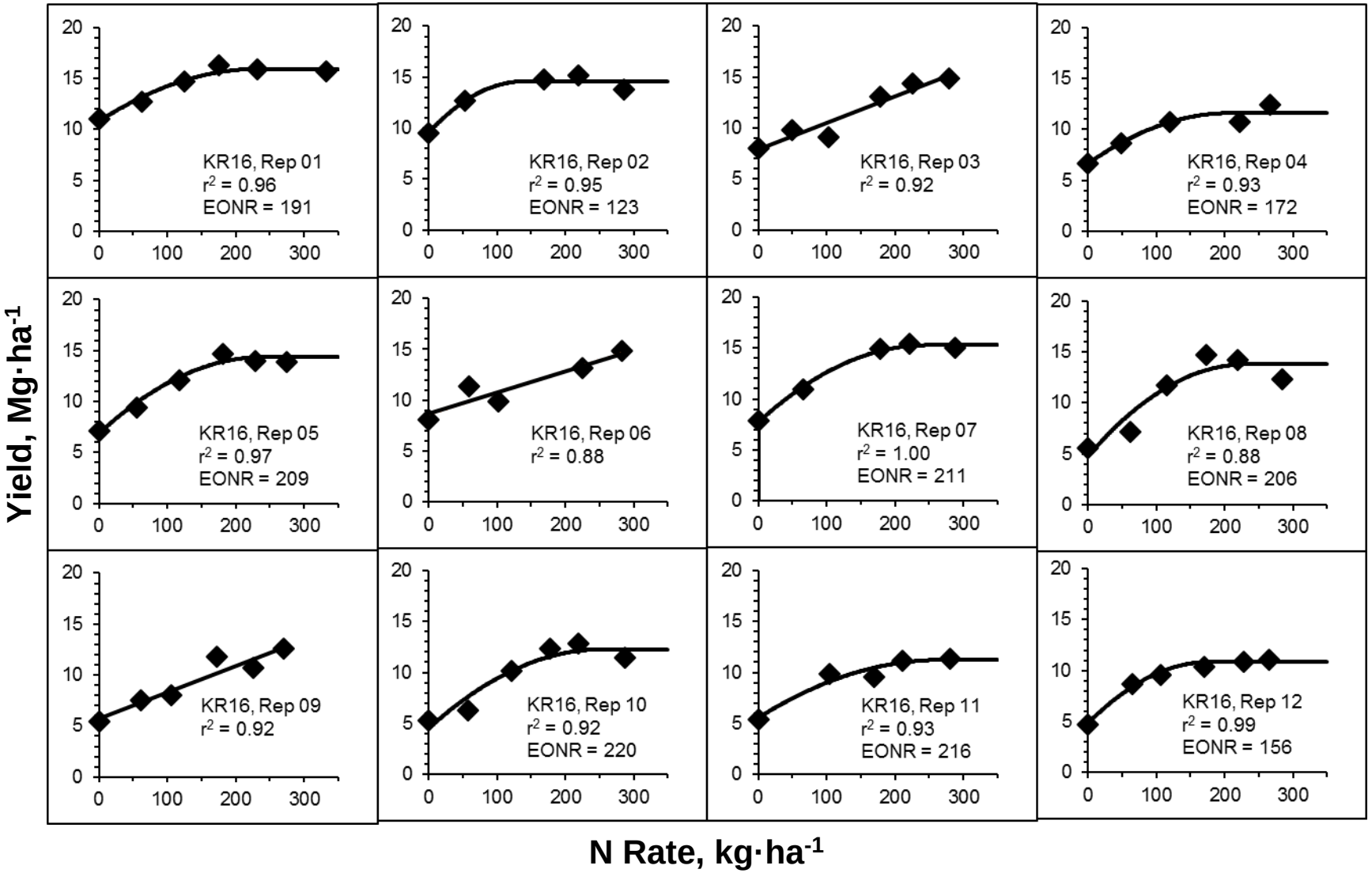

Fig. A1.20. Yield response to N rate models for treatment blocks in Field KR16.

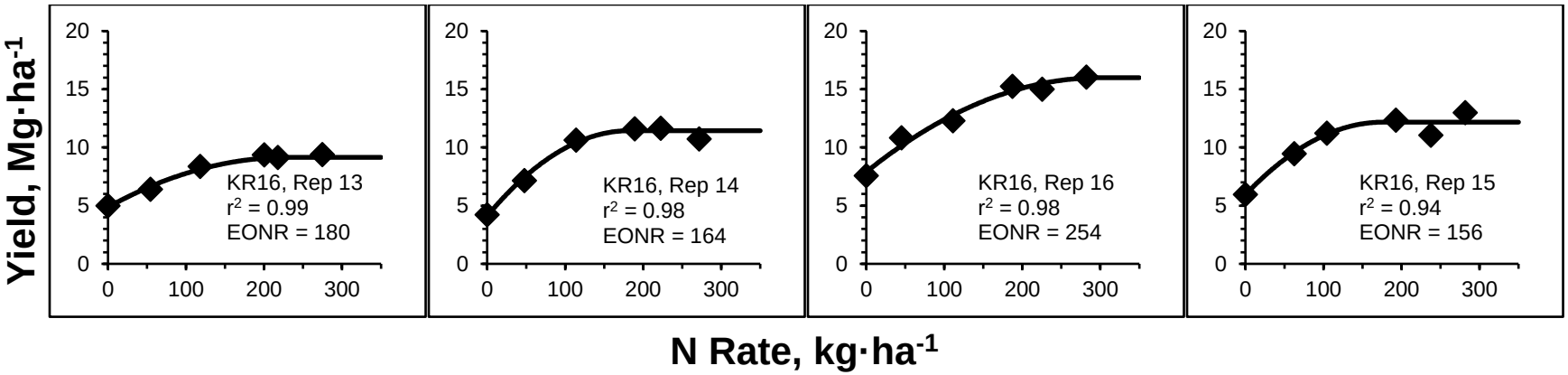

Fig. A1.20. Yield response to N rate models for treatment blocks in Field KR16.

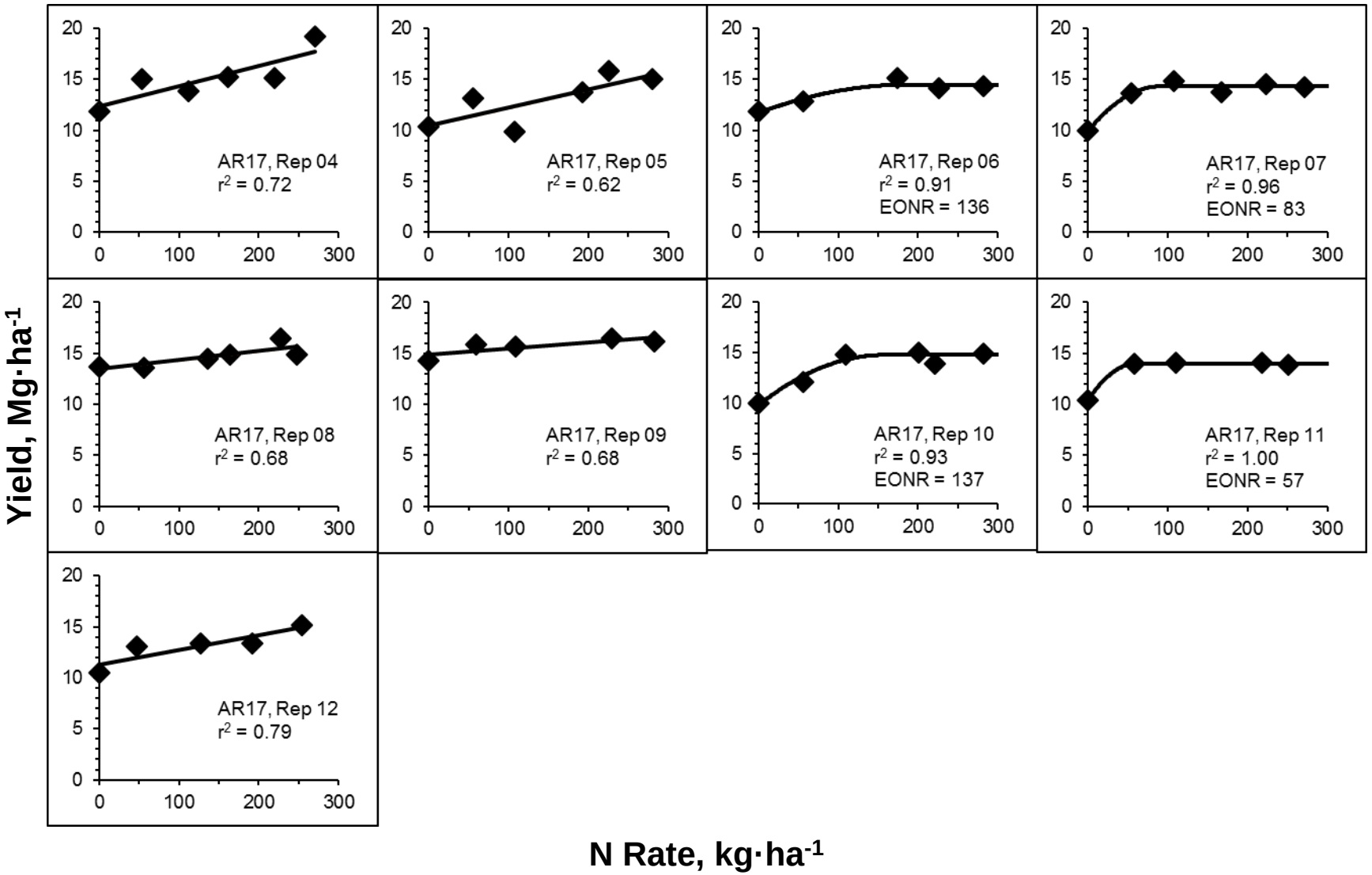

Fig. A1.21. Yield response to N rate models for treatment blocks in Field AR17.

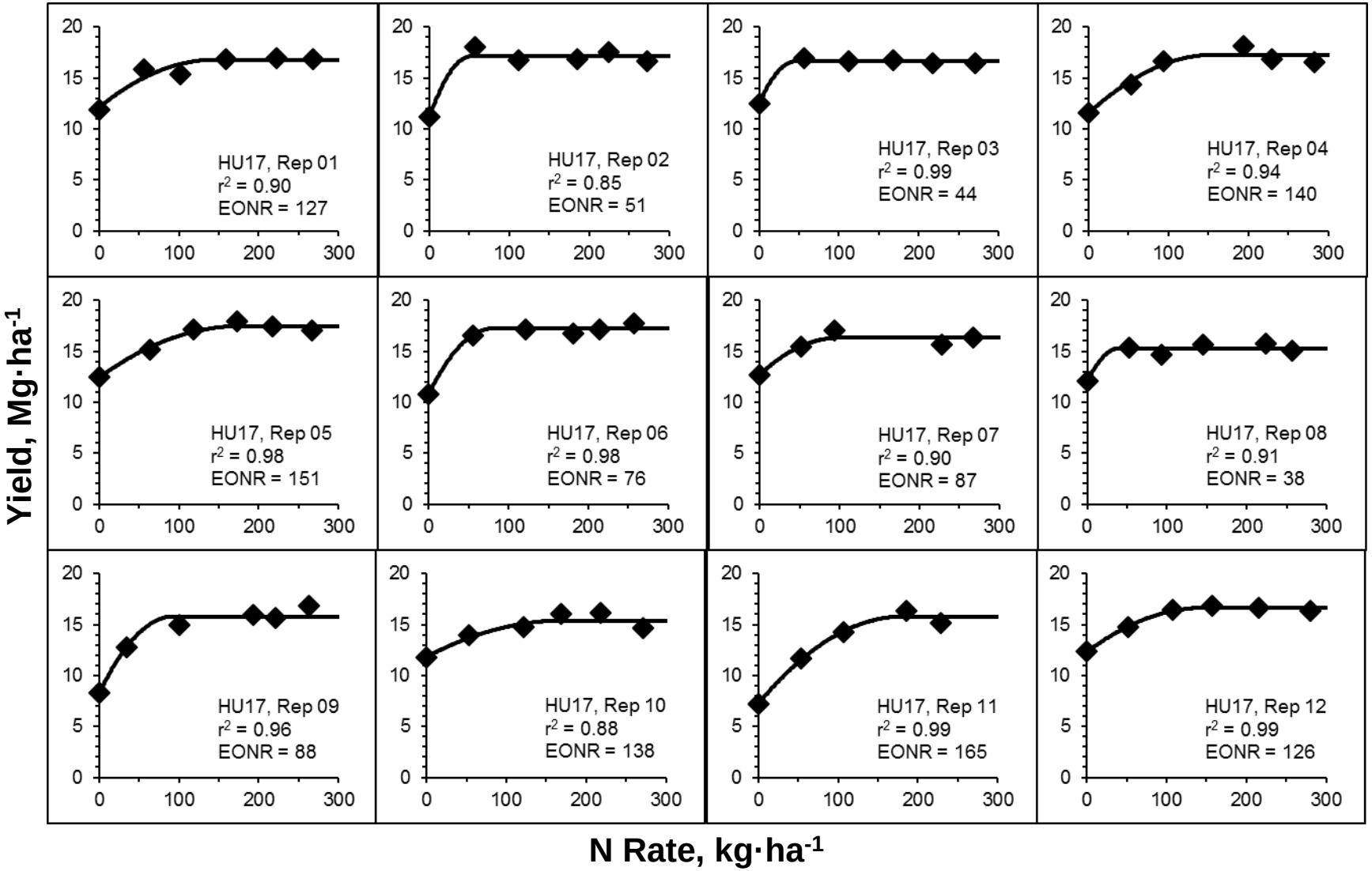

Fig. A1.22. Yield response to N rate models for treatment blocks in Field HU17.

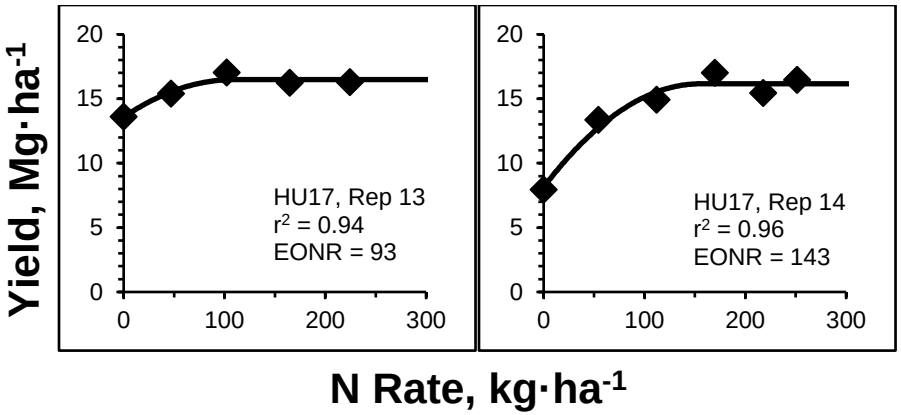

Fig. A1.22. Yield response to N rate models for treatment blocks in Field HU17.

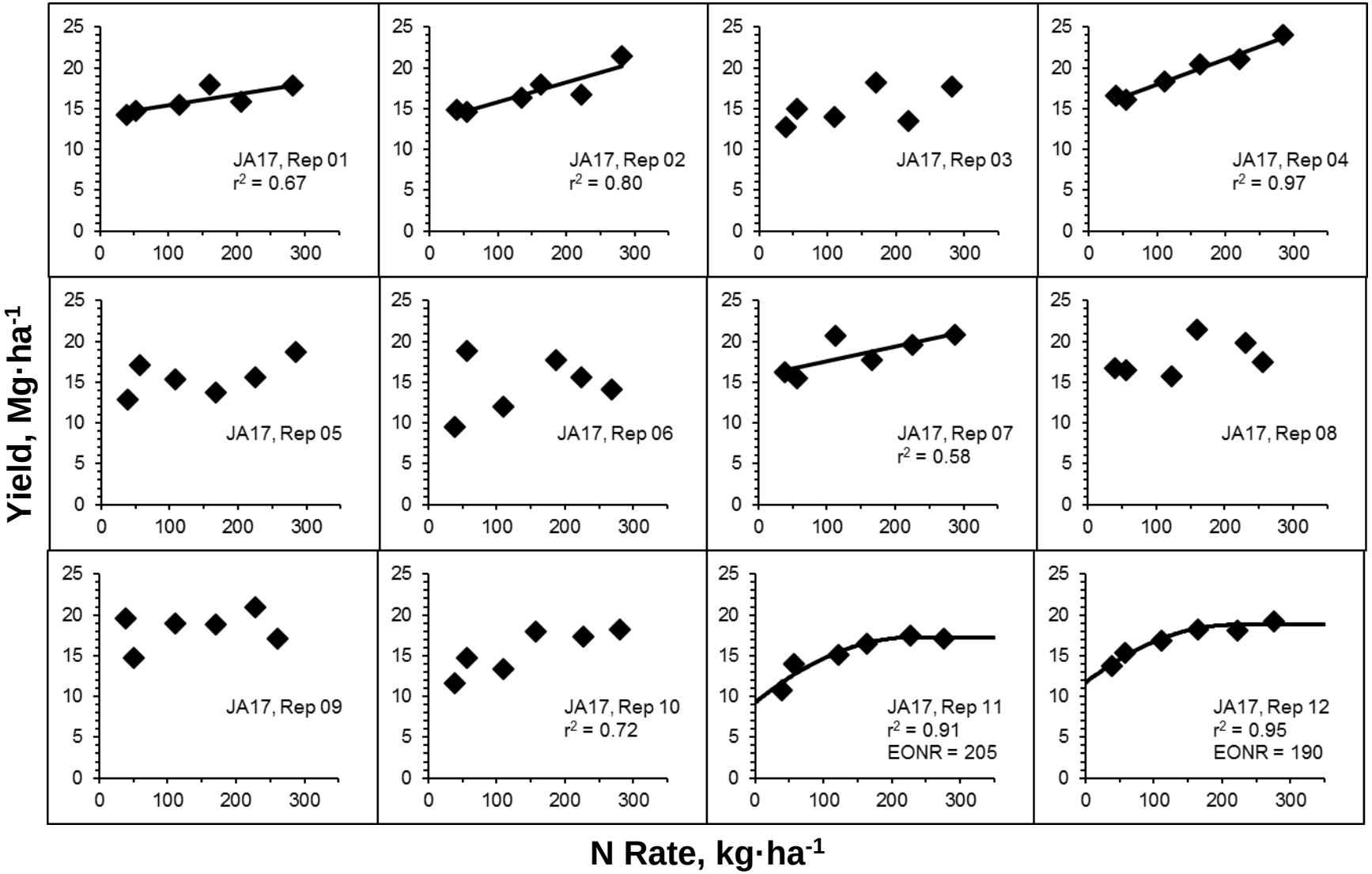

Fig. A1.23. Yield response to N rate models for treatment blocks in Field JA17.

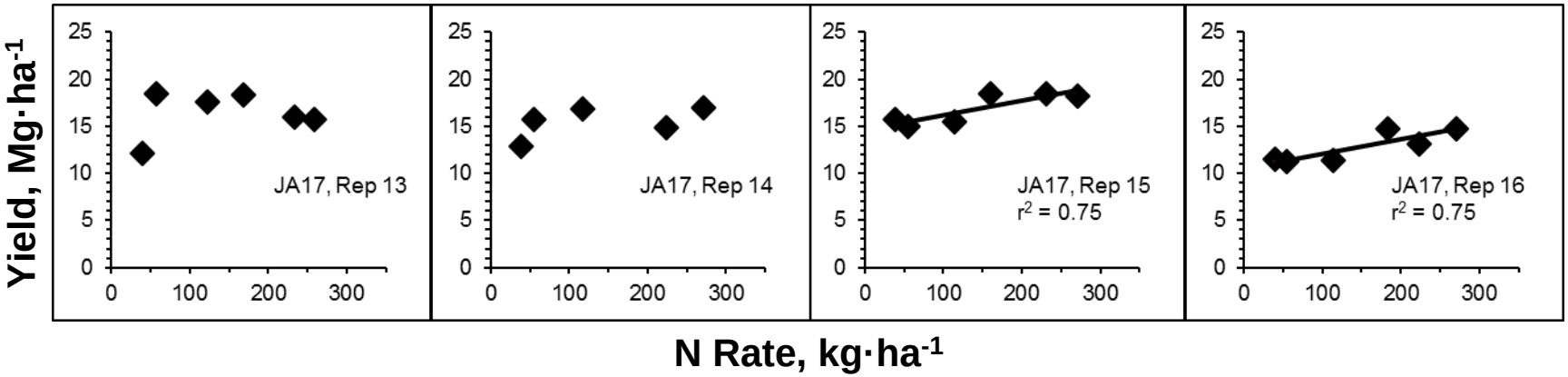

Fig. A1.23. Yield response to N rate models for treatment blocks in Field JA17.

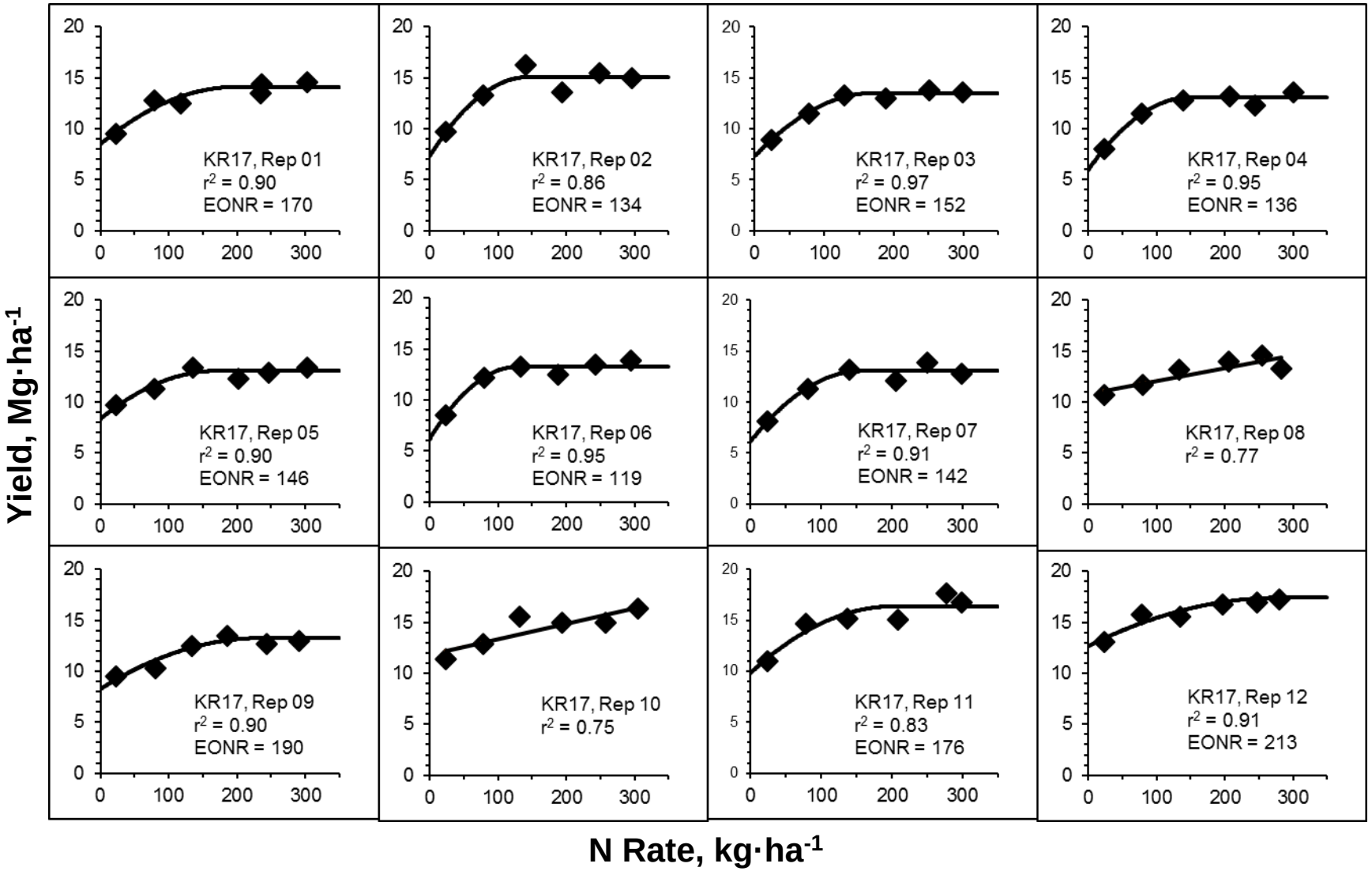

Fig. A1.24. Yield response to N rate models for treatment blocks in Field KR17.

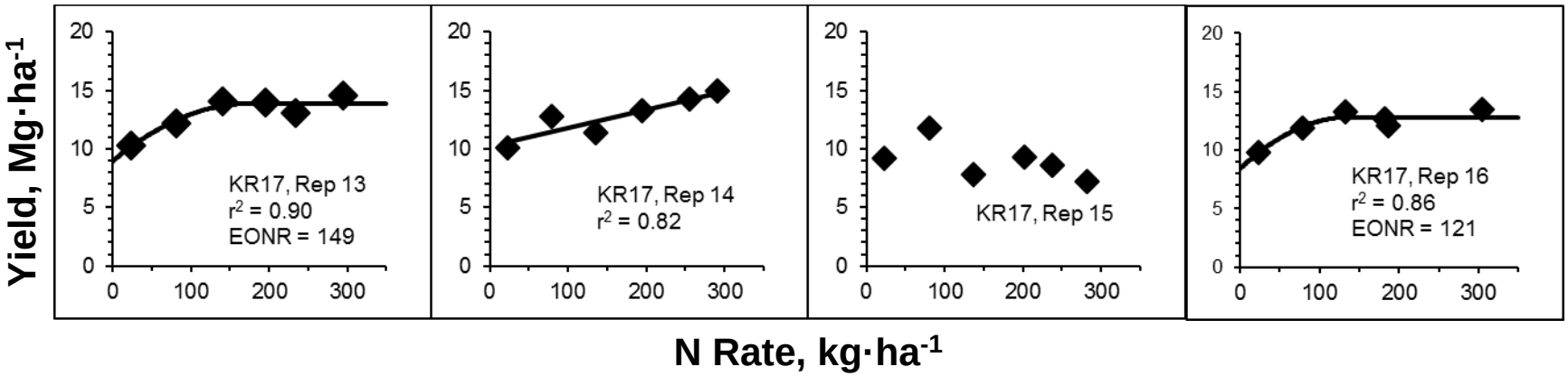

Fig. A1.24. Yield response to N rate models for treatment blocks in Field KR17.

Table A1.1. Pearson correlation coefficients of soil and topographic variables to check plot yield and in-season NDRE for Field AR16 (n = 10).

			Apparent Electrical Conductivity		Soil Optical Reflectance		Landscape	
	Yield	**NDRE**	**EC_s**	**EC_d**	**SR_{soil}**	**SOM**	**$Elev_{rel}$**	**Slope**
Yield	1							
NDRE	-0.21	1						
EC_s	0.46	-0.86**	1					
EC_d	0.41	-0.83**	0.97***	1				
SR_{soil}	-0.30	0.69*	-0.43	-0.38	1			
SOM	-0.40	0.60#	-0.78**	-0.74*	0.21	1		
$Elev_{rel}$	0.28	-0.74*	0.84**	0.93***	-0.34	-0.54	1	
Slope	0.21	-0.65*	0.57#	0.39	-0.44	-0.44	0.16	1

Statistical significance at P < 0.10.
* Statistical significance at P < 0.05.
** Statistical significance at P < 0.01.
*** Statistical significance at P < 0.001.

Table A1.2. Pearson correlation coefficients of soil and topographic variables to in-season NDRE for all nonzero plots for Field AR16 (n = 50).

		Apparent Electrical Conductivity		Soil Optical Reflectance		Landscape	
	NDRE	**EC_s**	**EC_d**	**SR_{soil}**	**SOM**	**$Elev_{rel}$**	**Slope**
NDRE	1						
EC_s	-0.66***	1					
EC_d	-0.62***	0.96***	1				
SR_{soil}	0.27#	-0.17	-0.15	1			
SOM	0.40**	-0.66***	-0.55***	-0.03	1		
$Elev_{rel}$	-0.58***	0.93***	0.91***	-0.10	-0.59***	1	
Slope	-0.30*	0.46***	0.34*	-0.17	-0.52***	0.33*	1

Statistical significance at P < 0.10.
* Statistical significance at P < 0.05.
** Statistical significance at P < 0.01.
*** Statistical significance at P < 0.001.

Table A1.3. Pearson correlation coefficients of soil and topographic variables to check plot yield and in-season NDRE for Field CA16 (n = 13).

			Apparent Electrical Conductivity		Soil Optical Reflectance		Landscape	
	Yield	**NDRE**	**EC_s**	**EC_d**	**SR_{soil}**	**SOM**	**$Elev_{rel}$**	**Slope**
Yield	1							
NDRE	0.77**	1						
EC_s	0.43	0.55#	1					
EC_d	0.41	0.41	0.84**	1				
SR_{soil}	0.30	-0.20	-0.05	0.22	1			
SOM	-0.12	0.36	0.28	0.23	-0.63*	1		
$Elev_{rel}$	0.43	0.60*	0.26	0.16	-0.32	0.55#	1	
Slope	-0.18	-0.32	0.00	-0.06	0.14	0.09	-0.16	1

Statistical significance at P < 0.10.
* Statistical significance at P < 0.05.
** Statistical significance at P < 0.01.
*** Statistical significance at P < 0.001.

Table A1.4. Pearson correlation coefficients of soil and topographic variables to in-season NDRE for all nonzero plots for Field CA16 (n = 65).

		Apparent Electrical Conductivity		Soil Optical Reflectance		Landscape	
	NDRE	**EC_s**	**EC_d**	**SR_{soil}**	**SOM**	**$Elev_{rel}$**	**Slope**
NDRE	1						
EC_s	0.07	1					
EC_d	-0.06	0.90***	1				
SR_{soil}	0.01	-0.27*	-0.16	1			
SOM	0.06	0.36**	0.38**	-0.51***	1		
$Elev_{rel}$	0.23#	0.11	0.01	-0.29*	0.63***	1	
Slope	-0.15	-0.05	-0.08	0.16	-0.19	-0.02	1

Statistical significance at P < 0.10.
* Statistical significance at P < 0.05.
** Statistical significance at P < 0.01.
*** Statistical significance at P < 0.001.

Table A1.5. Pearson correlation coefficients of soil and topographic variables to check plot yield and in-season NDRE for Field HU16 (n = 12).

			Apparent Electrical Conductivity		Soil Optical Reflectance		Landscape	
	Yield	**NDRE**	**EC_s**	**EC_d**	**SR_{soil}**	**SOM**	**$Elev_{rel}$**	**Slope**
Yield	1							
NDRE	0.89***	1						
EC_s	-0.64*	-0.63*	1					
EC_d	-0.80**	-0.78**	0.91***	1				
SR_{soil}	0.42	0.44	-0.78**	-0.63*	1			
SOM	0.51#	0.52#	-0.85***	-0.74**	0.94***	1		
$Elev_{rel}$	0.46	0.51#	-0.78**	-0.69*	0.86***	0.93***	1	
Slope	-0.44	-0.52#	0.82**	0.68*	-0.85***	-0.91***	-0.94***	1

Statistical significance at P < 0.10.
* Statistical significance at P < 0.05.
** Statistical significance at P < 0.01.
*** Statistical significance at P < 0.001.

Table A1.6. Pearson correlation coefficients of soil and topographic variables to in-season NDRE for all nonzero plots for Field HU16 (n = 75).

		Apparent Electrical Conductivity		Soil Optical Reflectance		Landscape	
	NDRE	**EC_s**	**EC_d**	**SR_{soil}**	**SOM**	**$Elev_{rel}$**	**Slope**
NDRE	1						
EC_s	-0.60***	1					
EC_d	-0.57***	0.85**	1				
SR_{soil}	0.38***	-0.71***	-0.42***	1			
SOM	0.41***	-0.75***	-0.56***	0.85***	1		
$Elev_{rel}$	0.35**	-0.63***	-0.50***	0.65***	0.83***	1	
Slope	-0.35**	0.71***	0.44***	-0.81***	-0.83***	-0.81***	1

Statistical significance at P < 0.10.
* Statistical significance at P < 0.05.
** Statistical significance at P < 0.01.
*** Statistical significance at P < 0.001.

Table A1.7. Pearson correlation coefficients of soil and topographic variables to check plot yield and in-season NDRE for Field KR16 (n = 16).

			Apparent Electrical Conductivity		Soil Optical Reflectance		Landscape	
	Yield	**NDRE**	**EC_s**	**EC_d**	**SR_{soil}**	**SOM**	**$Elev_{rel}$**	**Slope**
Yield	1							
NDRE	0.94***	1						
EC_s	0.91***	0.83***	1					
EC_d	0.72**	0.67**	0.84***	1				
SR_{soil}	-0.74**	-0.65**	-0.78***	-0.56*	1			
SOM	.	.	.	.	.	1		
$Elev_{rel}$	0.22	0.15	0.22	0.30	0.23	.	1	
Slope	-0.08	-0.17	-0.05	0.17	-0.13	.	0.06	1

Statistical significance at P < 0.10.
* Statistical significance at P < 0.05.
** Statistical significance at P < 0.01.
*** Statistical significance at P < 0.001.

Table A1.8. Pearson correlation coefficients of soil and topographic variables to in-season NDRE for all nonzero plots for Field KR16 (n = 80).

		Apparent Electrical Conductivity		Soil Optical Reflectance		Landscape	
	NDRE	**EC_s**	**EC_d**	**SR_{soil}**	**SOM**	**$Elev_{rel}$**	**Slope**
NDRE	1						
EC_s	0.69***	1					
EC_d	0.66***	0.86***	1				
SR_{soil}	-0.55***	-0.74***	-0.55***	1			
SOM	.	.	.	.	1		
$Elev_{rel}$	0.14	0.16	0.18	0.14	.	1	
Slope	0.05	0.04	0.02	-0.11	.	0.12	1

Statistical significance at P < 0.10.
* Statistical significance at P < 0.05.
** Statistical significance at P < 0.01.
*** Statistical significance at P < 0.001.

Table A1.9. Pearson correlation coefficients of soil and topographic variables to check plot yield and in-season NDRE for Field AR17 (n = 11).

			Apparent Electrical Conductivity		Soil Optical Reflectance		Landscape	
	Yield	**NDRE**	**EC_s**	**EC_d**	**SR_{soil}**	**SOM**	**$Elev_{rel}$**	**Slope**
Yield	1							
NDRE	0.44	1						
EC_s	-0.55#	-0.40	1					
EC_d	-0.35	-0.27	0.41	1				
SR_{soil}	-0.24	0.44	-0.07	0.05	1			
SOM	0.62*	0.30	-0.09	-0.12	-0.57#	1		
$Elev_{rel}$	-0.36	-0.77**	0.74**	0.23	-0.61*	0.15	1	
Slope	-0.36	-0.23	0.06	0.00	0.46	-0.69*	-0.11	1

Statistical significance at P < 0.10.
* Statistical significance at P < 0.05.
** Statistical significance at P < 0.01.
*** Statistical significance at P < 0.001.

Table A1.10. Pearson correlation coefficients of soil and topographic variables to in-season NDRE for all nonzero plots for Field AR17 (n = 52).

		Apparent Electrical Conductivity		Soil Optical Reflectance		Landscape	
	NDRE	**EC_s**	**EC_d**	**SR_{soil}**	**SOM**	**$Elev_{rel}$**	**Slope**
NDRE	1						
EC_s	-0.22	1					
EC_d	-0.18	0.47***	1				
SR_{soil}	-0.08	-0.37**	0.07	1			
SOM	0.16	-0.15	-0.27#	-0.48***	1		
$Elev_{rel}$	-0.12	0.80***	0.17	-0.52***	-0.04	1	
Slope	0.14	0.40**	0.13	-0.04	-0.19	0.38**	1

Statistical significance at P < 0.10.
* Statistical significance at P < 0.05.
** Statistical significance at P < 0.01.
*** Statistical significance at P < 0.001.

Table A1.11. Pearson correlation coefficients of soil and topographic variables to check plot yield and in-season NDRE for Field HU17 (n = 14).

			Apparent Electrical Conductivity		Soil Optical Reflectance		Landscape	
	Yield	**NDRE**	**EC_s**	**EC_d**	**SR_{soil}**	**SOM**	**$Elev_{rel}$**	**Slope**
Yield	1							
NDRE	0.81***	1						
EC_s	-0.79***	-0.79***	1					
EC_d	-0.56*	-0.62*	0.80***	1				
SR_{soil}	0.07	-0.07	-0.34	0.01	1			
SOM	0.73**	0.73**	-0.69**	-0.27	0.28	1		
$Elev_{rel}$	-0.21	-0.40	0.48#	0.46#	-0.01	-0.43	1	
Slope	-0.64*	-0.56*	0.54*	0.10	-0.36	-0.93***	0.30	1

Statistical significance at P < 0.10.
* Statistical significance at P < 0.05.
** Statistical significance at P < 0.01.
*** Statistical significance at P < 0.001.

Table A1.12. Pearson correlation coefficients of soil and topographic variables to in-season NDRE for all nonzero plots for Field HU17 (n = 70).

		Apparent Electrical Conductivity		Soil Optical Reflectance		Landscape	
	NDRE	**EC_s**	**EC_d**	**SR_{soil}**	**SOM**	**$Elev_{rel}$**	**Slope**
NDRE	1						
EC_s	-0.57***	1					
EC_d	-0.34**	0.66***	1				
SR_{soil}	0.12	-0.02	0.17	1			
SOM	0.68***	-0.70***	-0.32**	0.17	1		
$Elev_{rel}$	-0.39**	0.45***	0.27*	0.25*	-0.42***	1	
Slope	-0.63***	0.52***	0.26*	-0.20	-0.81***	0.35**	1

Statistical significance at P < 0.10.
* Statistical significance at P < 0.05.
** Statistical significance at P < 0.01.
*** Statistical significance at P < 0.001.

Table A1.13. Pearson correlation coefficients of soil and topographic variables to check plot yield and in-season NDRE for Field JA17 (n = 16).

			Apparent Electrical Conductivity		Soil Optical Reflectance		Landscape	
	Yield	**NDRE**	**EC_s**	**EC_d**	**SR_{soil}**	**SOM**	**$Elev_{rel}$**	**Slope**
Yield	1							
NDRE	0.50*	1						
EC_s	0.19	0.40	1					
EC_d	0.27	0.31	0.91***	1				
SR_{soil}	0.07	-0.47#	-0.74**	-0.48#	1			
SOM	-0.02	0.47#	0.65**	0.40	-0.95***	1		
$Elev_{rel}$	-0.20	-0.30	-0.74**	-0.77***	0.35	-0.28	1	
Slope	-0.15	-0.45#	-0.80***	-0.68**	0.64**	-0.61*	0.70**	1

Statistical significance at P < 0.10.
* Statistical significance at P < 0.05.
** Statistical significance at P < 0.01.
*** Statistical significance at P < 0.001.

Table A1.14. Pearson correlation coefficients of soil and topographic variables to in-season NDRE for all nonzero plots for Field JA17 (n = 80).

		Apparent Electrical Conductivity		Soil Optical Reflectance		Landscape	
	NDRE	**EC_s**	**EC_d**	**SR_{soil}**	**SOM**	**$Elev_{rel}$**	**Slope**
NDRE	1						
EC_s	0.35**	1					
EC_d	0.18	0.90***	1				
SR_{soil}	-0.49***	-0.73***	-0.46***	1			
SOM	0.50***	0.63***	0.34**	-0.94***	1		
$Elev_{rel}$	-0.14	-0.80***	0.76***	0.44***	-0.34**	1	
Slope	-0.18	-0.61***	-0.49***	0.50***	-0.51***	0.62***	1

Statistical significance at P < 0.10.
* Statistical significance at P < 0.05.
** Statistical significance at P < 0.01.
*** Statistical significance at P < 0.001.

Table A1.15. Pearson correlation coefficients of soil and topographic variables to check plot yield and in-season NDRE for Field KR17 (n = 16).

			Apparent Electrical Conductivity		Soil Optical Reflectance		Landscape	
	Yield	**NDRE**	**EC_s**	**EC_d**	**SR_{soil}**	**SOM**	**$Elev_{rel}$**	**Slope**
Yield	1							
NDRE	0.52*	1						
EC_s	0.85***	0.53*	1					
EC_d	0.84***	0.46#	0.96***	1				
SR_{soil}	-0.08	-0.52*	-0.06	0.04	1			
SOM	-0.03	0.50*	-0.11	-0.25	-0.90***	1		
$Elev_{rel}$	0.42	-0.14	0.36	0.50*	0.75***	0.75***	1	
Slope	0.22	-0.54*	0.07	0.27	0.53*	0.53*	0.66**	1

Statistical significance at P < 0.10.
* Statistical significance at P < 0.05.
** Statistical significance at P < 0.01.
*** Statistical significance at P < 0.001.

Table A1.16. Pearson correlation coefficients of soil and topographic variables to in-season NDRE for all nonzero plots for Field KR17 (n = 80).

		Apparent Electrical Conductivity		Soil Optical Reflectance		Landscape	
	NDRE	**EC_s**	**EC_d**	**SR_{soil}**	**SOM**	**$Elev_{rel}$**	**Slope**
NDRE	1						
EC_s	0.45***	1					
EC_d	0.26*	0.91***	1				
SR_{soil}	-0.30**	-0.04	0.15	1			
SOM	0.44***	-0.05	-0.24*	-0.92***	1		
$Elev_{rel}$	0.12	0.53***	0.65***	0.54***	-0.51***	1	
Slope	-0.36**	0.14	0.28*	0.53***	-0.67***	0.32**	1

Statistical significance at P < 0.10.
* Statistical significance at P < 0.05.
** Statistical significance at P < 0.01.
*** Statistical significance at P < 0.001.

Table A1.17. Summary statistics for soil and topographic variables for all 2016 fields.

Field	Variable	Units	Min	Max	Range	Mean	Standard Deviation	CV
AR16	EC_s	$dS \cdot m^{-1}$	11.4	73.4	62.0	31.9	11.85	37.2%
	EC_d	$dS \cdot m^{-1}$	22.0	101.8	79.8	48.9	16.75	34.3%
	SR_{soil}	-	1.7	2.0	0.3	1.9	0.05	2.6%
	SOM_{cal}	%	3.1	4.6	1.5	3.9	0.22	5.5%
	SOM	%	2.9	5.0	2.1	3.9	0.39	9.9%
	CEC	$cmol_c \cdot kg^{-1}$	13.6	24.8	11.2	18.5	2.86	15.5%
	$Elev_{rel}$	m	0.0	4.4	4.4	2.1	0.83	40.4%
	Slope	%	0.0	15.1	15.1	2.1	1.26	60.7%
CA16	EC_s	$dS \cdot m^{-1}$	19.4	82.2	62.8	46.3	11.29	24.4%
	EC_d	$dS \cdot m^{-1}$	26.5	119.9	93.4	69.6	15.50	22.3%
	SR_{soil}	-	1.7	1.9	0.2	1.8	0.04	2.1%
	SOM_{cal}	%	2.3	3.7	1.4	3.1	0.20	6.6%
	SOM	%	1.9	3.6	1.7	3.0	0.42	14.0%
	CEC	$cmol_c \cdot kg^{-1}$	13.7	25.4	11.7	19.6	3.02	15.4%
	$Elev_{rel}$	m	0.0	20.0	20.0	9.7	4.84	49.6%
	Slope	%	0.0	26.5	26.5	7.0	3.38	48.1%
HU16	EC_s	$dS \cdot m^{-1}$	14.4	95.1	80.7	38.6	11.72	30.3%
	EC_d	$dS \cdot m^{-1}$	24.8	136.2	111.4	66.1	14.88	22.5%
	SR_{soil}	-	1.7	2.0	0.3	1.9	0.05	2.8%
	SOM_{cal}	%	1.7	3.6	1.9	2.9	0.32	11.1%
	SOM	%	1.9	3.8	1.9	2.9	0.46	15.9%
	CEC	$cmol_c \cdot kg^{-1}$	13.3	22.7	9.4	16.6	2.75	16.6%
	$Elev_{rel}$	m	0.0	8.5	8.5	6.3	1.64	25.9%
	Slope	%	0.0	19.8	19.8	2.9	2.93	101.4%
KR16	EC_s	$dS \cdot m^{-1}$	1.3	27.1	25.7	4.1	2.69	66.4%
	EC_d	$dS \cdot m^{-1}$	2.0	24.2	22.3	7.1	4.13	58.5%
	SR_{soil}	-	1.8	2.2	0.4	2.0	0.06	3.0%
	SOM_{cal}	%	-	-	-	-	-	-
	SOM	%	0.6	1.7	1.1	1.0	0.30	31.0%
	CEC	$cmol_c \cdot kg^{-1}$	3.8	9.1	5.3	5.1	1.41	27.8%
	$Elev_{rel}$	m	0.0	4.7	4.7	2.0	0.62	32.0%
	Slope	%	0.0	12.6	12.6	1.5	1.26	84.0%

EC_s, shallow apparent electrical conductivity
EC_d, deep apparent electrical conductivity
SR_{soil}, simple ratio of soil optical reflectance
SOM_{cal}, calibrated soil organic matter
SOM, measured soil organic matter
CEC, measured cation-exchange capacity
$Elev_{rel}$, relative elevation

Table A1.18. Summary statistics for soil and topographic variables for all 2017 fields.

Field	Variable	Units	Min	Max	Range	Mean	Standard Deviation	CV
AR17	EC_s	$dS \cdot m^{-1}$	14.5	67.0	52.5	29.2	8.65	29.6%
	EC_d	$dS \cdot m^{-1}$	11.4	155.3	143.9	52.9	20.91	39.5%
	SR_{soil}	-	1.6	1.9	0.2	1.8	0.03	1.8%
	SOM_{cal}	%	2.2	3.8	1.5	3.0	0.19	6.5%
	SOM	%	1.9	4.7	2.8	3.0	0.55	18.5%
	CEC	$cmol_c \cdot kg^{-1}$	14.6	25.2	10.6	19.5	2.75	14.1%
	$Elev_{rel}$	m	0.0	4.0	4.0	1.5	0.81	54.2%
	Slope	%	0.0	13.5	13.5	2.1	1.47	68.9%
HU17	EC_s	$dS \cdot m^{-1}$	6.6	70.6	64.0	31.9	9.59	30.1%
	EC_d	$dS \cdot m^{-1}$	12.7	95.2	82.6	55.0	13.56	24.6%
	SR_{soil}	-	1.6	2.3	0.7	2.1	0.10	4.6%
	SOM_{cal}	%	1.8	4.2	2.4	3.3	0.36	10.9%
	SOM	%	2.2	4.4	2.2	3.3	0.42	12.6%
	CEC	$cmol_c \cdot kg^{-1}$	15.4	24.0	8.6	18.5	1.95	10.5%
	$Elev_{rel}$	m	0.0	5.1	5.1	2.2	1.06	47.6%
	Slope	%	0.0	10.2	10.2	1.3	1.17	90.1%
JA17	EC_s	$dS \cdot m^{-1}$	2.3	37.9	35.6	7.8	4.63	59.2%
	EC_d	$dS \cdot m^{-1}$	2.6	48.5	46.0	12.7	8.24	65.1%
	SR_{soil}	-	1.7	2.2	0.4	1.9	0.08	4.1%
	SOM_{cal}	%	0.0	2.5	2.5	1.4	0.50	36.0%
	SOM	%	0.9	3.1	2.2	1.4	0.57	39.7%
	CEC	$cmol_c \cdot kg^{-1}$	5.3	16.7	11.4	8.6	3.08	36.0%
	$Elev_{rel}$	m	0.0	7.0	7.0	2.2	1.51	68.9%
	Slope	%	0.0	16.0	16.0	3.2	2.42	76.1%
KR17	EC_s	$dS \cdot m^{-1}$	1.7	26.2	24.6	5.8	3.94	67.5%
	EC_d	$dS \cdot m^{-1}$	0.0	55.5	55.5	6.0	5.40	90.6%
	SR_{soil}	-	1.7	2.1	0.4	1.9	0.06	3.3%
	SOM_{cal}	%	0.3	1.7	1.4	1.2	0.24	20.2%
	SOM	%	0.7	2.0	1.3	1.2	0.39	32.8%
	CEC	$cmol_c \cdot kg^{-1}$	3.8	13.9	10.1	6.8	2.39	35.1%
	$Elev_{rel}$	m	0.0	2.9	2.9	1.2	0.46	38.9%
	Slope	%	0.0	7.9	7.9	1.8	1.35	76.1%

EC_s, shallow apparent electrical conductivity
EC_d, deep apparent electrical conductivity
SR_{soil}, simple ratio of soil optical reflectance
SOM_{cal}, calibrated soil organic matter
SOM, measured soil organic matter
CEC, measured cation-exchange capacity
$Elev_{rel}$, relative elevation

APPENDIX 2

A2.1. SAS Code for estimation of EONR by quadratic-plateau function.

```
*Quadratic-Plateau Model;
Title 'Quadratic-Plateau Analysis';
PROC NLIN DATA=All;
      by Site Rep;
      parms       a=7
                  b=0.05
                  c=-0.0002;
x0=-.5*b/c;
db=-.5/c;
dc=.5*b/c**2;
output out=quadplat p=QPpred r=QPresid ess=QPess parms = a b c;
if AppN<x0 then do;
model Yld=a+b*AppN+c*AppN*AppN;
der.a=1; der.b=AppN; der.c=AppN*AppN;
end;
else do;
model Yld=a+b*x0+c*x0*x0;
der.a=1; der.b=x0+b*db+2*c*x0*db; der.c=b*dc+x0*x0+2*c*x0*dc;
end;
if _obs_=1 & _model_=1 then do;
plateau=a+b*x0+c*x0*x0;
put x0= plateau=;
end;
ods output ConvergenceStatus=CS ANOVA=AN;
run;

PROC SORT DATA=CS;
BY site rep;
RUN;
PROC SORT DATA=AN;
BY site rep;
RUN;
PROC SORT DATA=quadplat;
BY site rep;
RUN;
DATA merge1;
MERGE quadplat (in=in1) AN;
BY site rep;
IF in1;
RUN;
DATA merge2;
MERGE merge1 (in=in1) CS;
BY site rep;
IF in1;
RUN;
PROC PRINT DATA=merge2;
RUN;
```

A2.2. SAS code for linear regression of yield response to N.

```
PROC REG DATA=NOConverge plots=ResidualByPredicted
plots=predictions(X=AppN);
      by site rep;
      var AppN;
      model Yld=AppN / r clm cli;
ods output ANOVA=AN FitStatistics=FS ParameterEstimates=PE;
RUN;
ods graphics off;

DATA merge1;
MERGE AN (in=in1) FS;
IF in1;
RUN;
DATA merge2;
MERGE merge1 (in=in1) PE;
IF in1;
RUN;
PROC PRINT DATA=merge2;
RUN;
```

A2.3. R code for an alternative MZ delineation method.

Several methods of cluster analysis are available for management zone (MZ) delineation. Fuzzy *k*-means cluster analysis has been used often to identify MZ for precision agriculture. In addition to using the original soil and topographic variables as inputs, some have used Principal Component Analysis (PCA) to build linear combinations of those variables, which are then used in the *k*-means clustering algorithm. Classical PCA summarizes the variability of several variables in new synthetic variables.

One issue with traditional *k*-means cluster analysis is that it does not include spatial autocorrelation or any reference to the geographical position of the data points. These clustering algorithms were not developed for spatial data, and often high zone fragmentation occurs when the spatial nature of the data is ignored.

Recent research by Córdoba et al. (2013) sought to apply a method proposed by Dray et al. (2008) that first takes into account spatial autocorrelation and then uses a fuzzy *k*-means clustering algorithm using spatial principal components from PCA as input variables. Dray et al. (2008) had applied this at a macrogeographical scale, and Córdoba et al. (2013) applied it to precision agriculture, finding it to be a more successful method for MZ delineation than traditional fuzzy *k*-means cluster analysis. They called this method cluster fuzzy *k*-means from spatial PCA (KM-sPC).

To test if MZ are delineated appropriately, MZ are evaluated to determine if there are differences among the zones in terms of crop response, yield, or other validation traits. However, conventional statistical models such as ANOVA are not recommended for use in evaluating mean differences between zones. One assumption of ANOVA is that all observations are independent, but independence is not met when the dataset is

spatially referenced (Lawes and Bramley, 2012). Mixed Linear Models (MLM) are preferred because they can account for spatial correlation in the dataset.

Cordoba et al. (2016) developed a protocol using R software for delineating MZ using the KM-sPC method and for testing the appropriateness of MZ using four MLM, all with a fixed zone effect. The four models were spherical and exponential spatial correlation functions, with and without a nugget effect. Akaike information criterion (AIC) was used to select the best-fitting model.

This method was explored for analyzing MZ in this thesis research. However, uncertainty as to the accuracy of this method precluded its conclusion in the thesis, and the more widely adopted fuzzy *k*-means clustering algorithm using Management Zone Analyst (MZA) was used in this study. Future research should consider the implications of these findings.

Córdoba, M., C. Bruno, J. Costa, and M. Balzarini. 2013. Subfield management class delineation using cluster analysis from spatial principal components of soil variables. Comput. Electron. Agric. 97:6-14.

Córdoba, M.A., C.I. Bruno, J.L. Costa, N.R. Peralta, and M.G. Balzarini. 2016. Protocol for multivariate homogeneous zone delineation in precision agriculture. Biosyst. Eng. 143:95-107.

Dray, S., S. Saïd, and F. Débias. 2008. Spatial ordination of vegetation data using a generalization of Wartenberg's multivariate spatial correlation. J. Veg. Sci. 19:45-56.

Lawes, R.A., and R.G.V. Bramley. 2012. A simple method for the analysis of on-farm strip trials. Agron. J. 104:371-377.

R Code for delineating MZ using the KM-sPC method (Córdoba et al., 2016)

```
## INSTALLATION AND LOADING OF REQUIRED PACKAGES----------
     ------------------------------
install.packages
     ("spdep","rgdal","geoR","gstat","ade4","e1071","sampli
     ng")
library(spdep)
library(rgdal)
library(geoR)
library(gstat)
library(ade4)
library(e1071)
library(nlme)
library(lsmeans)


## LOAD DATA SET-----------------------------------------
     ------------------------------
data0 <-read.table("C:\\.....\\name.txt", header = TRUE)

## 1. REMOVAL OF OUTLIERS--------------------------------
     ------------------------------

# Histogram and summary measures before outlier removal
summary(data0$ECa30)
boxplot(data0$ECa30,col='gray',ylab='ECa30
     (mS/m)',main="Box-Plot")

# Mean and standard deviation calculation
Mean <- mean(data0$ECa30)
stde <- sd(data0$ECa30)
Lower <- Mean-3*stde
Upper <- Mean+3*stde

# Selection of data that are located between the mean ± 3
     SD
data0$ECa30[Upper<data0$ECa30|data0$ECa30<Lower] <-NA
```

```
data0 <- subset(na.omit(data0),select=c(x,y,ECa30))

# Histogram and summary measures after outlier removal
summary(data0$ECa30)
boxplot(data0$ECa30,col='gray',ylab='ECa30
     (mS/m)',main="Box-Plot")



## 2. REMOVAL OF INLIERS----------------------------------
     ------------------------------

# Spatial weights matrix
cord <- coordinates(data0[,1:2])
gri <- dnearneigh(cord,0,25)
lw <- nb2listw(gri, style = "W")

# Local Moran's Index
LM <-
     localmoran(data0$ECa30,lw,p.adjust.method="bonferroni"
     ,alternative ="less")
LM

# Moran Plot
MP <- moran.plot(data0$ECa30,
     lw,quiet=T,labels=F,col=3,zero.policy=F,xlab="ECa30",
     ylab="ECa30 Spatially Lagged")
summary(MP)

# Identification of inliers
Influ <- MP$is.inf ; Influ
data0 <- data.frame(data0,LM,Influ); data0

# Removal data with negative local Moran and statistically
     significant (p <0.05)
data1 <- subset(data0,data0[,4] > 0 | data0[,8] > 0.05 ) ;
     data1

# Elimination of inliers identified with Moran Plot
data2 <- data1[data1$dfb.1_ == FALSE & data1$dfb.x == FALSE
     & data1$dffit == FALSE
& data1$cov.r == FALSE & data1$cook.d  == FALSE & data1$hat
     == FALSE, ]
```

```
## 3. SPATIAL INTERPOLATION OF DATA-----------------------
     -------------------------------

# Fit the empirical and theoretical semivariogram
coordinates(data2) <- ~x+y

ECa30vario <- variogram(ECa30~1, data2, cutoff=250)
Exp_wls <- fit.variogram(fit.method=1,ECa30vario, vgm(25,
     "Exp", 80,10))
Exp_wls
plot(ECa30vario,Exp_wls,main="ECa30",xlab="Distance between
     field sites",ylab="Semivariance of
     ECa30",cex=1,cex.axis=10)
attr(Exp_wls, 'SSErr')

Esf_wls <- fit.variogram(fit.method=1,ECa30vario, vgm(25,
     "Sph", 80,10))
Esf_wls
plot(ECa30vario,Esf_wls,main="ECa30",xlab="Distance between
     field sites",ylab="Semivariance of ECa30")
attr(Esf_wls, 'SSErr')

# Cross Validation
val_exp <- krige.cv(ECa30~1, data2, model = Exp_wls,
     nfold=200,verbose=F,nmin=7,nmax=25)
val_sph <- krige.cv(ECa30~1, data2, model = Esf_wls,
     nfold=200,verbose=F,nmin=7,nmax=25)

# Mean square error-MSE(ideally small)
MSE_exp <- mean(val_exp$residual^2)
MSE_sph <- mean(val_sph$residual^2)

# Root mean squared error-RMSE (ideally small)
RMSE_exp <- sqrt(mean(val_exp$residual^2))
RMSE_sph <- sqrt(mean(val_sph$residual^2))

# mean squared deviation ratio-MSDR (ideally close to 1)
MSDR_exp <- mean(val_exp$zscore^2)
MSDR_sph <- mean(val_sph$zscore^2)

# Load data set with the georeferenced points that make up
     the plot polygon,
# i.e., points representing the field boundaries
Bound <-read.table("C:\\.....\\Bound.txt", header = TRUE)

# Regular grid of 10 x 10 m
```

```
gr <- pred_grid(Bound, by=10)
gri <- polygrid(gr, bor=Bound)
plot(gri,col = "red", pch = 10, cex =
     0.2,xlab="X",ylab="Y")
gridded(gri) = ~Var1+Var2

# Interpolation using block kriging
Kg_wls <- krige(ECa30~1, data2, gri, model = Exp_wls, block
     = c(40,40), nmin=7, nmax=25)
spplot(Kg_wls["var1.pred"],
     col.regions=terrain.colors(100))

# Interpolated data extraction
PredECa30 <- as.data.frame(Kg_wls)
PredECa30 <- PredECa30[,1:3]

names(PredECa30)[1]<-paste("x")
names(PredECa30)[2]<-paste("y")
names(PredECa30)[3]<-paste("ECa30")



## 4. MULTIVARIATE SITE CLASSIFICATION ----------------------
     -------------------------------

# After all the variables have been processed from step 1
     up to the interpolation with the same prediction grid
     (step 5),
# the different data sets obtained should be concatenated
     using the cbind function.
# Below the R code was deactivated because a new database
     that has been concatenated is used.

# Pred <- cbind(PredECa30[,1:3], PredECa90[,3],
     PredElev[,3],PredSd[,3])
# names(Pred)[3]<-paste("ECa30")
# names(Pred)[4]<-paste("ECa90")
# names(Pred)[5]<-paste("Elev")
# names(Pred)[6]<-paste("Sd")

Pred <-read.table("C:\\.....\\Pred.txt", header = TRUE)

# Spatial principal component analysis (MULTISPATI-PCA)
pca <- dudi.pca(Pred[,3:6], center=T,scannf = FALSE,  nf =
     5)
```

```
cord_1 <- coordinates(Pred[,1:2])
gri_1 <- dnearneigh(cord_1,0,25)
lw_1 <- nb2listw(gri_1, style = "W")

ms <- multispati(pca, lw_1, scannf = F, nfposi = 5)
s.arrow(ms$c1,xax = 1, yax = 2, clabel = 1)

# Extraction of spatial principal components
sPC <- ms$li[,1:4]
PredMA <- cbind(Pred,sPC) ;PredMA

#  Fuzzy k-means cluster analysis
MC_2<-cmeans(PredMA[,7:8],2,100,method="cmeans",m=1.3)
MC_3<-cmeans(PredMA[,7:8],3,100,method="cmeans",m=1.3)
MC_4<-cmeans(PredMA[,7:8],4,100,method="cmeans",m=1.3)

# Indices for selecting the number of classes: two (I2MC),
     three (I3MC) and four (I4MC)
I2MC <- fclustIndex(MC_2,PredMA[,7:8], index=c("xie.beni",
     "fukuyama.sugeno",
"partition.coefficient", "partition.entropy"))

I3MC <- fclustIndex(MC_3,PredMA[,7:8], index=c("xie.beni",
     "fukuyama.sugeno",
"partition.coefficient", "partition.entropy"))

I4MC <- fclustIndex(MC_4,PredMA[,7:8], index=c("xie.beni",
     "fukuyama.sugeno",
"partition.coefficient", "partition.entropy"))

Indices0 <- cbind(I2MC,I3MC,I4MC)

XieBeni <-Indices0[1,]
FukSug <-Indices0[2,]
PartCoef_1 <-Indices0[3,]
PartCoef <- 1/PartCoef_1
PartEntr <-Indices0[4,]

Indices <-
     as.data.frame(rbind(XieBeni,FukSug,PartCoef,PartEntr))
Indices

# Summary indices
XieBeniMax<-max(Indices[1,])
FukSugMax<-max(Indices[2,])
PartCoefMax<-max(Indices[3,])
```

```
PartEntrMax<-max(Indices[4,])

XieBeniN<- XieBeni/XieBeniMax
FukSugN<- FukSug/FukSugMax
PartCoefN<- PartCoef/PartCoefMax
PartEntrN<-PartEntr/PartEntrMax

IndicesN <-
     as.data.frame(rbind(XieBeniN,FukSugN,PartCoefN,PartEnt
     rN))
IndicesN2 <- (IndicesN)^2

Indice2MC <- sqrt(sum(IndicesN2[,1]))
Indice3MC <- sqrt(sum(IndicesN2[,2]))
Indice4MC<- sqrt(sum(IndicesN2[,3]))

# Summary indices for selection of two, three or four
     management zones
Indice2MC; Indice3MC; Indice4MC

# Maps with management classes delimited
MC_22 <-as.data.frame(MC_2$cluster)
MC_33 <-as.data.frame(MC_3$cluster)
MC_44 <-as.data.frame(MC_4$cluster)

baseMC <- cbind(PredMA[,1:2],MC_22,MC_33,MC_44)

coordinates(baseMC) <- ~x+y
gridded(baseMC) <- T
spplot(baseMC["MC_2$cluster"],col.regions=gray.colors(2),co
     lorkey = F)

spplot(baseMC["MC_3$cluster"],col.regions=gray.colors(10),c
     olorkey = F)

spplot(baseMC["MC_4$cluster"],col.regions=gray.colors(4),co
     lorkey = F)



## 5. SMOOTHING OF CLASSIFICATION RESULTS ----------------
     ------------------------------

# Median filter function
smooth <-function(mytable,mywindow){
```

```
  newtable<-
     matrix(1:(dim(mytable)[1]*dim(mytable)[2]),dim(mytable
     )[1],dim(mytable)[2])
      vecinity<-function(pos) {
        col=as.integer((pos-1)/nrow(newtable))+1
        row=pos-((nrow(newtable)*col)-nrow(newtable))
        if (is.na(mytable[row,col])) NA else{
        myrow1<-ifelse(row-mywindow<1,1,row-mywindow)
        mycol1<-ifelse(col-mywindow<1,1,col-mywindow)
        myrow2<-
     ifelse(row+mywindow>dim(newtable)[1],row,row+mywindow)
        mycol2<-
     ifelse(col+mywindow>dim(newtable)[2],col,col+mywindow)

        neighbor<-
     na.omit(as.vector(mytable[myrow1:myrow2,mycol1:mycol2]
     ))
        round(median(neighbor),digits=0)
      }}
      as.matrix(apply(newtable,c(1,2),vecinity))}

# Function to obtain a matrix
obtainM <- function(mytable){
  x<-as.numeric(names(table(mytable$x)))
  y<-as.numeric(names(table(mytable$y)))
  myframe <- matrix(1:(length(x)*length(y)), length(x),
     length(y))
  position<-function(pos) {
    col=as.integer((pos-1)/nrow(myframe))+1
    row=pos-((nrow(myframe)*col)-nrow(myframe))
    myindex=which(mytable$x==x[row] &
     mytable$y==y[col],arr.ind=T)
    if(length(myindex)==0) return(NA) else
     mytable[myindex,3]
  }
 thematrix<-as.matrix(apply(myframe,c(1,2),position))
 rownames(thematrix)<-x
 colnames(thematrix)<-y
 thematrix}

base0 <- cbind(PredMA[,1:2],MC_22)
datafilter <- obtainM(base0)

# Windows 5 x 5
smoot5x5 <- smooth(datafilter,5)
```

```
# Windows 7 x 7
smoot7x7 <- smooth(datafilter,7)

# Windows 9 x 9
smoot9x9 <- smooth(datafilter,9)

par(mfrow=c(2,2))
image(datafilter, main= "Original Zonification", axes =
     FALSE,
     xlab="",ylab="",col=palette(c("grey94","grey34")))
image(smoot5x5, main= "Median Filter 5 x 5",axes = FALSE,
     xlab="",ylab="",col=palette(c("grey94","grey34")))
image(smoot7x7, main= "Median Filter 7 x 7",axes = FALSE,
     xlab="",ylab="",col=palette(c("grey94","grey34")))
image(smoot9x9, main= "Median Filter 9 x 9",axes = FALSE,
     xlab="",ylab="",col=palette(c("grey94","grey34")))

# Data set with smoothing classification
# Function to ransform a matrix to table
MtoT <- function(mymatrix){
position <- function(ij){
data.frame(x=rownames(mymatrix)[ij[1]],y=colnames(mymatrix)
     [ij[2]],z=mymatrix[ij[1],ij[2]])
}
myindex <-
     which(!is.na(mymatrix),arr.ind=T);rownames(myindex)=NU
     LL
b <- apply(myindex,1,position)
b <- do.call("rbind",b);b}

# New data set
base1 <- as.data.frame(smoot9x9)
base2 <- MtoT(base1)
base2[order(base2[,1], base2[,2]),]
PredMA[order(PredMA[,1], PredMA[,2]),]
Finalbase <- cbind(PredMA[,1:6],base2[,3])
names(Finalbase)[7]<-paste("Zone")
```

R Code for evaluating the appropriateness of delineated MZ using four MLM

```
## INSTALLATION AND LOADING OF REQUIRED PACKAGES----------
     ------------------------------

library(nlme)
library(estimability)
library(lsmeans)

## VALIDATION OF MANAGEMENT ZONES-------------------------
     ---------------------------

# Load data set
Sample <-read.table("C:\\...\\name.txt", header = TRUE)
Sample$Zone<-as.factor(Sample$Zone)

# NDRE data ----------------------------------------------
     -------------------
# Model with exponential spatial correlation
mod1_NDRE <-gls(NDRE~1+Zone
,correlation=corExp(form=~as.numeric(as.character(X))+as.nu
     meric(as.character(Y))
,metric="euclidean"
,nugget=FALSE)
,method="REML"
,na.action=na.omit
,data=Sample)

# Model with exponential spatial correlation and nugget
     effect
mod2_NDRE <-gls(NDRE~1+Zone
,correlation=corExp(form=~as.numeric(as.character(X))+as.nu
     meric(as.character(Y))
,metric="euclidean"
,nugget=TRUE)
,method="REML"
,na.action=na.omit
,data=Sample)

# Model with spherical spatial correlation
mod3_NDRE <-gls(NDRE~1+Zone
,correlation=corSpher(form=~as.numeric(as.character(X))+as.
     numeric(as.character(Y))
,metric="euclidean"
,nugget=FALSE)
,method="REML"
```

```
,na.action=na.omit
,data=Sample)

# Model with spherical spatial correlation and nugget
     effect
mod4_NDRE <-gls(NDRE~1+Zone
,correlation=corSpher(form=~as.numeric(as.character(X))+as.
     numeric(as.character(Y))
,metric="euclidean"
,nugget=TRUE)
,method="REML"
,na.action=na.omit
,data=Sample)

# Model of independent errors
mod5_NDRE <-gls(NDRE~1+Zone
,method="REML"
,na.action=na.omit
,data=Sample)

# Selecting spatial correlation model using the Akaike
     information criterion
AICmod1_NDRE <- AIC(mod1_NDRE)
AICmod2_NDRE <- AIC(mod2_NDRE)
AICmod3_NDRE <- AIC(mod3_NDRE)
AICmod4_NDRE <- AIC(mod4_NDRE)
AICmod5_NDRE <- AIC(mod5_NDRE)

AICmod1_NDRE
AICmod2_NDRE
AICmod3_NDRE
AICmod4_NDRE
AICmod5_NDRE

# LSMeans Summaries for Each Attribute----------------------
     ------------------
# Select the correct model below based on AIC values-------
     ------------------

# Summary of selected model (NDRE)
NDREmeans <- summary(lsmeans(mod4_NDRE, pairwise~Zone));
     NDREmeans
```